ANALYTICAL CHARACTERIZATION OF ANTHOCYANINS FROM NATURAL PRODUCTS BY REVERSE-PHASE LIQUID CHROMATOGRAPHY-PHOTODIODE ARRAY-ELECTROSPRAY IONIZATION-ION TRAP-TIME OF FLIGHT MASS SPECTROMETRY

by

JEREMY S. BARNES

Presented to the Faculty of the Graduate School of

The University of Texas at Arlington in Partial Fulfillment

of the Requirements

for the Degree of

MASTER OF SCIENCE IN CHEMISTRY

THE UNIVERSITY OF TEXAS AT ARLINGTON

December 2010

ACKNOWLEDGEMENTS

I would like to acknowledge my research mentor, Dr. Kevin Schug, who has always believed in me and has never doubted my abilities. His great ideas and encouragement have helped me accomplish many things. Also, to the professors who serve on my committee, Dr. Frank Foss and Dr. Purnendu Dasgupta, I would like to thank them for the time and effort they have given me.

I must acknowledge my loving wife's devotion and dedication. She inspires me to do my best at everything I do. Finally, my father has blessed me with many tools in life, most importantly of which are a sense of responsibility and work ethic.

November 18, 2010

ABSTRACT

ANALYTICAL CHARACTERIZATION OF ANTHOCYANINS FROM NATURAL PRODUCTS BY REVERSE-PHASE LIQUID CHROMATOGRAPHY-PHOTODIODE ARRAY-ELECTROSPRAY IONIZATION-ION TRAP-TIME OF FLIGHT MASS SPECTROMETRY

Jeremy S. Barnes, M.S.

The University of Texas at Arlington, 2010

Supervising Professor: Kevin Schug

Anthocyanins are known to be one of the most powerful phytochemical antioxidant and believed to have a positive influence on a variety of health conditions. Numerous studies continue on these compounds that are readily found in most plants. Red hybrid-tea rose petals and wild blueberries were used as model systems for optimizing the extraction and identification process of anthocyanins in plant material using high performance liquid chromatography (HPLC) and mass spectrometry (MS) without the use of authentic standards. A number of extraction parameters, including sample homogenization, solvent selection and acid type and amount, were varied to examine the effects on anthocyanin extraction from blueberries. Individual anthocyanins within the extract solution were separated by reverse phase HPLC and identified by elution order and tandem mass spectrometry. Further definitive identification of anthocyanins from other isobaric flavonoid species was demonstrated by multi-dimensional tandem mass spectrometry fragmentation (MS^n). Cyanidin-3,5-diglucoside and pelargonidin-3,5-diglucoside were isolated from an extract of freeze dried rose petals via fractionation. These compounds were then structurally-characterized by multi-stage mass spectrometry

fragmentation (up to MS^6). Variations in the collision energy of the ion trap resulted in cleavage of the glycosides at the MS/MS, and MS^3 stages; fragmentation of the anthocyanidin was recorded at the MS^4 stage and beyond. Computational modeling was used to investigate the cross-ring cleavage fragment ions of cyanidin.

TABLE OF CONTENTS

LIST OF ILLUSTRATIONS

Figure Page

LIST OF TABLES

CHAPTER 1

INTRODUCTION

Polyphenolic species are ubiquitous in nature, and are often found in complex mixtures, with each plant type offering its own unique profile of individual species[1]. Anthocyanins are one of the many compound classes that fall under the polyphenolic flavonoid group, and this group of species is distinguished for their role in conferring the bright red, blue and purple colors of berries and fruits[2]. Recently and importantly, they have been the focus of significant beneficial health claims due to their antioxidant capacity[3]. Consumer and academic interest continues in the understanding of the medicinal, therapeutic and nutritional value provided by these naturally occurring phytochemical compounds. This interest further urges the development of analytical techniques to determine the identity and quantities of anthocyanins in natural products, as well as their effects *in vivo* and *in vitro*.

The wide array of phenolic species and the general complexity of plant matrices make qualitative and quantitative chemical analysis of anthocyanins challenging. Adding to the difficulties is the fact that most phenolic species are made up of only carbon, hydrogen and oxygen, sometimes differing by only one atom and many differing by only their related constitutional and stereochemical isomers. Due to subtle changes in structure, it may be difficult to confidently identify species. In order to overcome these challenges, a combination of complimentary techniques needs to be used.

Proper sample preparation is needed to bring these compounds into a liquid phase, where they can be analyzed by liquid chromatography with photodiode array detection, which is currently the most popular technique for separation[4]. Qualitative identification can then be achieved using tools offered by technological advancements in mass spectrometry, such as the soft ionization ability of electrospray ionization (ESI), the selective fragmentation ability of an ion trap (IT), and the high resolution ability of time-of-flight (TOF) mass spectrometry detection.

Determining the fragmentation pathways of individual species through optimized multi-dimensional mass spectrometry may extend the ability to identify anthocyanin species in complex matrices[5]. Reliable identification of anthocyanin mass signals from other isobaric flavonoid species can be assessed through diagnostic fragment signals. Unfortunately, higher order fragmentation may be limited by signal strength, especially in higher order fragmentation stages. Using unoptimized settings may leave the user with little or no fragmented species. The collision energy settings for the ion-trap can be systematically varied to enhance certain fragment signals and thus a higher degree of fragmentation (MS^n) can be achieved by improving on the signal strength.

The focus of this work was to develop a set of techniques to extract anthocyanins from plant material and identify them by high performance liquid chromatography (HPLC) and mass spectrometry (MS) without the use of rare and expensive standards. Wild blueberries, which contain a vast number of anthocyanin species, and the petals of a red hybrid-tea rose ("Liberty", *R. gallica*), were used as model systems for optimizing the extraction and identification process.

In order to find the most efficient extraction system, blueberries were subjected to varying sample homogenization techniques and multiple extraction solvents, along with varying the types and amounts of acid used in the extraction solvent. Once in solution, separation of the individual anthocyanin species was achieved by observing the chromatographic elution order by a reversed phase separation mode and selective detection by virtue of their characteristic absorption at 520 nm. Observation of distinct UV spectra provided by a photodiode array can be used to differentiate the anthocyanin from the other flavonoid classes.

Further definitive identification of anthocyanins from other isobaric flavonoid species was demonstrated by multi-dimensional fragmentation (MS^n). Cyanidin-3,5-diglucoside and pelargonidin-3,5-diglucoside were isolated from an extract of freeze dried rose petals via fractionation. These compounds were then structurally-characterized by multi-stage tandem mass spectrometry fragmentation (up to MS^6). By varying the collision energy of the ion trap, changes in the intensities of fragment ions due to cleavage of the glycosides were observed at the MS/MS, and MS^3 stages; fragmentation of the anthocyanidin (aglycone species) was recorded at the MS^4 stage and beyond. Iterative fragmentation pathways and

high mass accuracy were used to propose structures for observed mass signals. Structural characterization was attempted by identifying the fragments created by cross-ring cleavage (CRC) and small neutral molecule loss. An investigation of the overall energy of the CRC fragments of cyanidin by means of a computational study was also performed.

Efficiency and cost must be considered during the development of ideal analytical assays. Most of the time and effort dedicated towards the analysis of anthocyanins from natural products is in sample clean up,and separation of individual anthocyanin species from other isomeric flavonoids. Costs can accrue from consumables and the high price of standards. By using MS^n for iterative fragmentation of anthocyanins, unequivocal qualitative identification of all species within a mixture can be determined by matching observed signals with fragmentation pathways previously determined. This ability to identify species by directly infusing extracted plant solutions could help analysts bypass some of the many challenges they currently face.

CHAPTER 2

GENERAL BACKGROUND

2.1 Structure of Anthocyanins

Flavonoids are one of the largest groups of phenolics found in nature. It has been estimated that 2% of all carbon produced by plants is converted into flavonoids[6]. There are well over 9000 known flavonoids, which can be classified into 12 subclasses based on the degree of oxidation of their central pyran ring[7]. Deconstruction of the total phenolic content of natural products leads to either simple phenolics, made up of coumarins and phenolic acids, or polyphenolics, which includes a much broader subclass of flavonoids and tannins (Figure 2.1). One unique subset of flavonoid compounds is the water-soluble anthocyanins. Anthocyanins are polyphenolic secondary metabolites synthesized in almost all higher order plants and are partly responsible for the purple, blue and red color found in leaves, flowers, fruits and vegetables.

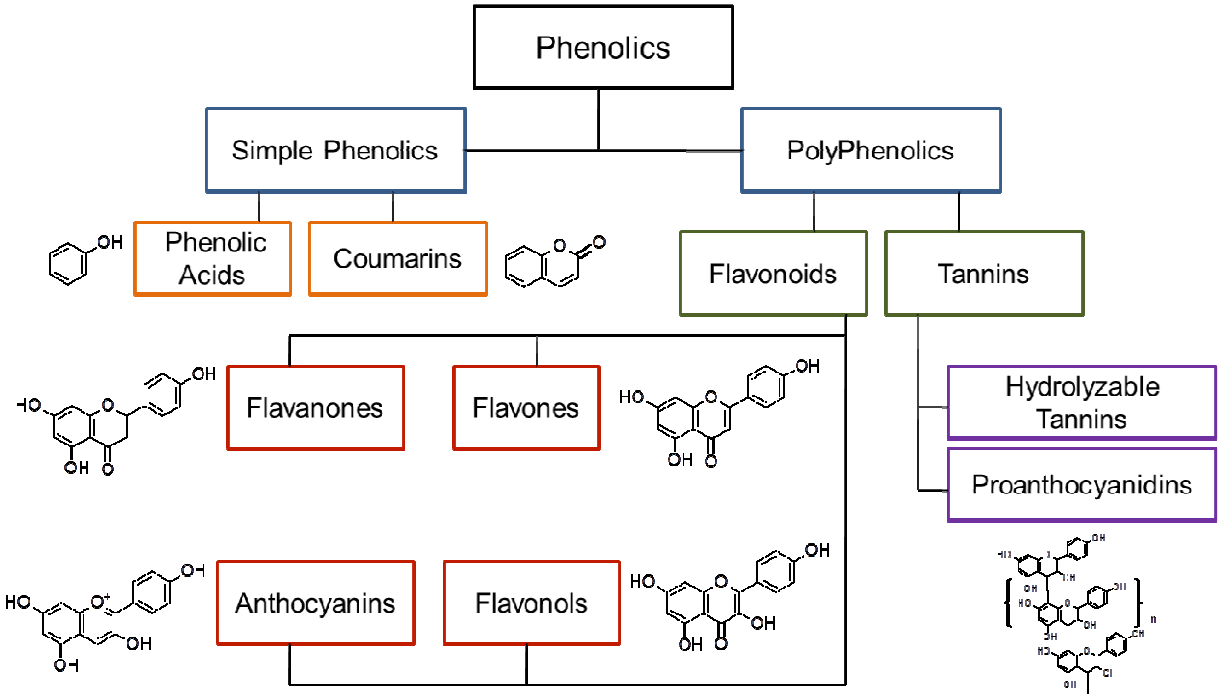

Figure 2.1: Structural organization of phenolics in natural products

The core structure of an anthocyanin is a C_6-C_3-C_6 skeleton consisting of a benzopyran with a phenolic ring connected at the 2 position of the pyran, and is referred to as a flavylium cation.

Traditionally the rings are labeled A, B and C, with the fused benzoyl ring labeled A, the attached phenolic labeled B and the center pyran ring labeled C. Anthocyanins differ from the rest of the flavonoid group by a formal positive charge found on the oxygen of the pyran ring (Figure 2.2). The A-C bicycle is naturally glycosylated and attachment can occur at the 3, 5, and 7 positions and, in rare instances, can occur at the 3', 4', and 5' positions on the B ring. The sugars that are naturally attached can include glucose, rhamnose, xylose, galactose, arabinose, and fructose. Many anthocyanins have been found to be acylated by aliphatic or aromatic acids, the most commonly seen acyl groups being coumaric, caffeic, ferulic, *p*-hydroxy benzoic, synapic, malonic, acetic, succinic, oxalic, and malic acids[8]. This variety allows for a multitude of potential structural and functional variants. Up to 600 different species have been reported[9].

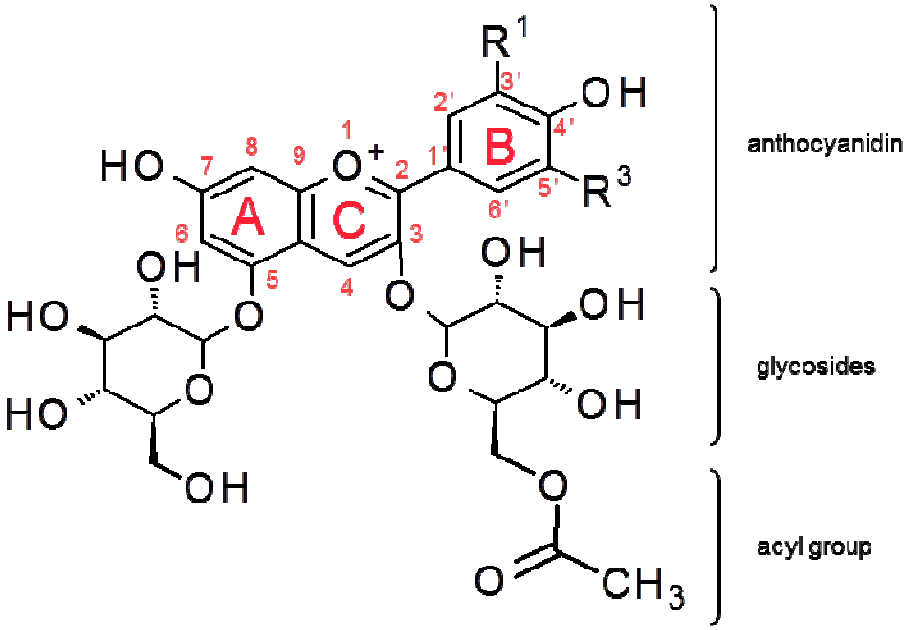

Figure 2.2: A generic structure of an acylated anthocyanin diglucoside

The aglycone flavylium cation is referred to as an anthocyanidin[10]. To date, there are 19 naturally occurring anthocyanidins (Table 2.1). The six most common anthocyanidins are pelargonidin, peonidin, cyanidin, malvidin, petunidin, and delphinidin. The differences between the six common

structures are based on variations of hydroxyl- and methoxy-substituent groups at two positions on the B-ring, 3' and 5'.

Table 2.1: Naturally Occurring Anthocyanidins and their substitution patterns

Anthocyanidin	**Substitution Pattern**					
Common	3	5	6	7	3′	5′
Pelargonidin	OH	OH	H	OH	H	H
Cyanidin	OH	OH	H	OH	OH	H
Peonidin	OH	OH	H	OH	OMe	H
Delphinidin	OH	OH	H	OH	OH	OH
Malvidin	OH	OH	H	OH	OMe	OMe
Petunidin	OH	OH	H	OH	OMe	OH
3-deoxyanthocyanidins						
Apigeninidin	H	OH	H	OH	H	H
Luteolinidin	H	OH	H	OH	OH	H
Tricetinidin	H	OH	H	OH	OH	OH
Riccionidin A[1]	H	H	OH	OH	H	H
Others						
Aurantinidin	OH	OH	OH	OH	H	H
6-Hydroxycyanidin	OH	OH	OH	OH	OH	H
6-Hydroxydelphinidin	OH	OH	OH	OH	OH	OH
Hirsutidin	OH	OH	H	OMe	OMe	OMe
Rosinidin	OH	OH	H	OMe	OMe	H
Europinidin	OH	OMe	H	OH	OMe	OH
Capensinidin	OH	OMe	H	OH	OMe	OMe
5-Methylcyanidin	OH	OMe	H	OH	OH	H
Pulchellidin	OH	OMe	H	OH	OH	OH

[1] 3 and 6' has ether bond and 2' has OH

2.2 Plant Physiology

Anthocyanins are present in almost all higher order plants. They are very rare in fungi/algae, but 3-deoxyanthocyanidins have been reported in moss groups of bryophyte[11]. Anthocyanins are found in the epidermal and subepidermal cells in roots, stems, petals, fruits, leaves and bracts. These compounds are believed to be dissolved in the cell sap found in vacuoles within the cells[12,13]. Furthermore, the anthocyanins can exist within specialized packets within the vacuole, referred to as anthocyanoplasts (ACP), a membrane bound compartment which contains other compounds responsible for anthocyanin biosynthesis[14]. They may also exist in the vacuole as an anthocyanic vacuolar inclusion (AVI); a non-membrane bound structure consisting of a hydrophobic proteinaceous matrix which binds anthocyanins creating a concentrated region of color in some plants[15].

It is believed that anthocyanins have multiple functions in plant physiology. These functions can be classified into two categories, plant-animal/insect interaction, or response to stress. The difference in chemistry between the aglycones along with other color-modifying factors, serves as a basis for color variation in fruits and flowers. The bright colors attract potential pollinating and/or seed-dispersing insects and animals[10]. One misconception is that leaves change colors during autumn senescence because the degradation of chlorophyll unmasks the anthocyanin pigment. Instead, this has been linked to anthocyanin production, which may be a warning to insects and herbivores that the leaves may be toxic or low in nutrition[16]. A more subtle animal-plant interaction, which is currently being debated, is over the dietary antioxidant contribution and other therapeutical aspects caused by ingestion of anthocyanin-enriched plants.

Speculation suggests that the anthocyanin plays a key role in a plant's response to stresses, such as UV radiation and attack by insects, microbes and fungi. It is known that the polyphenolic structure of anthocyanins absorb UV-B light, particularly the acylated forms, which reduces the photoinhibition and damage of DNA[17]. Second, since the anthocyanin is at the end of the flavonoid biosynthetic pathway, it is believed that the compound is biologically active[16]. In some studies of insect attack on leaves, an increase in production of anthocyanins was observed[18,19]. Anthocyanins have also been observed surrounding fungal lesions, although fungal inhibition is low[20]. Interestingly, fungal inhibition by 3-deoxyanthocyanidin has been reported[21].

2.3 Nutritional and Therapeutic Interests

Many epidemiological studies have shown that diets with fruits and vegetables are positively correlated with reduced mortality by coronary heart disease (CHD), stroke and cancer[22]. A phenomenon known as the "French Paradox" correlated the low mortality rates from CHD of the French demographic, whose diets are high in saturated fats, with an above average consumption of red wine, which contain large amounts of anthocyanins and pro-anthocyanidins. One study suggests, though, that there has been an insufficient amount of data to link saturated fat with CHD[23]. Nevertheless, fruits and vegetables contain high flavonoid content, which are believed to be the reason behind these physiological benefits.

Numerous studies[24 -28] have shown that anthocyanins are powerful antioxidants. In addition they have been linked to anticancer effects[29], and their capacity to deter apoptosis of healthy cells[30], which may be attributed to their powerful antioxidant abilities, as well as their promotion of other cellular functions, which suppress cancerous cellular growth. Recently, attention has been given to anthocyanins and their role in biochemical signaling cascades[31]. Some related studies suggested cancer chemoprevention[32] and tumor cell inhibition[33] by shutting down signaling cascades that are responsible for growth factors. One study suggests anthocyanins are more effective than isolated applications of phenolic acids, tannins and flavonols at inhibiting colon cancer cells and inducing their apoptic demise[34]. In contrast, the same research group showed in another studied that cellular anthocyanin transport/absorption efficiencies were relatively low compared to other polyphenols, citing that free hydroxyl groups and methoxy groups hindered bioavailability[35].

The debate here between *in vitro* results and *in vivo* possibilities is justifiable, and warrants the increased need for further studies and improved analytical techniques to support these paramount conquests. Results of anthocyanin analysis in human urine demonstrated a very low concentration, near 0.1% of the ingested dose, suggesting that anthocyanins remained in the system for some time[36]. Another study demonstrated detection of anthocyanins in plasma, meaning these compounds do appear in the bloodstream[37]. New techniques are revealing methylated, glucoronidated and sulphated anthocyanin compounds in urine[38,39], while previous methods were not sensitive enough to detect these metabolites[36,40].

Many *in vitro* studies have been performed, which have resulted in an array of suggested mechanisms by which anthocyanins provide physiological health benefits. In addition to cancer cell inhibition and apoptosis, anthocyanins act as scavengers of free radicals and may help prevent the negative effects of reactive oxygen species (ROS)[41]. Free metal ions can also act as oxidants. One example demonstrated that the antioxidant capability of ascorbic acid (which also deactivates ROS), a compound ubiquitous in animal and plant systems, was decreased due to oxidation by free copper ions. When a cyanidin derivative was introduced the metal ion oxidation was prevented through metal chelation. The authors proposed a unique ascorbic acid-metal-anthocyanin complex[42]. In the case of

CHD, atherogenesis may be escalated by oxidized low density lipoproteins (LDL). Oxidized LDL damages the cells that line the blood vessels. Antioxidant anthocyanins were shown to lower the amount of oxidized LDL[43].

Three possible mechanisms for neutralization of free radicals by anthocyanins are 1) a transfer of a hydrogen atom to the free radical, 2) an electron transfer, then proton transfer from the polyphenolic to the free radical, and 3) sequential proton loss-electron transfer, where the anthocyanin loses a proton, forming an anion, then transfers an electron to the free radical, upon which the anionic free radical sequesters a free proton (Figure 2.3). Some computational studies of anthocyanins which used ionization potentials, homolytic O-H bond dissociation enthalpies and heterolytic O-H bond dissociation enthalpies, suggested that the most likely mechanism would be mechanism (1), hydrogen atom transfer, although, any mechanism may be plausible based on the pH of the system[44-46].

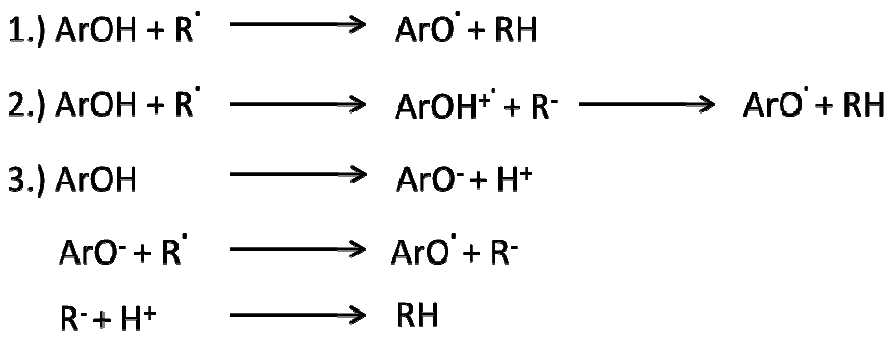

Figure 2.3: Three possible mechanisms by which anthocyanins neutralize free radicals**.**

2.4 Natural Product Extraction

The term anthocyanin, which is derived from the Greek words *anthos* meaning flower and *kyanos* meaning blue, was first coined by L.C. Marquart in 1835 when describing “colored cell sap” observed

using light microscopy[16]. Anthocyanins were studied in roses as early as 1914 in a study by Willstater and Nolan on the isolation of cyanidin[47]. One of the first major books covering the characterization of anthocyanins was by Onslow in 1916, The Anthocyanin Pigments of Plants, a later edition of which was published in 1926[48].

Anthocyanins were probably one of the first flavonoids to be analyzed, owing to their visibility to the eye and the ease at which isolation and precipitation can be achieved due to their high concentrations[11]. As the demand for bioactive compounds in dietary supplements, pharmaceuticals and food additives grows, an increased understanding of how to extract and purify anthocyanins from a variety of sources is sought. Similarly, as academic research on anthocyanins continues, the need for efficient and homogenous sample preparation is required. Extraction of anthocyanins from natural sources may be more favorable than laboratory synthesis because of the labile nature of the compound[49]. For natural products, extraction of anthocyanins typically involves some form of solid-liquid extraction, followed by solid phase and/or liquid-liquid extraction to help remove unwanted species, such as phenolic acids, sugars, proteins and other flavonoids.

2.4.1 Structural Changes Due to pH

The anthocyanin structure can exist in many different forms depending on the acidity of the environment to which it is subjected, which may significantly affect the extraction of it from a solid or liquid[50]. Delineation of these forms is shown in Figure 2.4. When the pH of a solution is below 2.5, the anthocyanin is in the flavylium cation state and a red color can be observed. In weakly acidic solutions, where the pH is between 4 and 6, the compound favors a secondary structure, a mixture of anhydrobases and pseudobases. The purple anhydrobases are formed first, and then they decolorize rapidly to form colorless pseudo bases, caused by nucleophilic attack from water on the pyran ring. Above a pH of 8, the pyran ring opens, creating a colorless chalcone structure [51,52]. In vivo, pH levels may not be lower than 4, but complexation of the anthocyanin can be present, which may alter its characteristics, due to stabilization of the anthocyanins by forming “tertiary structures”, through self-association, inter- and intramolecular copigmentation, and metal complex formation[10]. Co-pigmentation has been observed over a wide range of pH conditions[53].

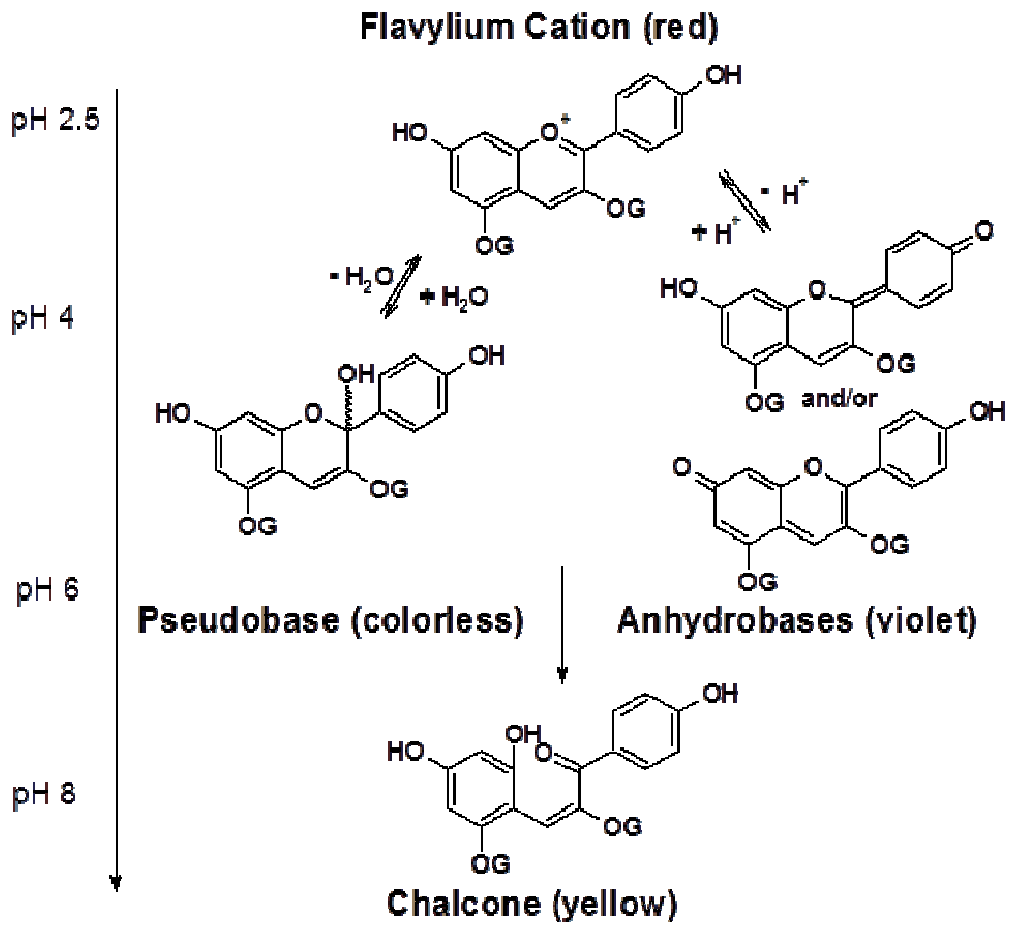

Figure 2.4: Anthocyanins undergo structural changes due to shifts in pH (adapted from Reference [52]).

.

2.4.2 Extract Stability

Although the flavylium cation is stabilized at low pH when using acidified extraction solvents, instability of the anthocyanin may occur in these conditions. Typically, mildly acidified solvents are used in solid-liquid extractions, showing increased extraction efficiency with some acidified solvents[50]. A study on the effects of acids (1% v/v) used in a variety of extract solvents of anthocyanins from red grapes reported hydrolytic degradation of acetylated anthocyanins, resulting in noticeable changes in the anthocyanin profiles detected which may falsely demonstrated improved extraction of some modified anthocyanins[50]. Neutral solvent extraction was demonstrated to be just as efficient in this study. Instability of anthocyanins, especially those with pendant acyl groups, should be considered when mineral acids are used[54,55]. Another study showed no degradation of anthocyanins when extracting with 0.1%

HCl in methanol[56]. In addition, the acidic environment promotes denaturing of the cell tissue membrane, which allows for improved extraction rates of natural products[57]. Therefore, very low amounts of acids (~0.1%) in the extraction solvents may be justifiable in stabilizing the anthocyanin compound in solution without degradation.

2.4.3 Solid-Liquid Extraction

In solid-liquid extraction, the concentration of each compound reaches an equilibrium between the solid and the solvent, which is described by the partition coefficient. The larger the coefficient, the more of the compound is extracted. This equilibrium can be further characterized by a compound's diffusivity, solubility and mass transfer[58]. Optimization of the solid-liquid extraction can be done through manipulation of these attributes. Natural products are typically lyophilized and ground. This reduces the particle size and allows the solute to reach the solvent quicker, increasing the diffusivity[58], as well as improves the homogeneity of the sample. Sonication of the solid-liquid extract can also improve on the extraction efficiency[59]. Increased temperature can improve extraction efficiencies, but some caution must be taken, since high heat can easily degrade the glycosylated and acylated compounds, hydrolyzing the sugar, leaving an anthocyanidin structure[60]. Solubility and diffusivity can be further affected by the solvent selection and the solvent/solid ratio.

2.4.4 Solvent Selection

Due to the large number of hydroxyl groups and the compound's formal charge, the water soluble compound has a fair degree of polarity. The polyphenolic structure adds a measure of hydrophobic character which gives the anthocyanin solubility in organic solvents. The combination of this polar and hydrophobic nature makes aqueous/organic solvent mixtures the ideal solvent. Typically, the organic solvent content varies from 50% to 100% of the mixture. The organic solvent is usually methanol but many other solvents have also been used such as acetone, ethanol or acetonitrile[2,54,59,61]. One study on the extraction of wine grape pomace, which compared the extraction efficiency of ethanol, methanol and water, determined that methanol was 23% more efficient than ethanol and 73% more efficient than water[62]. In a study on isoflavone extraction in methanol, which has a structure closely

related to that of an anthocyanin, evidence suggested that the alcohol group of the solvent provided strong hydrogen bonding with the isoflavone[63].

2.4.5 Solid-Phase and Liquid-Liquid Extraction

Natural products contain numerous other matrix components, such as sugars, phenolic acids, proteins, salts and other flavonoids that will be extracted along with anthocyanins during solid-liquid extraction. Additionally, liquid-liquid extraction and solid phase extraction can be used to further purify an solution containing anthocyanins. For solid phase extraction, due to the polar and hydrophobic functionality of anthocyanins, a number of different column chemistry packings can be used. Many studies use C_{18}, but others have used alumina, insoluble polyvinylpyrrolidone (PVP), Sephadex, Toyopearl, polyamide and ion-exchange resins[2,57,60,64-66]. Oxygen in the peptide of PVP and polyamide packings is believed to form hydrogen-bonds with the phenolic hydroxyl groups of the anthocyanins, which facilitates extraction[57].

Fractionation of red wine has had much attention and can be done using a combination of C_{18} and Toyopearl packing (Figure 2.5)[67]. Acidified wine is loaded onto a pre-conditioned column and washed with an aqueous buffer. This washing elutes phenolic acids, sugars and other polar species. The cartridge is then washed with ethyl acetate which removes non-anthocyanin flavonoids and monomer and oligomer proanthocyanidins. The pigmented species are removed from the cartridges by elution with acidified methanol. This fraction is loaded onto a Toyopearl cartridge (an ion exchange packing material) where the anthocyanins can then be separated from the polymer proanthocyanidins by elution with methanol. One study suggested adding sodium bisulfate (0.1% w/v) before ethyl acetate extraction to help keep the anthocyanins in the aqueous phase[68].

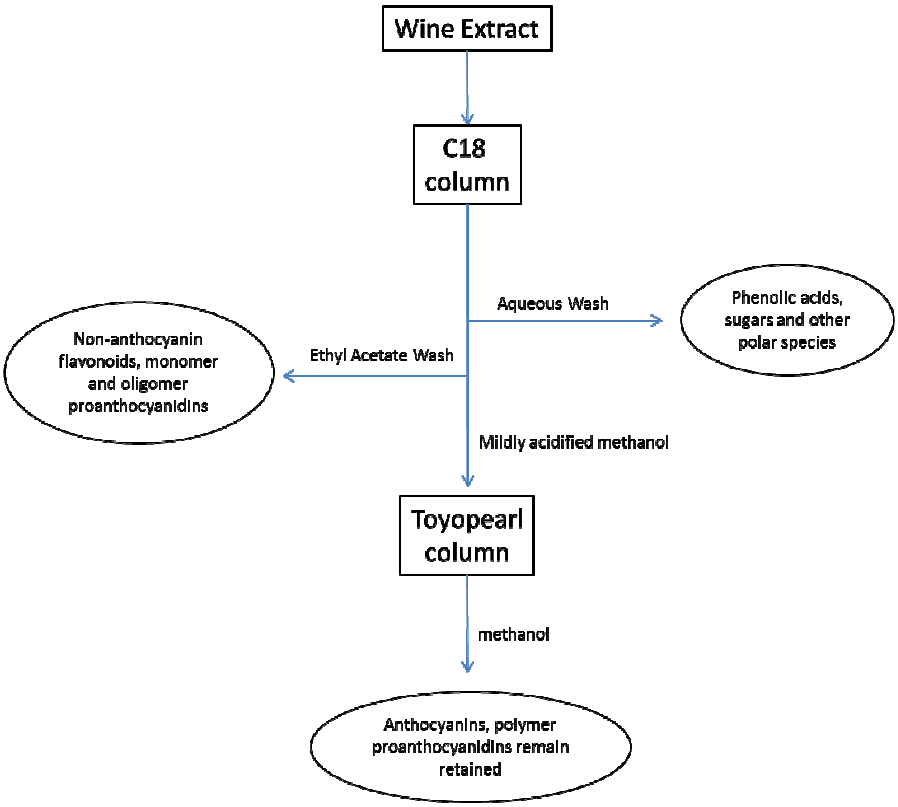

Figure 2.5: Flow diagram for purification of anthocyanins from a wine extract using mixed mode SPE[67].

Non-acylated anthocyanins with adjacent hydroxyl groups (petunidin, cyanidin and delphinidin) can be separated from anthocyanins without adjacent hydroxyl groups (peonidin, malvidin, and pelargonidin) by loading a mixed anthocyanin sample onto a C_{18} SPE cartridge and then eluting with an alkaline borate solution[69]. Anthocyanins with adjacent hydroxyl groups form charged borate complexes. These complexes have a hydrophilic character and are eluted from the column. It is important to note that acylated anthocyanins may have enough hydrophobic character to overcome the hydrophilic character of the charged species and remain retained to the column packing. Also, this solution completely destroys any anthocyanidin species, which adds a unique way (although destructive) to separate anthocyanidins from an anthocyanin solution. Further isolation of individual anthocyanins for identification of unknown species can be performed by paper chromatography or fractionation by collection of the liquid chromatography eluent[57].

2.5 Methods of Analysis

2.5.1 Total Phenolic and Total Anthocyanin Content

The food industry has used two main methods that provide a ballpark measurement for total phenolic content and total anthocyanin content. The total phenolic content can be quantified based on the total reducing capacity determined by the Folin-Ciocalteu method[70]. Quantifiable concentrations for the total phenolic material of a sample can be established colorimetrically using the Folin-Ciocalteu (F-C) reagent method. This simple method involves comparing spectrophotometric absorption values of the sample treated with F-C reagent at 760 nm against a multi-point standard curve using gallic acid or Trolox (a water soluble vitamin E derivative), with the quantification expressed in standard equivalents. This method directly measures the amount of analyte needed to inhibit oxidation of the Folin-Ciocalteu reagent. Therefore, this test measures the total reducing power of a solution, rather than total phenolics. However, considering the sample type is of biological and phenolic nature, it has some basis.

The color change reaction is based on an electron transfer reaction. An alkali solution is required to create ionized phenolates in solution, which provide an electron when mixed with a yellow acidic solution comprised of a polymeric complex of phosphomolybdic and phosphotungstate compounds. The valence of the complex is lowered from +6 to +5, resulting in a blue color. Adequate linearity has been demonstrated and the method has been used extensively in testing biological samples[70].

Furthermore, the total anthocyanin content can be determined using a pH differential method with a spectrophotometer. At a pH of 1.0, anthocyanins are in the colored flavylium cation form; they are in the colorless hemiketal forms at pH 4.5. This method is accurate and specific, even in the presence of other interfering flavonoid compounds[71]. A sample at pH 1.0 and a sample at 4.5 are typically scanned by UV/Vis at 520 nm and 700nm, and then the total anthocyanin content can be determined by this calculation:

$$A = (A_{520} - A_{700})_{pH\ 1.0} - (A_{520} - A_{700})_{pH\ 4.5}$$

Total anthocyanin content (mg/liter) = (A x MW x DF x 1000) / (ε x 1)

where MW is the molecular weight, DF is the dilution factor and ε is the molar absorptivity. The molecular weight and molar absorptivity correspond to the major anthocyanin in the sample. If the molar absorptivity is not available or if the sample composition is unknown, the value for cyanidin-3-glucoside is used, where MW = 449.2 and ε = 26,900.

Although the methods described above are quick and provide some general estimation of anthocyanin content, they do not provide identification of individual anthocyanins. The identity of anthocyanins can be determined by a UV spectrum, but the solutions must be purely of one species. Chromatography can be used to provide adequate separation of the complex mixtures to aid in profiling and for this reason, identification by UV spectra will be discussed later.

2.5.2 Chromatographic Analysis

The profile and composition of anthocyanins for individual plant species is distinctive and is helpful in distinguishing between species. Interest in the genetics of flowers at the beginning of the twentieth century is the reason for the diverse understanding and development of spectral and chromatographic anthocyanin analysis[69]. Early chromatographic separation of anthocyanins first started with simple paper chromatography (PC) and thin layer chromatography (TLC). Separation can be performed (and still is) using Whatman filter paper, an equilibration tank and a suitable mobile phase. One of the most effective mobile phases used consists of butanol:formic acid:water (17:1:2, v/v) [57]. Separated visible spots can then be cut away and further dissolved in an organic solvent for additional analysis.

2.5.2.1 Reverse Phase-High Performance Liquid Chromatography

During the late 1970s and 1980s, reverse phase high performance liquid chromatography (RP-HPLC) became the dominant method for anthocyanin analysis. HPLC combines the ability to separate structurally similar species with multiple styles of detectors, such as UV-Vis and mass spectrometry. When photo-diode array (PDA) detection was developed, HPLC became an even greater tool for the identification of unique anthocyanin species. Now, with the onset of mass spectrometry (MS) detection, it is no wonder that HPLC is a common choice for qualitative, quantitative and preparative applications.

Reverse phase chromatography is usually performed using a column packed with C_{18} bonded to silica. The mobile phase system is consistently binary, with an acidified aqueous phase and either methanol or acetonitrile. It is important for the mobile phase system to have a low pH to keep the anthocyanins in their flavylium cation form, but caution must be exercised with regard to degrading the column at such low pH values[69]. High amounts of acids in the aqueous mobile phase, such as 10% formic acid, have been used to improved peak shape and resolution between closely eluting species[72]. Ion pairing reagents, such as trifluoroacetic acid can be used to modify the mobile phase, which helps to improve peak shape. Some type of sample cleanup, such as described previously, should also be applied due to possible co-elution of other structurally similar flavonoid compounds.

Within a reverse phase chromatographic system, anthocyanin separation is governed by polarity and stereochemistry. The general retention order is primarily affected by the three sections of an anthocyanin: 1) the anthocyanidin, 2) number and nature of the attached glycosides, and 3) any attached acyl groups.

1.) Anthocyanidins differ by their B-ring substituents, a variation of hydroxyl groups and methoxy groups. The most common anthocyanidins would follow this elution series (from shortest to longest retention time): delphinidin, cyanidin, petunidin, pelargonidin, peonidin, malvidin. Hydroxyl groups decrease dwell time, while methoxy groups increase it. Delphinidin has the greatest degree of polarity because it has the most hydroxyl groups, thus eluting first, while malvidin has the most methoxy groups, giving it more hydrophobic character and making it the last to elute from a reverse phase column.

2.) The number of glycosides would follow this elution series (from shortest to longest retention time): 3,7-diglycoside, 3,5-diglycoside, 3-diglycoside; and then the nature of the glycoside would follow this order (from shortest to longest retention time): galactoside, sambubioside, glucoside, arabinoside, rutinoside, xyloside. This is advantageous, since TLC and PC do not separate glycosides very well[11].

3.) Anthocyanins that differ only by their acylation would elute after any non-acylated species and would elute based on polarity. Acylation that differ by their stereochemistry will also affect elution

order. For instance, *cis* isomers of coumaroyl-glycosides will elute earlier than *trans* isomers of coumaroyl-glycosides[72].

HPLC is not without its share of drawbacks. Many methods require a gradient composition scheme which usually requires a fair amount of optimization to successfully separate solutions with multiple species. Also, peak retention times vary from method to method and from column to column. The second and third elution order rules are not strict and analyte elution may be switched depending on pH, solvent type and column chemistry of the system. Finally, the qualitative and quantitative analysis of anthocyanins is still hampered by the limitation of available calibration standards (only a few anthocyanin reference compounds are available commercially and they are expensive)[73].

2.5.2.2 Identification by HPLC-UV/Vis

Once separated, the chromophores of the anthocyanin can be used to differentiate them from other flavonoid classes as well as help identify between individual anthocyanin species. Anthocyanin spectra have been well characterized and unknown species can easily be compared to the literature. Caution should be exercised here due to the effect of the pH and solvent changes on the spectra. For instance Harborne reported that, in general, there is a 15-nm shift toward shorter wavelengths when water is substituted for methanol[69,74]

Characterization by spectral data provides 1) selective identification of anthocyanins from other flavonoid classes, 2) the nature of the anthocyanidin, 3) the position of the attached glycoside, 4) and if the species in question is acylated with an organic acid, the number of organic acids that are attached.

1) The spectral data differentiates an anthocyanin from other flavonoid classes based on a maximum absorbance in the visible region, primarily ~500 nm, also known as $\lambda_{vis,\ max}$ (Figure 2.6).
2) Based on shifts in the $\lambda_{vis,\ max}$ the nature of the anthocyanidin can be differentiated between three classes (which are based on their visible color), cyanidin derivatives (cyanidin/peonidin; magenta), delphinidin derivatives (delphinidin/malvidin/petunidin; purple) and pelargonidin derivatives (pelargonidin; orange). Pelargonidin derivatives have a lower visible $\lambda_{vis,\ max}$ than cyanidin derivatives, which in turn have a lower visible $\lambda_{vis,\ max}$ than the delphinidin derivatives. Pelargonidin exhibits the lowest visible wavelength maxima[69]. Additionally, to differentiate

between individual species in a pigment class, two techniques can be used. The first is the addition of aluminum chloride to the sample solution[74]. The aluminum metal complexes with an anthocyanin with two adjacent hydroxyl substituents and causes a shift in the $\lambda_{vis,\ max}$. With this technique, cyanidin can be differentiated from peonidin, and malvidin can be distinguished from petunidin/delphinidin. The second technique uses the solid phase extraction technique with alkaline borate solution, previously described, in which anthocyanins with adjacent hydroxyl groups are separated from anthocyanins without adjacent hydroxyl groups[69].

3) Anthocyanidins can be differentiated from anthocyanins based on a bathochromic shift of 6-12 nm. The largest shift is observed when the glycosylation is at the 3 position and a lower shift is observed when glycosylation occurs at the 5 position. A shift in the 400-450 nm region is also indicative of glycosylation position. A 3-glycosylated species would have a shoulder in this region, while 3,5-glycosylated species would not[69,74].
4) Lastly, the presence of anthocyanins with acylated organic acids can be determined by the presence of a peak near 310 nm, and is described symbolically as $\lambda_{acyl,\ max}$. Furthermore, the amount of acylated organic acids a compound contains can be determined by the ratio of the $\lambda_{acyl,\ max}$ versus the $\lambda_{vis,\ max.}$ This ratio is proportional to the molar ratio of acyl groups:anthocyanin. When $\lambda_{acyl,\ max}/\lambda_{vis,\ max}$ is around 48-71% then the ratio is 1:1 when it is 83-107% it is 2:1[69]. Higher ratios have also been estimated analytically by this method which is now known as “Harborne’s rule”[75]. Acylation by acetic acid and malonic acids are not detectable by this method, but instead can be determined by alkaline hydrolysis. The ester link which bonds the acyl group is susceptible to hydrolysis in alkaline conditions. When samples are treated with these conditions, any peaks that disappear when observing at 520 nm, would therefore be acylated[74].

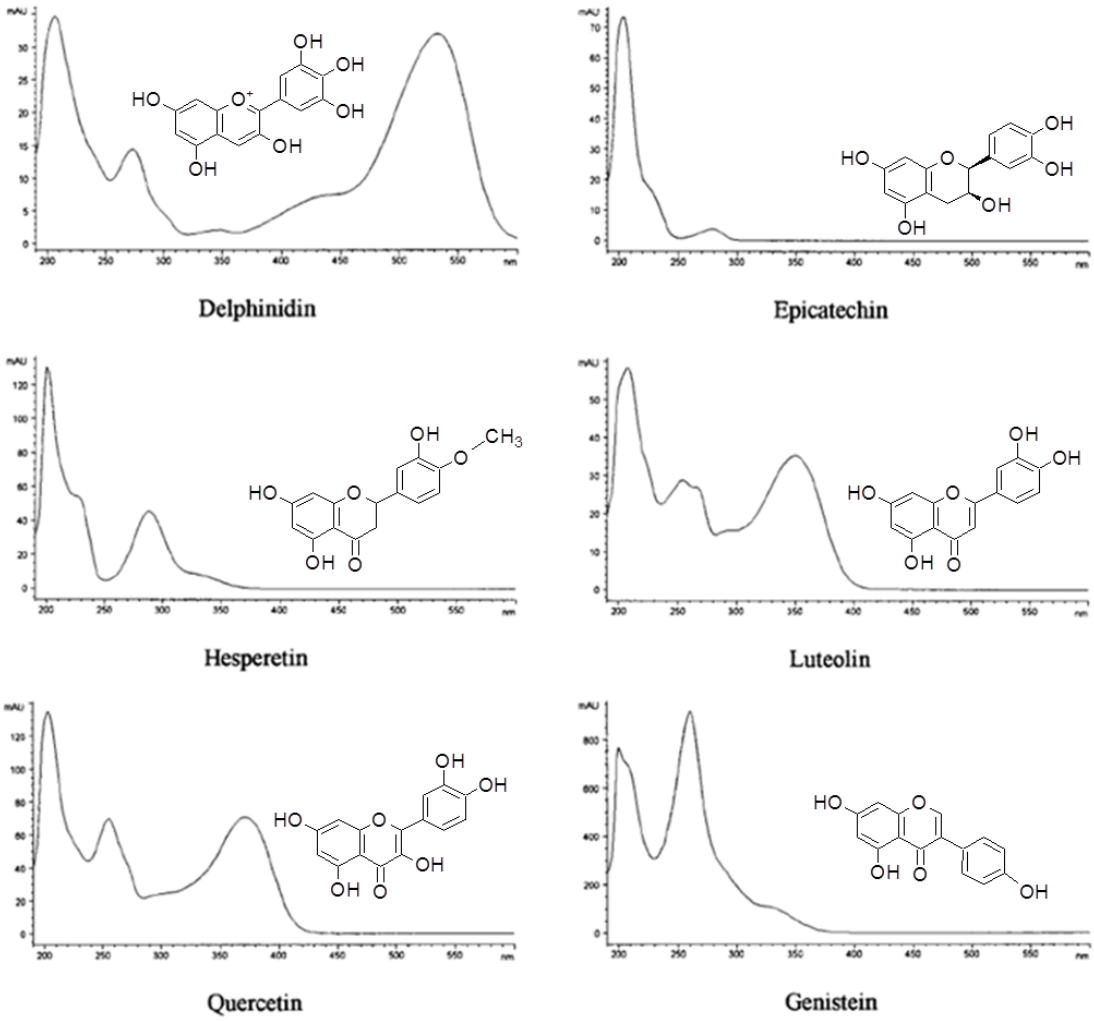

Figure 2.6: UV/Vis spectra of select flavonoids. Figure adapted from reference[76]

2.5.2.3 Quantification by HPLC-UV/Vis

Quantification can be performed by HPLC-UV/Vis, but due to limitation in available standards, there are some drawbacks. Three methods are generally used in practice, 1) quantitation of anthocyanidins after acid hydrolysis, 2) quantitation of all species based on peak area of a single anthocyanin standard (mostly cyanidin-3-glucoside), expressing as standard equivalents, and 3) quantitation based on multi-standards of similar nature, correcting with a molecular weight factor for those that differ[9].

Hydrolysis of O-glycosides can be achieved with a strong acid, such as hydrochloric acid, and elevated temperature. Quantitation can then be assessed against an anthocyanidin standard. All of the

naturally-occurring anthocyanidins can be acquired commercially. This technique is often done first in screening of anthocyanins in plants with unknown profiles[11]. In contrast, acid hydrolysis does not affect the C-C bond of C-glycosides, thus providing an additional characterization tool[10].

2.5.3 Analysis by HPLC-ESI-MS^n

2.5.3.1 Ionization

Mass spectrometry offers structural identification in complement to HPLC-UV/Vis. Many types of ionization are used in the field of mass spectrometry. One type, electrospray ionization (ESI), is useful because it is soft enough to avoid fragmentation of the molecular ion, providing the user with the molecular mass of the analyte. In LC-ESI-MS, the eluent from the LC is directed into a capillary upon which a charge is applied. The charged liquid leaves the capillary at a tip, which nebulizes the liquid and disperses it into a fine aerosol. The solvent evaporates from the charged droplets, making them smaller and smaller, eventually delivering the charged analyte to the gas phase. At this point the ion can enter the mass spectrometer (Figure 2.7). Electrospray uses high voltages and the source is operated at atmospheric pressure.

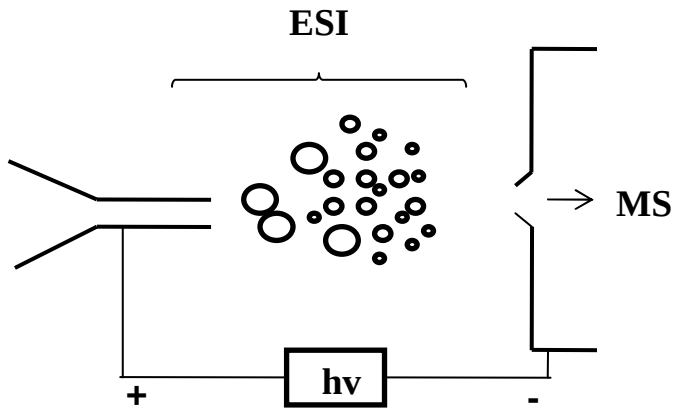

Figure 2.7: Diagram of electrospray ionization source.

With the development of “soft ionization” techniques such as electrospray ionization (ESI), the ability to analyze anthocyanins using mass spectrometry has increased. Anthocyanins are polar, non-volatile and thermally labile, which makes them unsuitable for ionization techniques that require analytes to be in the gas phase; electron impact (EI) and chemical ionization (CI) are unsuitable[77]. With ESI,

the anthocyanin compound can be ionized and observed with the glycoside and any acylation still attached, although in-source cleavage of the weak glycoside bond is often reported[78,79].

The formal positive charge of the anthocyanin makes it a great candidate for positive ionization mode ESI, in which $[M]^+$ ions are observed. Ionization in the negative mode can also be achieved, creating a deprotonated ion $[M-H]^-$. Negative mode offers less sensitivity and peak intensity, so it is only used in specific cases[80], such as selective ionization of anthocyanins with carboxylic acylation, anthocyanin-flavonoid adducts and differentiation of anthocyanins from isomeric signals generated from other interfering flavonoid species[2].

The composition of the solvent being introduced must be considered due to the direct influence it has on the ionization efficiencies of analytes. HPLC methods with phosphate buffers should be avoided at all costs, due to increased background, signal suppression, and rapid contamination of the ion source resulting in decreased sensitivity and stability. RP-HPLC is often facilitated with high acid content [72] and this can be detrimental to ionization, especially when TFA is used. Higher signal intensities are observed when solvent composition is higher in organic content, versus aqueous content due to the ease of evaporation[81].

2.5.3.2 Collision Induced Dissociation

Collision induced dissociation (CID) can be achieved through the use of ion-trap (IT) and triple quadrupole (QqQ) instruments. These instruments select an ion of a certain mass-to-charge (m/z) and allow it to be fragmented. The ions within the cell are accelerated by an electric potential and fragmentation is induced by collision with a neutral gas. Argon and helium are commonly used.

Controlled fragmentation of the anthocyanin adds an extra degree of species confirmation by identifying the nature, number and order of attached sugars, acyl groups and anthocyanidins. In some rough estimates, the position of the sugar and acylated moieties can be determined.

The *O*-glycosidic bond is fairly weak and is easily cleaved by low energy CID, with neutral loss of the sugar. Cleavage of the bond is accompanied by transfer of an O-linked hydrogen atom from the sugar unit to the anthocyanidin ion, returning a fragment ion equal to the mass of the anthocyanidin, and which is always singly-charged[82]. The nature of the glycoside can be determined by monitoring the

mass of the neutral loss (Figure 2.8), although differentiation of diasteroisomeric sugars is a known problem[78]. In this case, reverse phase elution order is needed for identification.

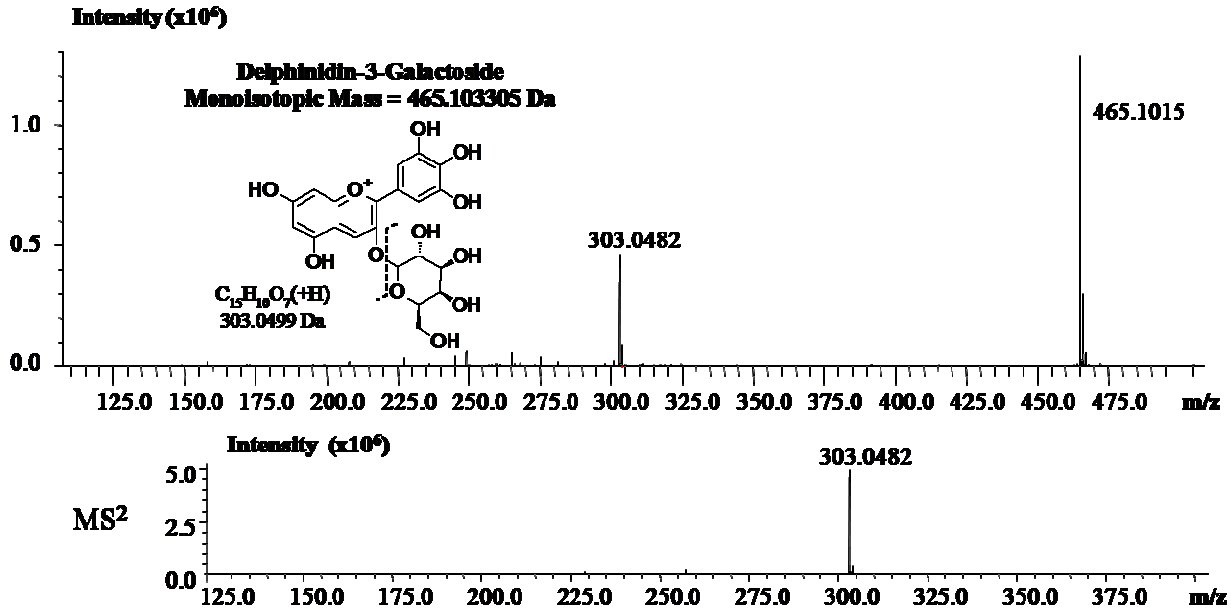

Figure 2.8: In-source fragmentation and CID fragmentation of an anthocyanin with an O-glycoside bond.

The *C*-glycosidic bond is much stronger and will not cleave easily. When fragmentation of this compound is attempted, the signals observed are of fragment ions generated from cleavage of the internal C-C bonds within the sugar moiety and not at the glycosidic bond or from the anthocyanidin[82]. Cleavage of the ester bond linking the acylated moiety is not typically observed in low energy CID, although cleavage of unstable malonoyl acylation has been reported[61]. A rough estimation of the position of the sugar and acylated moieties can be determined based on the fragment signals. For instance, this can be seen in fragmentation of species that have the same acylated moiety attached to the sugars at the 3 and 5 positions versus a species with two of the same acylation attached to one sugar[78].

2.5.3.3 Higher Order Tandem Mass Spectrometry (MS^n (n>3))

Tandem MS has been used extensively for identification of anthocyanins in many plant species. In one thorough summary, Wu and Prior used this technique to identify and characterize many common

fruits and berries[9]. Only a few studies report fragment signals beyond MS^3, the stages in which the anthocyanidin is fragmented[72,79,82,83] The flavylium cation has been shown to be very stable and does not possess a site of facile rupture. The ability to fragment the aglycone may further improve anthocyanin identification and characterization. Often times, anthocyanin species can be isomers of other flavonoids and in complex mixtures, they cannot be identified without authentic standards and a separation technique. These isomeric signals could be differentiated based on unique diagnostic fragmentation patterns without the use of commercial standards or lengthy sample cleanup procedures.

Anthocyanin fragmentation can generally be classified into two categories, 1) cross-ring cleavage (CRC) of the C-ring, and 2) ring-opening followed by subsequent loss of small neutral molecules, such as CO, C_2H_2O and H_2O (Figure 2.9). Cross-ring cleavage involves breaking of two bonds of the C-ring. The A-type fragments are the same for most common anthocyanidin species, but the B-type fragments differ for each anthocyanidin species based on the substitution of the B ring[82]. These diagnostic B-type fragment ions can aid in confirming the identity of anthocyanidins. The nomenclature described by Ma et al[84] for labeling fragment ions is commonly used. The labels $^{i,j}A^+$ and $^{i,j}B^+$ correspond to the fragment ions that contain either the A or B ring and were formed by cleavage of the i^{th} and j^{th} bonds of the C-ring (Figure 2.9).

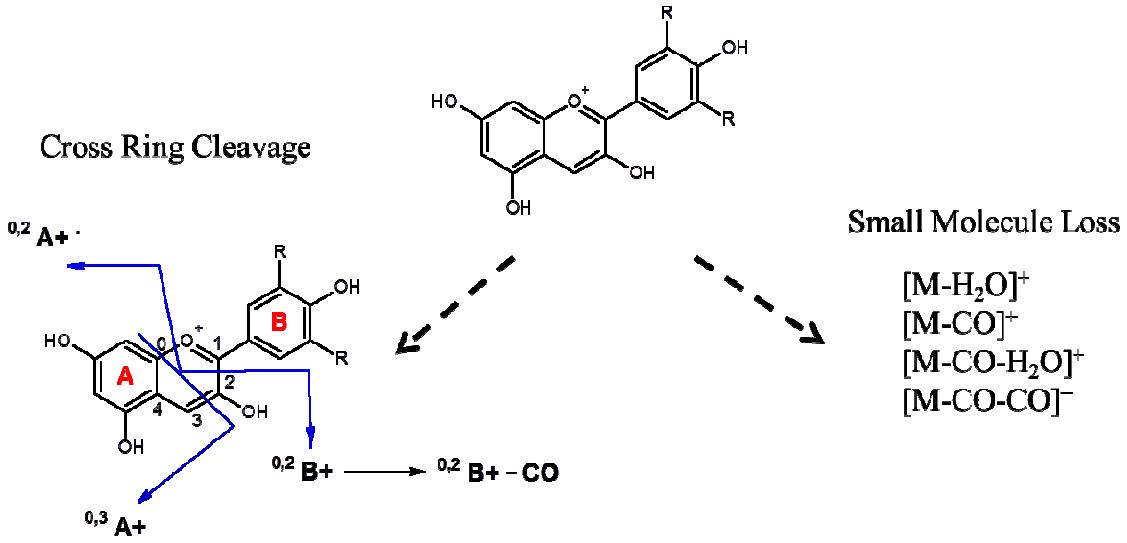

Figure 2.9: Fragmentation schemes of the anthocyanidin by CID. Figure based from [82].

Surprisingly, there only a few literature references regarding the mass signals and proposed structures for CRC and small molecule loss fragments for the naturally occurring anthocyanidins. One significant study was done with high energy CID by using electrospray ionization and with orthogonal acceleration—time-of-flight (oa-TOF) tandem mass spectrometry[82]. Another study involved anthocyanidin fragmentation from the berries of a myrtle shrub using ESI-IT-MS[79]. In contrast, numerous fragmentation studies have been performed on other flavonoids such as flavones, flavonols, flavanone[84,85] and proanthocyanidins[86,87]. Vuckis and Guttman provide a nice review of structural characterization of flavanone glycosides[88].

2.5.3.4 High Mass Resolution by Time-of-Flight Mass Spectrometry

In low resolution instruments, an observed ion may be fit by multiple elemental formula possibilities, particularly with organic compounds, which only contain carbon, hydrogen and oxygen, as in the case of anthocyanins. Increasing the resolution with higher mass accuracy eliminates erroneous choices and can provide the user with the exact elemental formula. Determining the structures from the signals of the fragment pathways can be improved upon by using high mass resolution. By hyphenating a CID-capable instrument with time-of-flight (TOF), high mass resolution can be achieved. In this class of detection, the ions are accelerated by an electric field towards a detector at the end of a flight tube. All of the ions have the same kinetic energy, but will travel at different speeds within the flight tube due to differences in their mass and charge. Therefore, their mass/charge ratio (m/z) can be determined based on their flight time with great accuracy.

Due to the relatively short amount of time that this hyphenated technique has been available, to the author's knowledge, there is only one study in which the mass-to-charge of parent ions for anthocyanins were reported with high mass accuracy[89]. Two other studies have reported values for non-anthocyanin flavonoids. One investigated fragmentation of an isoflavone, where MS^7 was achieved using ESI-IT-TOF-MS[90]. The other was a study of kampferol fragmentation[91].

2.6 Conclusion

There have been volumes of research and study concerning anthocyanin species, and for good reason. The colors offered by these compounds have attracted our attention before interest in their chemical character developed. From genetic diversity and modification to dietary antioxidant intake, continued analytical research is still needed to unfold the intricacies of this ever-present class of polyphenolics. Further development of methods based on LC-MS is warranted, as it is a technique which may be able to handle the sample complexity.

CHAPTER 3

GENERAL METHOD FOR EXTRACTION OF BLUEBERRY ANTHOCYANINS AND IDENTIFICATION USING HIGH PERFORMANCE LIQUID CHROMATOGRAPHY-ELECTROSPRAY IONIZATION-ION TRAP-TIME OF FLIGHT MASS SPECTROMETRY

3.1 Abstract

A systematic approach for optimizing the extraction and identification of anthocyanins from blueberries was explored using HPLC-UV and HPLC-ESI-IT-TOF-MS. Sample homogenization effects, extraction solvent selection, type of acid and amount used in extraction solvent were investigated. A mixture of methanol:water:trifluoroacetic acid (70:30:1, v:v:v) was found to be the best solvent system for blueberry anthocyanin extraction. Differences in total anthocyanin content due to commercial blueberry processing were explored as an application using the optimized extraction technique and HPLC-UV analysis. A methodical system for anthocyanin identification by HPLC-ESI-IT-TOF-MS without the use of standards was also reviewed and applied. Consideration was given to elution order by chromatographic separation with selective detection at 520 nm, high mass accuracy *m/z* values, tandem MS fragmentation, and previously published literature. Overall, 25 anthocyanins from a wild type highbush blueberry were identified and reported.

3.2 Introduction

Anthocyanins represent a unique subset of phenolic secondary metabolites found in plant tissues. They are one of many compound classes that fall under the flavonoid group, possessing a bi-phenolic structure. The core structure of the anthocyanin, a flavylium cation, may be described as a C_6-C_3-C_6 skeleton, having a phenolic ring fused to a pyran with an additional phenolic ring connected at the 2 position of the pyran. This structure can be glycosylated, and the glycosides may be acylated, giving rise to a plethora of potential structural and functional variants [9]. The aglycone flavylium cation is referred to

as an anthocyanidin. Anthocyanins differ from the rest of the flavonoid group by a formal positive charge found on the oxygen of the pyran ring [3] (Figure 3.1, Table 3.1). Up to 600 different species have been reported. These compounds are known to be responsible for the purple, blue and red colors found in many plant tissues [92] and are believed to be dissolved in the cell sap found in the vacuole of a plant's epidermis cells [12,57].

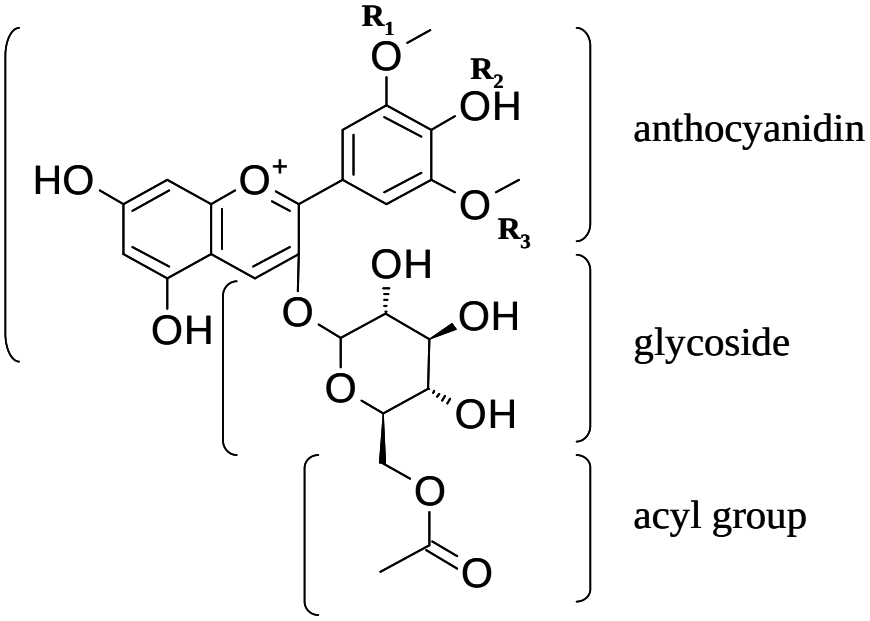

Figure 3.1: The skeletal structure of an acylated anthocyanin (malvidin-3-(6''-acetoyl)glucoside; monoisotopic mass = 535.14517 amu). R1, R2, and R3 designated for reference to Table 3.1.

Table 3.1:The common anthocyanidins and substituents found in natural anthocyanins.

Anthocyanidin	R_1	R_2	R_3	Glycoside	Acylation
Delphinidin	OH	OH	OH	Galactose Sambubiose Glucose Arabinose Rutinose Xylose	Acetoyl Malonoyl Coumaroyl
Cyanidin	OH	OH	H		
Petunidin	OMe	OH	OH		
Pelargonidin	H	OH	H		
Peonidin	OMe	OH	H		
Malividin	OMe	OH	OMe		

It was noted as early as 1914 that an individual anthocyanin species can result in many different colors [47]. The color of anthocyanins depends on their structure, the acidity of the environment, and the presence of metals. When the pH of a solution is below 2.5, the anthocyanin is in the flavylium cation state, the primary structure of the compound, and a red color can be observed. In weakly acidic solutions, where the pH is between 4 and 6, the compound favors a secondary structure, a mixture of anhydrobases and pseudobases. The purple anhydrobases are formed first, and then they decolorize rapidly to form colorless pseudo bases, caused by nucleophilic attack from water on the pyran ring. Above a pH of 8, the pyran ring opens, creating a colorless chalcone structure (Figure 3.2) [51,52]. In vivo, pH levels may not be lower than 4, but color remains due to stabilization of the anthocyanins by forming “tertiary structures”, through self-association, inter- and intramolecular copigmentation, and metal complex formation [1]. Co-pigmentation has been observed over a wide range of pH [53].

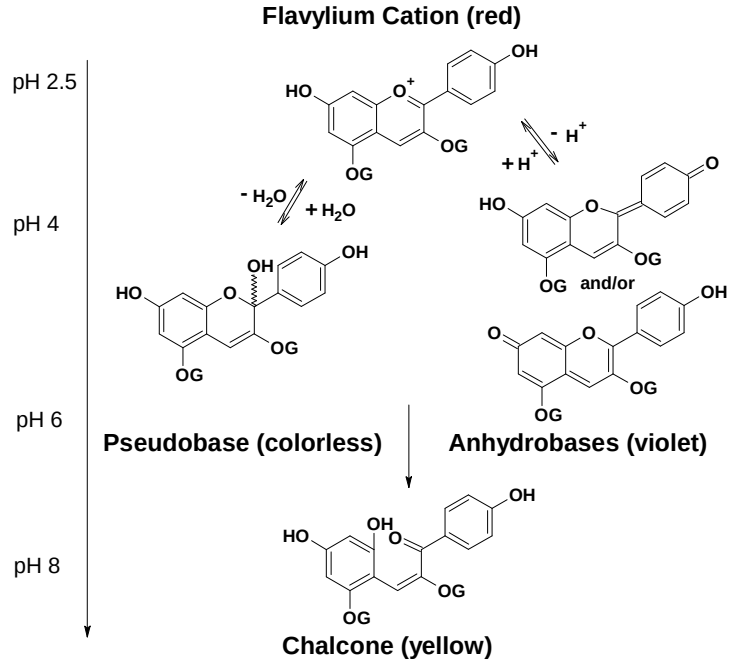

Figure 3.2: Variation in the anthocyanin structure and pigmentation with changes in pH of a solution (adapted from Reference [52]). G = glycoside

Numerous studies [24-28] have shown that anthocyanins are powerful antioxidants. Antioxidants protect against oxidative damage from radical reactive species by various mechanisms that ultimately

result in the neutralization of free radicals. Owing to the anthocyanin's positive charge and aromatic hydroxyl groups, these compounds can easily donate protons to the free radicals. This protects cells from oxidative damage that leads to aging and various diseases [27]. Moreover, epidemiological studies have revealed that the antioxidant activity presented by fruit consumption is positively correlated with reduced mortality by cardiovascular disease and some types of cancer [28]. Further studies in this area support the need for optimal methods to extract, isolate, and identify anthocyanins from natural products.

Extraction of anthocyanins may be more favorable than synthesis because of the labile nature of the compound [49]. Anthocyanins are reactive compounds and sensitive to pH changes [49]. High heat can easily degrade the glycosylated and acylated compounds, hydrolyzing the sugar, leaving an anthocyanidin structure [60]. They are normally extracted with acidified solvents under mild conditions. The extraction solvents consist of polar organic solvents, water and acids [2]. The organic solvent is usually methanol but many other solvents have also been used such as acetone [54], ethanol [59] or acetonitrile [61]. The organic solvent content varies from 50% to 100% of the mixture while the acid content is usually less than 7%. Strong acids (trifluoroacetic acid, hydrochloric acid) or weaker acids (formic acid, acetic acid) can be employed. A consideration should be given when mineral acids are used because of the possible loss of pendant acyl groups [54]. A systematic study for optimizing blueberry anthocyanin extraction appears to be lacking, despite a large number of publications on the subject. In one study, limited to only the use of methanol and water as the extraction solvent, Downey *et al.* reported optimized conditions for a stable extraction of anthocyanins and flavanols in grape skins [55]. For analytical purposes, extraction methods should be thoroughly checked for a specific case [25].

Several papers have been published on analytical studies of blueberries. Referring to the research of Ballinger *et al*. [93], 14 anthocyanins were first identified in the ripe blueberries of highbush variety in 1970. Later, this group confirmed the presence of 15 anythocyanins, which were the combination of five aglycone anthocyanidins (cyanidin, delphinidin, malvidin, peonidin, petunidin) with three sugars (glucose, galactose, arabinose) [94]. Several years later, the groups of Vershkovski [95] and Sapers [96] separated 16 anthocyanins from highbush blueberry extracts. Since then, there have been many more anthocyanins detected in blueberries. Wu and Prior recently found up to 27

anthocyanins in lowbush blueberry extracts and five of them were reported to be isolated for the first time [61].

The qualitative and quantitative analysis of anthocyanins in blueberries has been extensively studied but is still hampered by the limitation of available calibration standards (only a few anthocyanin reference compounds are available commercially) [73]. Classical chromatographic methods, such as planar chromatography (paper chromatography and thin layer chromatography) and open column chromatography still play a role in analytical analysis of anthocyanins, but HPLC is now the standard method for both analytical and preparative applications [97]. HPLC coupled with UV-Vis, photodiode array (PDA), or mass spectrometer detectors (MS) [97,98] are commonly used. Anthocyanin identification and characterization may be enhanced by high mass resolution and multiple fragmentation as demonstrated by a similar study on isoflavones, where fragmentation up to MS^7 was achieved using electrospray ionization-ion trap-time of flight-mass spectrometry (ESI-IT-TOF-MS) [90]. High mass accurate measurements of anthocyanins appear to be limited in the literature. For further structure elucidation of the large and complex anthocyanin compounds, nuclear magnetic resonance (NMR) is also a powerful instrument to approach, but is limited by the need to isolate milligram quantities of pure material [1].

The aim of this study was to optimize the extraction conditions for anthocyanins in blueberries by comparing the extraction efficiencies of solvent and acid types used in conjunction with reversed phase chromatography and UV-Vis detection and to describe a system which confirms the identity of anthocyanin species without the use of external standards. Optimal instrumental conditions for qualitative and quantitative analysis using HPLC-UV and HPLC-MS were given considerable attention. Separation and identification of anthocyanins using HPLC with electrospray ionization-mass spectrometry (ESI-MS) was performed by correlating results from published data with high accuracy full scan and tandem mass spectrometry measurements using an ESI-IT-TOF-MS instrument.

3.3 Materials and Methods

3.3.1 Chemicals

Isopropanol, propanol, tetrahydrofuran (THF), HPLC-grade acetonitrile and hydrochloric acid (HCl) were purchased from Merck (Darmstadt, Germany). Methanol, acetone, acetic acid and water were obtained from Mallinckrodt Baker, Inc. (Phillipsburg, NJ, USA). Trifluoroacetic acid (TFA) and ethanol were purchased from Sigma-Aldrich (St. Louis, MO, USA) and formic acid was purchased from Fluka (Stainheim, Germany). All solvents and water used for HPLC-UV measurements were of HPLC grade. LC-MS grade acetonitrile and water were purchased from Burdick and Jackson (Muskegon, MI, USA) and used exclusively in the mobile phases used for HPLC-ESI-IT-TOF-MS measurements.

3.3.2 Blueberry Sample Preparation

Southern highbush blueberries (*Vaccinium darrowii x Vaccinium corymbosum*) were bought from a local market. A drying house within the US also provided pre- and post-processed blueberries of wild and cultivated origins. Processed blueberries were soaked in a sugar solution and then dried by heating to remove moisture using a proprietary procedure. All blueberry samples were kept in a freezer at -16 ºC until prepared for analysis. A variety of homogenization procedures were tested, including smashing samples with a mortar and pestle, grinding samples in a Braun KSM 2B aromatic coffee grinder (Proctor and Gamble, South Boston, MA, USA), and lyophilization with a FreeZone 6 lyophilizer (Labconco, Kansas City, MO, USA). Based on these results, a set of optimal conditions was elucidated for treating the samples prior to extraction for additional experimental sets.

3.3.3 Extraction Solvent Preparation

The effect of solvent variation on total anthocyanin extraction was observed through the variation of three parameters: type of organic solvent used; type of acid used; and amount of acid used. The extraction solvent used for anthocyanin extraction was, in general, a mixture of organic solvent:water:acid (70:30:1, v:v:v). The selected organic solvents used for evaluation were methanol, ethanol, propanol, isopropanol, acetonitrile, and acetone. The selected acids used for evaluation were TFA, HCl, formic acid, and acetic acid. To study the effects of acid concentration, an extraction solvent of methanol:water

(70:30, v:v), was prepared with varying amounts of TFA. The selected amounts of acids used were 0, 0.1, 0.5, 0.7, 1, 3, 5, and 10 volume parts.

3.3.4 Sample Extraction

Blueberry anthocyanins were extracted by adding 100 mg of fresh blueberries, which had been lyophilized and ground, and 1 mL of extraction solvent into a 1.5-mL microcentrifuge tube. The sample was vortexed at high speed and left undisturbed for 1 hour. The sample was sonicated for 20 minutes and then centrifuged at 2000 x g for 20 minutes using a micro-centrifuge (Clover Labs, Whitehouse, OH, USA). The supernatant was filtered through a 13 mm syringe filter with a 0.2 µm PTFE membrane (VWR International, West Chester, PA, USA) into an HPLC vial.

3.3.5 Instrumentation

Total anthocyanin content was determined using two different methods on a stand-alone Finnigan SpectraSYSTEM®-HPLC (Thermo-Fisher Scientific, Inc., Waltham, MA, USA) comprised of a P2000 solvent delivery system, an AS3000 autosampler and a UV6000LP diode array detector. "Method 1" utilized a ODS Hypersil column (200 mm x 4.6 mm, 5 µm; Agilent Technologies, Santa Clara, CA, USA). Following the methods described by Price *et al*. [99], anthocyanin separation was achieved using a gradient profile with an aqueous solvent mixture of Water:THF:TFA (98:2:0.1, v:v:v) as solvent A, and acetonitrile as solvent B. The elution scheme was modified due to differences in instrumentation, column selection and to improve on peak resolution: isocratic 5% B, 0-2 min; linear gradient from 2% B to 25% B, 2-8 min; to 35% B, 8-18 min; to 50 % B, 18-23 min; to 90% B, 23-28 min; isocratic 90% B, 28-38 min; linear gradient to 5% B, 38-39 min; post-time re-equilibration14 min before next injection; flow rate 1 ml/min; injection volume 5 µL. "Method 2" followed work done by Kahkonen [100], and used a Zorbax SB-C18 column (150 mm x 4.6 mm, 3.5 µm, Agilent Technologies, Santa Clara, CA, USA). Anthocyanin separation was achieved by gradient elution using 10% formic acid in water as solvent A, and acetonitrile as solvent B. The elution scheme was modified due to differences in instrumentation, column selection and to improve on peak resolution: isocratic 2% B, 0-5 min; linear gradient from 10% B to 25% B, 5-20 min; isocratic 10% B, 20-40 min; gradient to 30% B, 40-60 min; to 95 % B, 60-61 min; isocratic elution

95% B, 61-71 min; linear gradient to 2% B, 71-72 min; post-time re-equilibration 10 min before next injection; flow rate 1 ml/min; injection volume 5 µL.

Separately, anthocyanin identification was performed by HPLC-ESI-IT-TOF-MS on a LCMS-IT-TOF (Shimadzu Scientific Instruments, Kyoto, Japan), equipped with a Prominence HPLC system (LC-20AD pumping system, a SIL-20AHT autosampler, SPD-M20A diode array detector; Shimadzu). On this system, a Gemini C18 column (100 mm x 2.0 mm, 3µm; Phenomenex, Torrance, CA, USA) and a Gemini C18 guard column (4.0 x 2.0 mm, 3µm; Phenomenex, Torrance, CA, USA) were used to chromatographically separate anthocyanin species using 1.0% formic acid in water as solvent A and acetonitrile as solvent B. The elution scheme was: linear gradient from 5% B to 10% B, 0-5 min; isocratic elution 10% B, 5-30 min; linear gradient from 10% B to 13.5% B, 30-75 min; linear gradient from 13.5% B to 25% B, 75-90 min. The heat block and curved desolvation line (CDL) were maintained at 250 ℃. Nitrogen was used as the nebulizing gas and drying gas, set at 1.5 L/min and 10 L/min, respectively. The ESI source voltage was set at 4.5kV and the detector voltage was set at 1.62 V. This method was denoted “Method 3”. Shimadzu’s *LCMS Solutions* software was employed for data analysis. The *Formula Predictor* function of *LCMS Solutions* was utilized in identification and confirmation of unknown signals. Ionization was performed using a conventional ESI source in the positive ionization mode. The instrument was calibrated to < 5 ppm error in mass accuracy with an external standard of sodium TFA solution (sodium hydrate, 0.1 g/L; triflouracetic acid, 0.25 mL/L).

3.4 Results and Discussion

Optimizing extraction conditions for HPLC analysis enhances the ability to quantitate and identify anthocyanins in plant materials. Increased response and sensitivity aid in confirming identification and may augment the detection of rare anthocyanins present in trace amounts. Conditions that enhance UV response may also offer insight into which solvents work best with varying plant matrices. The extraction solvent plays a part in the transfer of anthocyanins from the plant, to an analyzable liquid, one that may provide a suitable environment to the otherwise labile species.

3.4.1 Total Anthocyanin Content

The total anthocyanin content can be approximated by the total summation of peak areas observed at 520 nm during HPLC-UV analysis. At this wavelength, anthocyanins can be selectively detected in the presence of other flavanoids, which have maximum absorbance at characteristic wavelengths other than 520 nm, such as flavones (260 nm), flavanols (278 nm), flavanones (278 nm), proanthocyanidins (278 nm), and flavonols (370 nm) [73,101]. Monitoring the total peak area offers a convenient way to measure the efficiency of the extraction technique. Solid phase extraction (SPE) techniques are commonly employed for flavanoid analysis, but due to the scope of this study's focus on anthocyanin response, they were not utilized. Preliminary results did not show a noticeable difference between chromatographic profiles at 520 nm for SPE extracted samples compared to. non-SPE extracted samples (data not shown), although it is conceivable that a preparative method to purify anthocyanins for further use could benefit from SPE preconcentration and clean-up. For the purpose of this work, an HPLC instrument equipped with a PDA detector provide sufficient means to avoid UV signal interference without extra cleanup steps.

Homogenization of the samples followed lyophilization, grinding the dried blueberries to provide a powder-like substance. Lyophilization was shown not to deleteriously affect the total anthocyanin content, whereas reproducibility of results was shown to increase dramatically between unprepared blueberries and their homogenized counterparts (Figure 3.3). These results may be explained by the fluctuation and variability of anthocyanin concentrations between individual blueberries and supports the need for bulk sample homogenization. Any determination of changes in total anthocyanin content or quantitative applications requires good reproducibility.

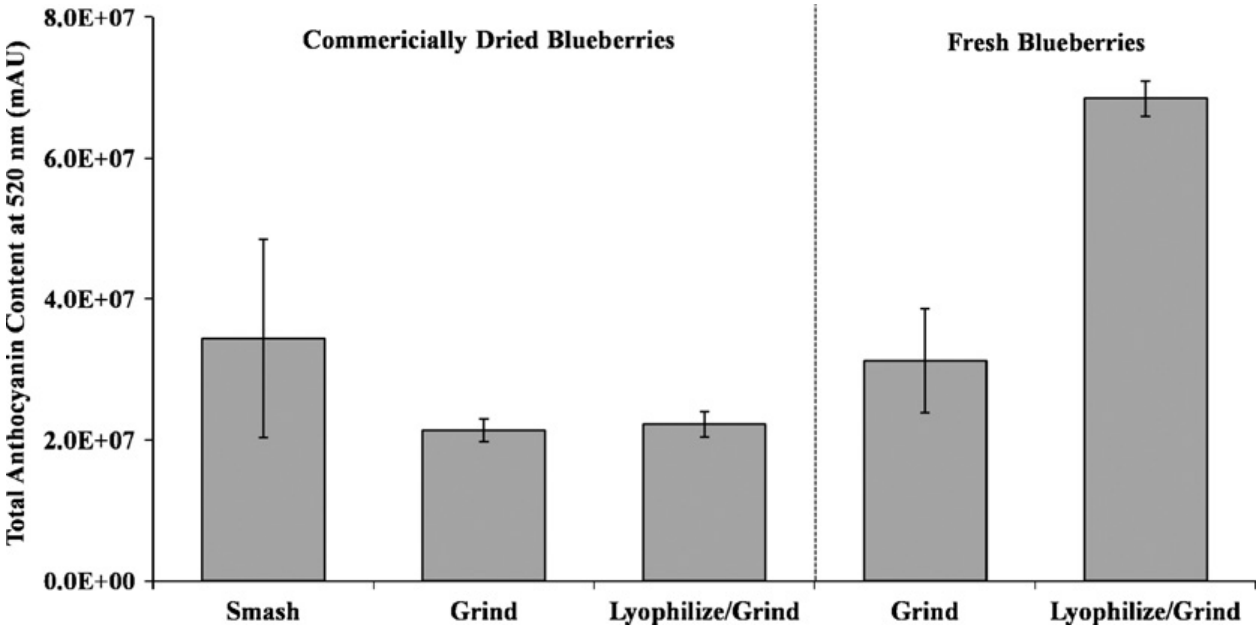

Figure 3.3: Effects of homogenization techniques on commercially dried blueberries and fresh blueberries (Method 1). n=5.

In liquid extractions, solvent selection is vitally important for achieving the highest efficiency. The anthocyanin, with its polyphenolic structure, can be extracted by an organic solvent. Furthermore, structures contain multiple hydroxyl groups and a formal charge of the oxygen on the pyran ring, providing a polar characteristic, suggesting a mixture of organic solvent and water would provide maximum extraction efficiency. In addition, a slightly acidic environment provides a favorable environment for the flavylium cation to be solubilized.

A mixture of organic solvent:water:acid (70:30:1, v:v:v) was used for a screening of varying types of organic solvents and acids. It was determined that the combination of methanol and TFA with water provided the greatest summed peak area at 520 nm (Figure 3.4). Respectively, ethanol, acetone and methanol were the best solvents overall when considering results between all the acids (Figure 3.4). In a study of isoflavone extraction in methanol by Sandoval *et al*., evidence suggested that the alcohol provides strong hydrogen bonding between alcoholic solvents and the isoflavone, whose structure is very closely related to the anthocyanins [63]. Consistent with this assessment, acetonitrile showed the lowest extraction response.

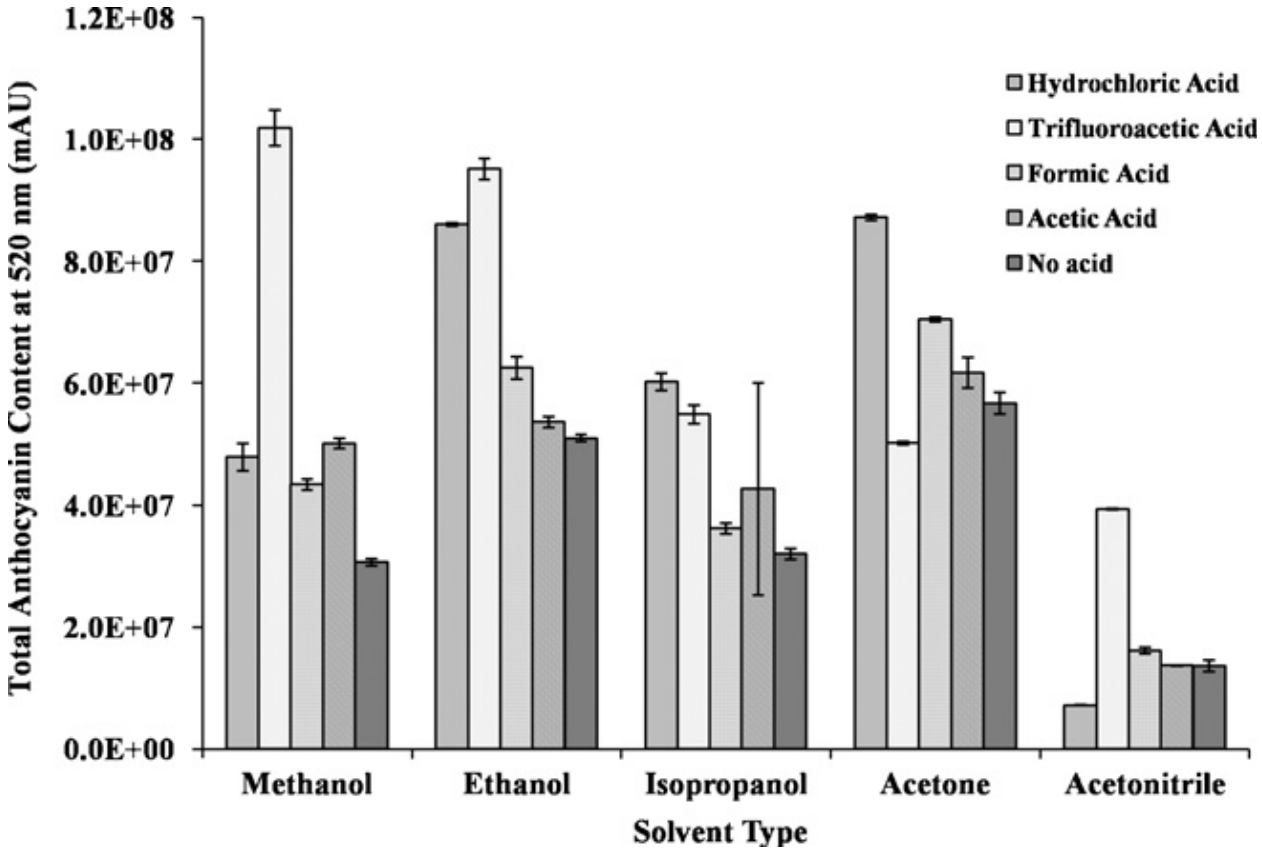

Figure 3.4: Blueberry samples were extracted with different combinations of organic solvent:water:acid (70:30:1, v/v/v) (Method 1). *n*=3.

In terms of acid use, TFA and HCl resulted in the greatest absorption of blueberries (Figure 3.4). Formic acid and acetic acid had a minimal increase in absorption compared to solutions without acid

added. As mentioned in previous literature, HCl and other strong acids can induce degradation via hydrolysis, obscuring a realistic profile of anthocyanins present in samples. TFA acts as a strong ion pairing agent with anthocyanins, providing better extraction efficiency and chromatographic resolution, although it can hinder mass spectrometry signals for the same reason [60].

The pH of the extraction solvent is a factor in providing a suitable environment for the anthocyanin. Based on the results described above, TFA was chosen to be the optimal acid for extraction. The effect of TFA concentration was then studied. The only significant increase in total anthocyanin content was seen between samples extracted with and without acid (Figure 3.5). Changes in individual peak responses and appearance of additional peaks were observed as the acid concentration was increased, but not enough to significantly change the total peak area values measured.

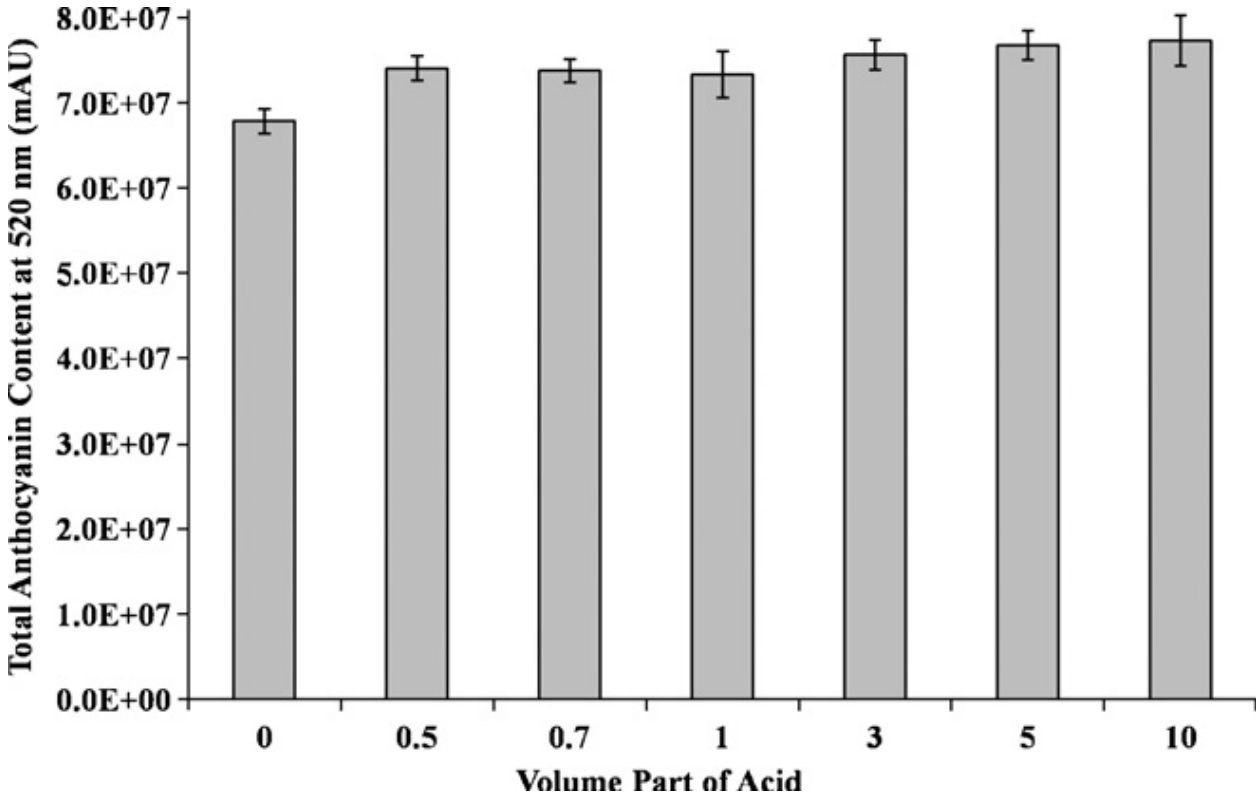

Figure 3.5: The effects of varying the TFA concentration in an extract mixture of methanol:water (70:30, v/v) on total anthocyanin content of blueberries (Method 1). *n*=5.

A number of applications can be explored by using the optimized extraction conditions determined from the latter discussion. One study conducted was on differing types of processed blueberries, which were analyzed for total anthocyanin content using separation Method 2. Three sets of pre- and post-processed highbush blueberries were provided by a drying house within the US. The first set was of a cultivated batch which underwent the sweetening and drying process. The second set was of the same cultivated batch and underwent only the drying process. The final set was of a wild highbush blueberry batch that underwent the same sweetening and drying process. There was a significant decrease in total anthocyanin content between the pre- and post-processed samples (Figure 3.6). The sweetened berries had slightly lower anthocyanin content than that of the unsweetened berries. There was also a significant difference in total anthocyanin content between the “cultivated” and “wild” blueberry types, with the cultivated berries having a higher overall anthocyanin content.

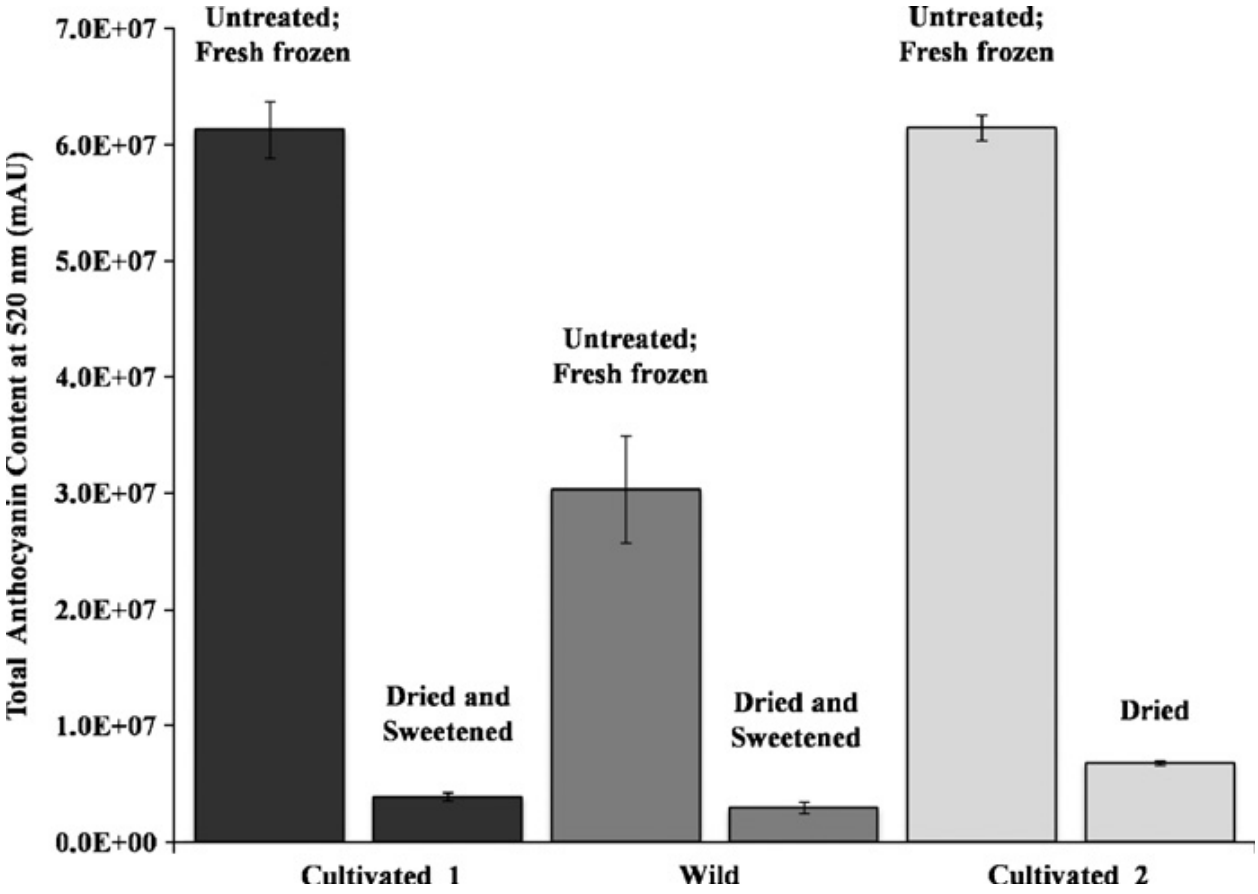

Figure 3.6:The effects of manufacturing processes on the total anthocyanin content of blueberries. Samples analyzed by HPLC-UV (Method 2). *n*=5.

3.4.2 Identification

Due to the large number of reported anthocyanins and the multitude of new compounds that are being reported every year, a general systematic approach may be useful in identifying compounds present in prepared solutions from natural sources. Through the combination of chromatographic separation and high mass accuracy mass spectrometric measurements, anthocyanins can be identified without the aid of standards.

Chromatographic separation and UV detection at 520 nm provides a convenient guide for subsequent mass spectrometric identification. In samples that have a variety of anthocyanins, separation is particularly important. Many anthocyanins have identical masses, and without proper chromatographic separation, these signals cannot be differentiated by mass spectrometry. For example, blueberries exhibit three types of glycosylation (glucose, galactose, arabinose) for five anthocyanidins, giving 15 major anthocyanins [64]. Two of the sugar substituents are isomers, glucose and galactose, thus making five pairs of isobaric compounds. Currently, the only known technique for identifying these peaks is by chromatographic separation. Once chromatographic separation is achieved, the anthocyanins can be identified, without standards, by following the reverse phase elution order set forth by previous researchers [4, 61,102].

Within a reverse phase chromatographic system, anthocyanins follow a general retention order based on the degree of polarity of the molecular structure, primarily affected by the three sections of an anthocyanin: 1) the anthocyanidin; 2) number and type of attached glycosides; and 3) any attached acyl groups.

1.) Anthocyanins that differ by only the anthocyanidin would follow this elution series (from shortest to longest retention time): delphinidin, cyanidin, petunidin, pelargonidin, peonidin, malvidin. A suggested explanation for this pattern is the differences in the hydroxyl and methoxy substituents attached to the anthocyanidin (Table 2). Delphinidin has the greatest degree of polarity because it has the most hydroxyl groups, thus eluting first, while malvidin has the most methoxy groups, giving it more hydrophobic character and making it the last to elute from a reverse phase column.

2.) Anthocyanins that differ only by their number and type of glycosides would follow this elution series (from shortest to longest retention time): 3,5-diglucoside, 3-diglucoside, galactoside, sambubioside, glucoside, arabinoside, rutinoside, xyloside. It is assumed, unless otherwise noted, that glycosides are attached at the 3-position of the flavylium cation.

3.) Anthocyanins that differ only by their acylation would elute after any non-acylated species and would follow this elution series (from shortest to longest retention time): malonoyl; acetoyl; coumoroyl. It is assumed the acyl groups are attached at the 6" position of the attached glycoside.

As a note of caution, it is important to remember that changes in column packings and chromatographic systems may alter retention of closely eluting species. This elution scheme should only be used in combination with other identification tools such as tandem MS fragmentation patterns and high mass accuracy measurements. Anthocyanidins and the conjugated structures of anthocyanins can be assessed through observation of fragmented ions and neutral loss [61]. The neutral loss of a glycogen from a precursor anthocyanin signal gives the telling fragmented ion of an anthocyanidin (Figure 3.7).

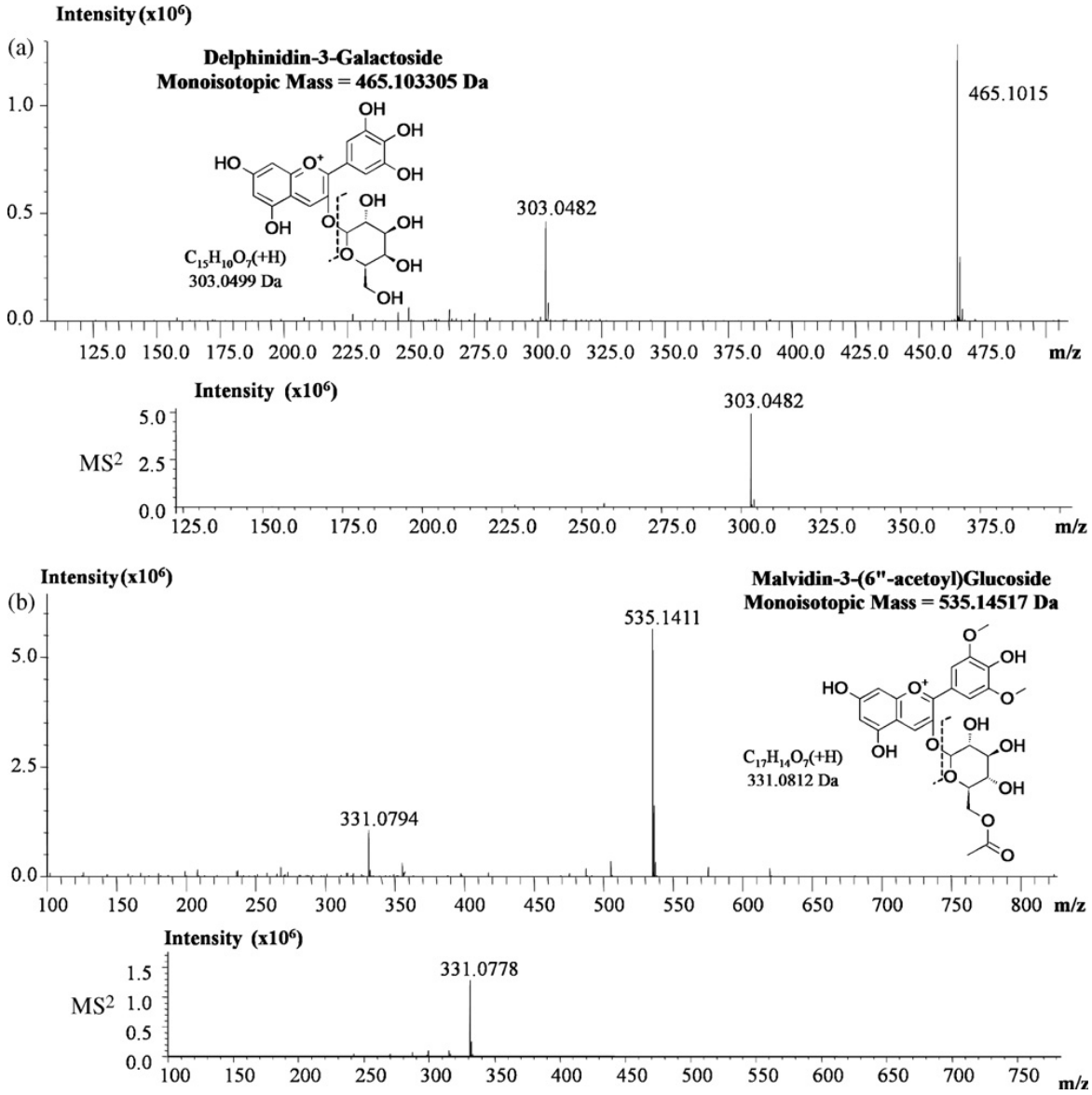

Figure 3.7: (a) Scan of delphinidin-3-galactoside from a blueberry sample and MS^2 scan from precursor ion 465.1015. (b) Scan of malvidin-3-(6-acetoyl)glucoside from a blueberry sample and MS^2 from precursor ion 535.1411 (Method 3).

Anthocyanins are a combination of only three elements, carbon, hydrogen and oxygen. Due to the inexact integral mass of hydrogen and oxygen, anthocyanins with unique formulas have unique masses and, with highly mass accurate measurements, species can be positively identified. Some species may have identical nominal masses, yet have slight different monoisotopic masses, indicating the need for high resolution, high mass accuracy measurements. For example, the theoretical monoisotopic

masses of cyanidin-3-(6”-malonoyl)glucoside ($C_{24}H_{23}O_{14}$) and malvidin-3-(6”-acetoyl)glucoside ($C_{25}H_{27}O_{13}$) are 535.108232 amu and 535.144617 amu, respectively, differing by only 0.036385 amu (68 ppm). By high mass accuracy measurements alone (generally less than 5 ppm error in the IT-TOF-MS system), these two species can be definitively differentiated without the use of a standard or tandem mass spectrometry.

The blueberry extracts contained numerous anthocyanins, including the fifteen major anthocyanins and acylated derivatives of these major species. In all, twenty-five anthocyanins were detected in a sample of the wild highbush berry (Figure 3.8, Table 3.2). These compounds were confirmed by following the identification steps described above and the results are in good agreement with previous literature [4, 61,100]. The average mass accuracy of measurements had less than 5 ppm error. As expected, monoglycosides of delphinidin, cyanidin, and malvidin dominate the chromatographic profile. Acylated derivatives appeared greater in size and number in the wild type samples compared to the cultivated samples.

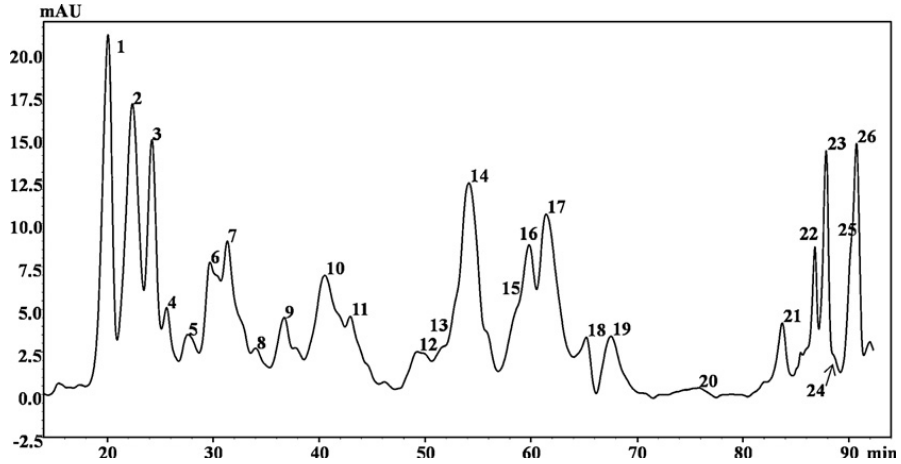

Figure 3.8:Chromatogram of a wild untreated fresh frozen blueberry extract using UV–Vis detection at 520nm (Method 3).

Table 3.2: Peak identification of anthocyanins in blueberry samples using HPLC–ESI-MS (Method 3).

Peak #	Species	Formula	Theor. m/z	Exp. m/z	Error (ppm)
1	Delphinidin-3-Galactoside	$C_{21}H_{21}O_{12}$	465.102753	465.1007	-4.414
2	Delphinidin-3-Glucoside	$C_{21}H_{21}O_{12}$	465.102753	465.1013	-3.196
3	Cyanidin-3-Galactoside	$C_{21}H_{21}O_{11}$	449.107838	449.1058	-4.612
4	Delphinidin-3-Arabinoside	$C_{20}H_{19}O_{11}$	435.092188	435.0922	0.104
6	Cyanidin-3-Glucoside	$C_{21}H_{21}O_{11}$	449.107838	449.1057	-4.835
7	Petunidin-3-Galactoside	$C_{22}H_{23}O_{12}$	479.118403	479.1167	-3.624
9	Cyanidin-3-Arabinoside	$C_{20}H_{19}O_{10}$	419.097273	419.0967	-1.288
10	Petunidin-3-Glucoside	$C_{22}H_{23}O_{12}$	479.118403	479.1164	-4.111
11	Peonidin-3-Galactoside	$C_{22}H_{23}O_{11}$	463.123488	463.1241	1.393
12	Petunidin-3-Arabinoside	$C_{21}H_{21}O_{11}$	449.107838	449.1060	-4.093
13	Peonidin-3-Glucoside	$C_{22}H_{23}O_{11}$	463.123488	463.1216	-4.149
14	Malvidin-3-Galactoside	$C_{23}H_{25}O_{12}$	493.134053	493.1335	-1.189
15	Peonidin-3-Arabinoside	$C_{21}H_{21}O_{10}$	433.112923	433.1112	-3.978
16	Malvidin-3-Glucoside	$C_{23}H_{25}O_{12}$	493.134053	493.1323	-3.622
18	Malvidin-3-Arabinoside	$C_{22}H_{23}O_{11}$	463.123488	463.1213	-4.652
20	Cyanidin-3-(6"-acetoyl)Galactoside	$C_{23}H_{23}O_{12}$	491.118403	491.1172	-2.450
21	Delphinidin-3-(6"-acetoyl)Glucoside	$C_{23}H_{23}O_{13}$	507.113317	507.1131	-0.428
21	Petunidin-3-(6"-acetoyl)Galactoside	$C_{24}H_{25}O_{13}$	521.128967	521.1268	-4.222
22	Cyanidin-3-(6"-acetoyl)Glucoside	$C_{23}H_{23}O_{12}$	491.118403	491.1172	-2.382
22	Peonidin-3-(6"-acetoyl)Galactoside	$C_{24}H_{25}O_{12}$	505.134053	505.1325	-3.074
23	Malvidin-3-(6"-acetoyl)Galactoside	$C_{25}H_{27}O_{13}$	535.144617	535.1435	-2.150
23	Petunidin-3-(6"-acetoyl)Glucoside	$C_{24}H_{25}O_{13}$	521.128967	521.1271	-3.647
24	Quercetin-3-Rutinoside (+H)	$C_{27}H_{30}O_{16}$	611.160661	611.1594	-2.009
25	Peonidin-3-(6"-acetoyl)Glucoside	$C_{24}H_{25}O_{12}$	505.134053	505.1361	3.986
26	Malvidin-3-(6"-acetoyl)Glucoside	$C_{25}H_{27}O_{13}$	535.144617	535.1438	-1.527

Caution must be exercised during identification due to the complexity of natural product matrices. During the identification of the blueberry anthocyanins, peak 24 (Figure 3.8) could not be correlated with previous literature reports of blueberries. At that retention time, a *m/z* signal of 611.1594 was observed, which had fragment ions at *m/z* 465.1007 and 303.0490. The fragment signal at *m/z* 303.0490 suggested

that this species might be a derivative of delphinidin. A literature search of berry anthocyanins was conducted for possible matches to these signals. Although coumaroyl-acylated anthocyanins have not been reported in blueberries, delphinidin-3-(6”-coumaroyl) glucoside was considered a candidate since acetoyl, and malonoyl acylated derivatives of delphinidin-3-glucoside had been observed in the analysis. An assessment of the theoretical mass of the predicted compound revealed that the experimentally measured mass had an error of ~20 ppm, a significant departure from the average of <5 ppm error observed with other identified anthocyanins from the blueberry samples.

The experimentally measured values underwent further scrutiny through the use of the *Formula Predictor* function provided in the *LCMS Solutions* software. Using isotopic ratio filtering, MS/MS fragmentation data, and deviation from mass accuracy, the formula predicted for this compound was $C_{27}H_{31}O_{16}$. Delphinidin 3-(6”-coumaroyl)glucoside was ruled out as a candidate because its formula of $C_{30}H_{27}O_{14}$ did not match. A further literature search of berry anthocyanins revealed that delphinidin-3-rutinoside, an anthocyanin commonly observed in black currant, matched this formula [103]. The experimental value recorded corresponded to ~5 ppm experimental error and had consistent fragmentation patterns. This species still seemed unusual for blueberry samples because of the glycoside, but appeared plausible to be present in trace quantities.

Further literature investigation revealed a glycosylated flavonol, quercetin-3-rutinoside [104], when protonated, to have exactly the same accurate mass and fragmentation pattern as delphnidin-3-rutinoside, although its maximum absorbance was expected near 260 and 370 nm (Figure 3.9). It was then noted that at the retention time of peak 24, larger absorbances were observed at 260 and 370 nm compared to 520 nm, presenting evidence that this species was likely quercetin-3-rutinoside and not delphindin-3-rutinoside. It is important to emphasize the use of multiple identification tools to confirm the identity of anthocyanins without standards due to their high degree of structural complexity and similarity. Here, results from accurate mass measurements alone were not sufficient to report a new natural product, even though such practice can sometimes be found in the literature.

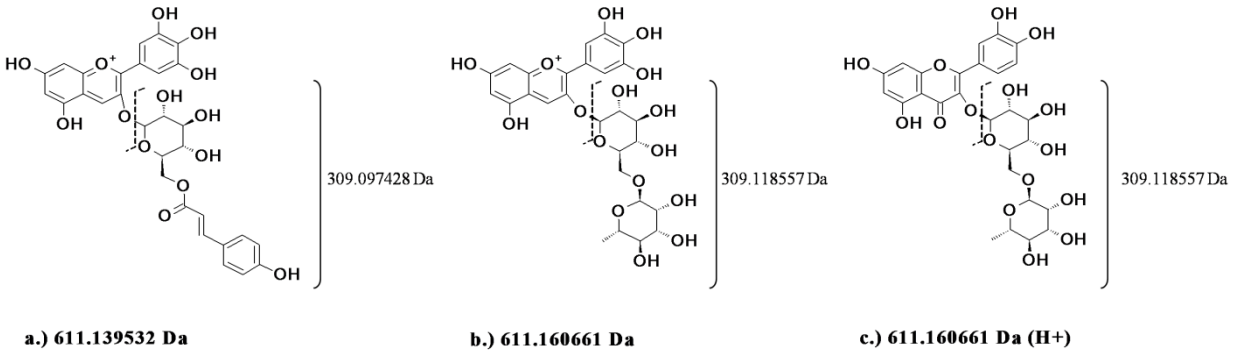

Figure 3.9: The molecular structures and monoisotopic masses of (a) delphindin-3-(6-coumaroyl)glucoside, (b) delphinidin-3-rutinoside, and (c) protonated quercetin-3-rutinoside. These structures have identical MS/MS fragmentation patterns (neutral loss masses indicated).

3.5 Conclusion

Anthocyanins can be extracted and identified in a facile manner from blueberries by employing optimal experimental conditions and utilizing proper identification tools. Homogenization by lyophilization and grinding showed improved reproducibility, without sacrificing UV response. Ethanol, acetone and methanol were found to be the most efficient solvent for blueberry extraction. Trifluoroacetic acid and hydrochloric acid were found to be the best suited acids to acidify the extraction solvents, although hydrochloric acid may not be the best choice for identification purposes due to anthocyanin degradation. Method 2 proved to be the most superior method for chromatographic separation using HPLC-UV, but may not be suitable for use with mass spectrometry due to the mobile phase's high formic acid content (10%). The high acid content can also be problematic for silica-based columns that are not suitably bonded for increased pH stability. For HPLC-ESI-IT-TOF-MS, Method 3 was shown to provide adequate separation and response of 25 individual anthocyanins in blueberries, further enabling the use of tandem MS fragmentation and high mass accuracy measurements for qualitative assignment.

Overall, interest in anthocyanin research is driven by the public's attention to nutritional aspects of fruits and vegetables as well as the therapeutic potential of natural products. Significant improvements in isolation and identification of anthocyanins is expected to improve the accessibility of these compounds for further academic and commercial pursuits.

3.6 Acknowledgements

The authors would like to thank Shimadzu Scientific Instruments, Inc. for their support in the form of an instrumentation grant, the University of Texas at Arlington for general research support and Dr. Jung-Mo Ahn, at the University of Texas at Dallas, for lyophilization of samples.

CHAPTER 4

STRUCTURAL CHARACTERIZATION OF CYANIDIN-3,5-DIGLUCOSIDE AND PELARGONIDIN-3,5-DIGLUCOSIDE ANTHOCYANINS: THEIR COMMON MULTI-DIMENSIONAL FRAGMENTATION PATHWAYS USING HIGH PERFORMANCE LIQUID CHROMATOGRAPHY-ELECTROSPRAY IONIZATION-ION TRAP-TIME OF FLIGHT MASS SPECTROMETRY

4.1 Abstract

Cyanidin-3,5-diglucoside and pelargonidin-3,5-diglucoside were identified from an extract of freeze-dried red hybrid-tea rose petals using high mass accuracy and multi-dimensional fragmentation using liquid chromatography-electrospray ionization-ion trap-time of flight mass spectrometry (LC-ESI-IT-TOF MS). The effects of varying the amount of collision energy applied to the trap at each MS stage were studied. Structural characterization of cyanidin and pelargonidin was attempted by identifying the fragments created by cross-ring cleavage (CRC) of the C-ring and small neutral molecule loss. These fragments were further determined to be diagnostic relative to each other. A computational study of the CRC fragments of cyanidin was performed in order to calculate the overall energy of the fragments. It was determined that the 0,2 CRC pathway was more favorable than the 0,3 CRC pathway.

4.2 Introduction

Anthocyanins are one of the many compound classes that fall under the polyphenolic flavonoid group; they are plentiful in nature and can be found in leaves, flowers, fruits and vegetables. The core structure of an anthocyanin is a phenolated benzopyran, referred to as a flavylium cation, and may be described as a C_6-C_3-C_6 skeleton. This skeleton has a phenolic ring fused to a pyran with an additional phenolic ring connected at the 2 position of the pyran. Two positions on the B-ring, at 3' and 5', provide sites for a variety of substituents and the AC bicycle is glycosylated at the 3, 5, and 7 positions, which allows for a multitude of potential structural and functional variants. The aglycone flavylium cation is

referred to as an anthocyanidin[1] (Figure 4.1). In addition, a positive charge is found on the oxygen of the pyran ring, and provides specific detection from other flavonoid species at 520 nm.

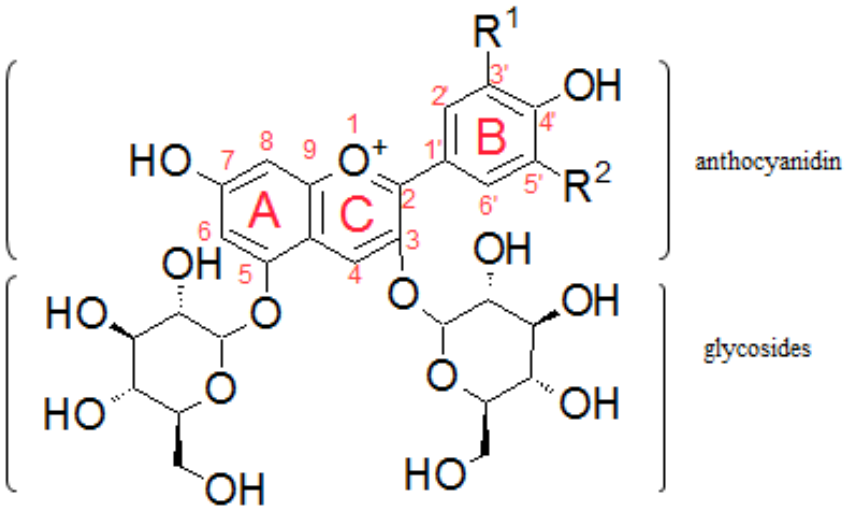

Figure 4.1:A generic diglucoside anthocyanin. For pelargonidin, R^1=R^2=H,. For cyanidin, R^1=OH and R^2=H.

Like many other fruits and flowers, the bright attractive colors of rose petals are partially due to their anthocyanin content. Anthocyanins were studied in roses as early as 1914 in a study by Willstater and Nolan on the isolation of cyanidin[47]. It was not until 1934 that pelargonidin was identified in a rose[92]. There are six naturally occurring anthocyanidins, which are differentiated by hydroxyl and methoxy groups on the B-ring. Each of these aglycones has been detected in one species of flower or another, and are found glycosylated with glucose, rhamnose, fructose, rutinose, and sophorose[104]. One of the most common roses is the red hybrid-tea rose (“Liberty”, *R. gallica*). The gallicanae section predominately contains cyanidin-3-5-diglucoside, along with small amounts of cyanidin-3-glucoside.

Additionally, other anthocyanins, such as pelargonidin-glucosides, can be introduced to these species through genetic recombination[105].

Anthocyanins have been linked to anticancer effects[29], and have demonstrated a capacity to deter apoptosis of cells[30], which may be attributed to their powerful antioxidant abilities[24-28]. Dietary ingestion of these antioxidant compounds is believed to combat oxidative damage by neutralizing reactive radical species. Epidemiological studies have shown that the antioxidant activity provided by the consumption of fruit is positively correlated with reduced mortality from cardiovascular disease and some types of cancer[28]. Recently, attention has been given to anthocyanins and their role in signaling pathways of cancer chemoprevention[32]. Increasing interest in these compounds due to their possible nutritional and therapeutical aspects has led to further need for structural characterization and identification techniques.

Efficient extraction of the compounds from natural material can be accomplished with an acidified aqueous/organic mixture[106]. Analysis is commonly performed using HPLC coupled with UV-Vis, photodiode array (PDA), or mass spectrometry (MS) detectors[97]. Often times, the anthocyanin species are isomers of other flavonoids and in complex mixtures, they cannot be differentiated without authentic standards and a separation technique. Unfortunately, qualitative identification is hindered by the limitation of available commercial standards[73]. Fragmenting the anthocyanidin using collision-induced dissociation (CID) may offer a solution. Positive identification may then be directly determined based on unique diagnostic fragmentation patterns of the anthocyanidin, without the use of commercial standards.

Numerous fragmentation studies have been reported for different flavonoid species, including flavones, isoflavones, flavanones, flavonols and proanthocyanidins[84-88,90,91,107]. Ma et al. demonstrated that the isomeric aglycones from a flavone and a flavonol could be directly identified based on fragmentation patterns of the aglycones[84]. The Brodbelt group used metal complexation to differentiate flavonoids glucuronides[108]. Kang et al. used deuterated isoflavones and fragmentation up to MS^5 to discern diagnostic fragmentation patterns[107]. Another study observed fragmentation up to MS^7 of isoflavones using ESI-IT-TOF-MS[90] and a study of kampferol fragmentation was examined

using high mass resolution. Vuckis and Guttman have provided a nice review of structural characterization of flavonoid glycosides by mass spectrometric fragmentation[88] .

Anthocyanin fragmentation by low energy CID using an ion trap is similar to the fragmentation of other flavonoids classes and can generally be classified into two categories, 1) cross-ring cleavage (CRC) of the C-ring, and 2) ring-opening followed by subsequent loss of small neutral molecules, such as CO, C_2H_2O and H_2O (Figure 4.2). Cross-ring cleavage involves breaking of two bonds of the C-ring. The A-type fragments are the same for most common anthocyanidin species (only very rare species have altered substituents on the A-ring), but the B-type fragments will differ based on the anthocyanidin type, due to changes of the substituents on the B ring[82]. These diagnostic B-type fragment ions can aid in confirming the identity of anthocyanins in complex mixtures or in the analysis of unusual plants.

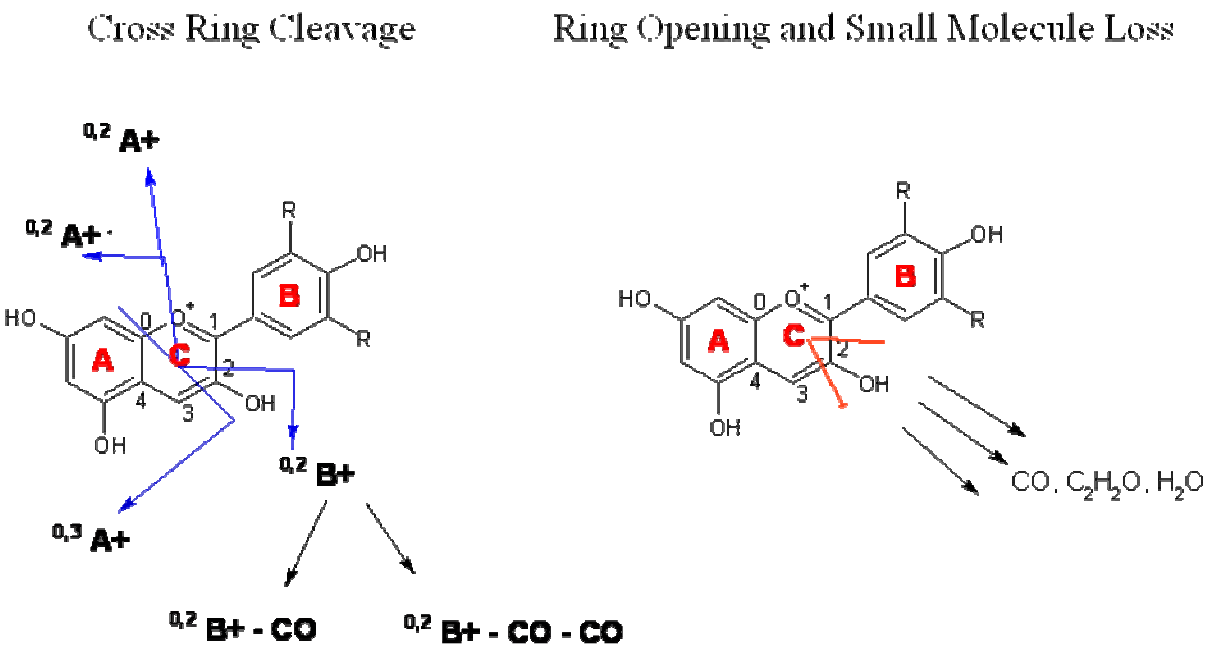

Figure 4.2: Fragmentation of the anthocyanidin occurs as either occurring from cross-ring cleavage (CRC) or from neutral small molecule loss from ring opening.

Surprisingly, the literature is incomplete with regard to the mass signals and proposed structures for CRC and small molecule loss fragments for naturally-occurring anthocyanidins. One significant study by Oliveira et al. revealed characteristics of fragmentation patterns for four of the common naturally

occurring anthocyanidins, cyanidin, peonidin, malvidin and delphinidin, using high energy CID by electrospray ionization and orthogonal acceleration—time-of-flight (oa-TOF) tandem mass spectrometry[82]. Other studies involved anthocyanidin fragmentation from natural products, such as berries from a myrtle shrub, grape skins and black carrots, all using ESI and ion trap tandem mass spectrometry[72,79,83]. Specifically, literature covering pelargonidin fragmentation is limited. A study of black carrots containing pelargonidin glycosides showed fragment data but stated that the intensities were too low to obtain reproducible data[83]. Another study attempted fragmentation of pelargonidin by plasma desorption but was not successful[109].

The limited knowledge of anthocyanidin fragmentation may be due to a few associated problems. The flavylium cation is particularly stable and does not easily fragment by low energy CID[82]. Using default instrument settings may leave the user with little or no fragmented species. Second, higher order fragmentation (MS^n) with an ion-trap may be limited because of signal strength, especially in increasing mass stages. By varying the energy applied to the ion-trap, mass signals can be optimized to produce increased signal output. Finally, in low resolution instruments, an observed fragment ion may have multiple elemental formula possibilities, particularly with organic compounds, which only contain carbon, hydrogen and oxygen, as in the case of anthocyanins. Increasing the resolution with higher mass accuracy can help eliminate erroneous choices and can provide the user with confidence to assign the exact elemental formula.

Molecular modeling and computational studies of flavonoid compounds may shed some light on the structures of these gas phase fragment ions, which otherwise would be difficult to structurally characterize. There have been a number of different studies focused on computational modeling of anthocyanidins these have used density functional theory (DFT)[46,110,111] and *ab initio*[112] approaches. One interesting study showed the effects of varying the hydroxyl substituents on the B-ring of a flavylium cation[113]. Another provided a conformational analysis of pelargonidin using density functional theory (DFT)[114].

In this study, an electrospray ionization-ion trap-time of flight mass spectrometer equipped with a liquid chromatograph (LC-ESI-IT-TOF-MS) was used to perform higher order fragmentation (up to MS^6)

on mono- and di-glucosides of cyanidin and pelargonidin found in the petals of a hybrid-tea rose ("Liberty", *R. gallica).* As the collision energy of the ion-trap was adjusted, variations in the signal intensities of product ions were observed, which were due to cleavage of the glycosides at the MS-MS, and MS^3 stages, and fragmentation of the anthocyanidin at the MS^4 stage. Iterative fragmentation pathways and high mass accuracy were used to assess the identity for observed mass signals. Software modeling using the density functional theory and the 6-31G basis set has been used to help delineate and assign possible CRC mechanisms and product structures.

4.3 Materials and Methods

4.3.1 Reagents and Materials

LCMS-grade acetonitrile, methanol, and water were purchased from Burdick and Jackson (Muskegon, MI, USA). Trifluoroacetic acid (TFA) was purchased from Sigma-Aldrich (St. Louis, MO, USA) and formic acid was purchased from Fluka (AG, Buchs, Switzerland). Red hybrid-tea roses ("Liberty", *R. gallica).* were purchased from a local market.

4.3.2 Instrumentation

Anthocyanin identification and fragmentation was performed on a LCMS-IT-TOF (Shimadzu Scientific Instruments, Kyoto, Japan), equipped with a Prominence HPLC system (LC-20AD pumping system, a SIL-20AHT autosampler, and SPD-M20A diode array detector; Shimadzu). *LCMS Solutions* software (version 3.41.324) was used for data analysis. The *Formula Predictor* function of *LCMS Solutions* was used to support identification and confirmation of unknown signals.

Fractionation was performed using a Finnigan SpectraSYSTEM®-HPLC (Thermo-Fisher Scientific, Inc., Waltham, MA, USA) comprised of a P2000 solvent delivery system, an AS3000 autosampler and a UV6000LP diode array detector. A Foxy® Jr. Fraction Collector (Teledyne-Isco, Inc., Lincoln, NE, USA) was placed online, after the detector.

4.3.3 Rose Petal Extraction

Rose petals were ground to a powder in a coffee grinder, and then lyophilized. Powder (0.1 g) was extracted in 70:30:0.1, methanol: water: triflouroacetic acid (1 mL) then centrifuged and filtered to remove any residual solids.

4.3.4 Chromatographic Analysis of Extraction

For HPLC-ESI-MS, a Gemini C18 column (100mm x 2.0 mm, 3µm; Phenomenex, Torrance, CA, USA) and a Gemini C18 guard column (4.0 x 2.0 mm, 3µm; Phenomenex, Torrance, CA, USA) were used to chromatographically separate anthocyanin species using 1.0% formic acid as solvent A and acetonitrile as solvent B. The elution scheme was: linear gradient at 0.1 mL/min from 5% B to 10% B, 0-5 min; isocratic elution 10% B, 5-30 min; linear gradient from 10% B to 13.5% B, 30-75 min; linear gradient from 13.5% B to 25% B, 75-90 min.

Ionization was performed using a conventional ESI source, in the positive ionization mode. The heat block and curved desolvation line (CDL) were maintained at 250 ℃. Nitrogen was used as nebulizing gas and drying gas, each set at 1.5 L/min and 10 L/min, respectively. The ESI source voltage was set to 4.5 kV and the detector voltage was 1.62 V. The instrument was calibrated to < 5 ppm error in mass accuracy with an external standard of sodium TFA solution.

4.3.5 Identification and Fractionation

Cyanidin-3,5-diglucoside, pelargonidin-3,5-diglucoside, cyanidin-3-monoglucoside, and pelargonidin-3-monoglucoside were identified in the chromatogram of the rose petal extraction (Figure 4.3). Cyanidin-3,5-diglucoside and pelargonidin-3,5-diglucoside were isolated by eluent collection using the fraction collector for use in ion-trap optimization experiments, via direct infusion. Infusion was performed using a NE-1010 syringe pump (New Era Pump Systems Inc. Wantagh, NY, USA) operated at 5µL/min.

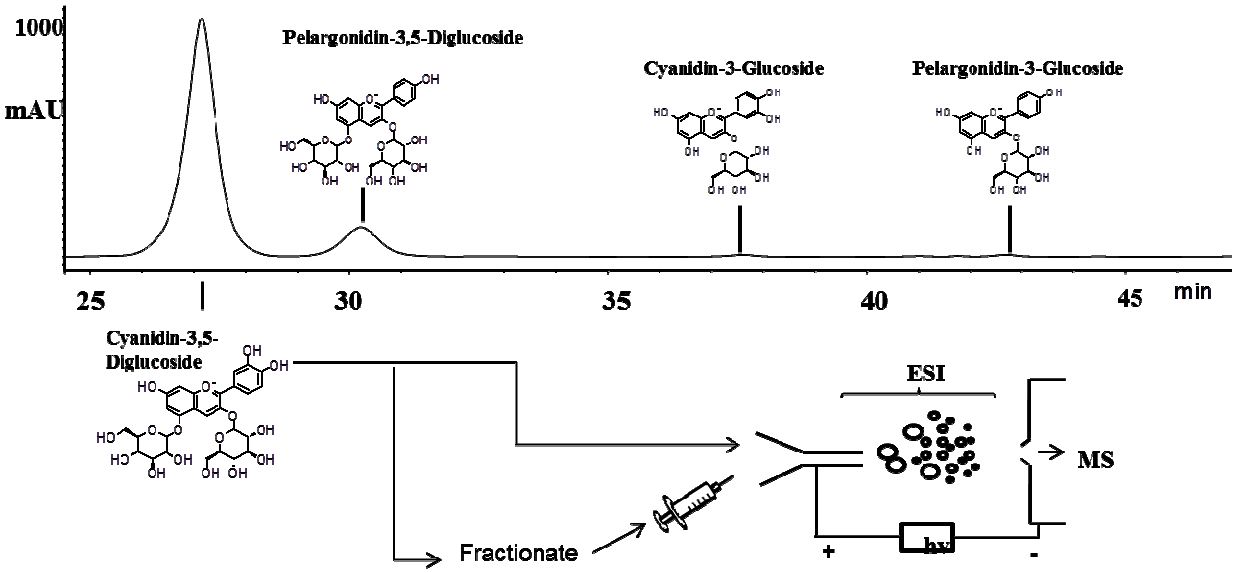

Figure 4.3: Reverse phase separation of rose petal anthocyanins and selective detection at 520 nm along with inline positive mode ESI-IT-TOF-MS results in identification of 4 anthocyanins. These compounds can be isolated through fractionation, if desired, and observed with positive mode ESI-IT-TOF-MS via direct infusion.

4.3.6 Ion-Trap Optimization

The ion accumulation time was set at 50 milliseconds. Precursor ion isolation parameters were set at a width of 3.000 amu and 20 milliseconds. The energy and collision gas CID parameters were varied as demonstrated in the results, while keeping the time and frequency (q) constant at 30 milliseconds and 0.251, respectively.

4.3.7 Computational Modeling

The 3-D structures of the anthocyanidin fragments and their Cartesian coordinates were submitted to Gaussian03[115] for optimization of energy using DFT/B3LYP and 6-31G basis set.

4.3.8 Nomenclature

The nomenclature described by Ma et al[84]for labeling fragment ions was used. The labels ${}^{i,j}A^{+}$ and ${}^{i,j}B^{+}$ correspond to the fragment ions that contain either the A or B ring and were formed by cleavage of the i and j bonds of the C-ring (Figure 4.2).

4.4 Results and Discussion

4.4.1 Optimization of glycoside cleavage

The effects of varying the energy applied to the ion-trap on the cleavage of the O-glycosidic bond of the di-glucoside and mono-glucoside species of cyanidin and pelargonidin were observed (Figure 4.4). Both of the anthocyanidin types showed similar trends in regards to loss of their glucose moiety. The loss of the first glucoside from the diglucoside compound was observed at 1% collision energy (the lowest setting). There is some uncertainty at what position this glucoside is lost (maybe a mixture of both), but it is depicted in the figures at the 3-position based on the prevalence of the 3-monoglucoside in nature. The mono-glucoside signal grows sharply from 5 – 10%, then reaches a maximum and levels out near 15% for cyanidin and 20% for pelargonidin. From 20% to 75% the signal from the mono-glucoside slowly diminishes.

Signals for cyanidin and pelargonidin were observed starting at 5% and 7% collision energy, respectively. At these energies, cleavage of both glucosides is achieved. Operating at collision energies lower than these thresholds may offers the ability to selectively fragment only one glucoside, which may be helpful in distinguishing rare species which have different two different sugar units attached. The anthocyanidin signal quickly overcomes the mono-glucoside signal at 15%, suggesting that the collisional energy needed to cleave both glucosides is not that much different than the energy for loss of only one glucoside. The anthocyanidin signals reach a maximum near 25% and begin to decrease with a mild slope as the collision energy approaches near 50%, marking the energy at which the anthocyanidin begins to fragment. The wide range of consistent signal response from 25% to 75% demonstrates the great stability of the anthocyanidin, while almost all of the collision energy is being directed into cleavage of the glycosides. No fragmentation of the glycoside moieties, besides that of the bond which links it to the anthocyanidin is observed, typical for product ion spectra of O-glycosides at low energy CID. Additionally, relatively low amounts of protonated signals, $[M+H]^{+\cdot}$, was observed for the diglucoside and mono-glucoside species.

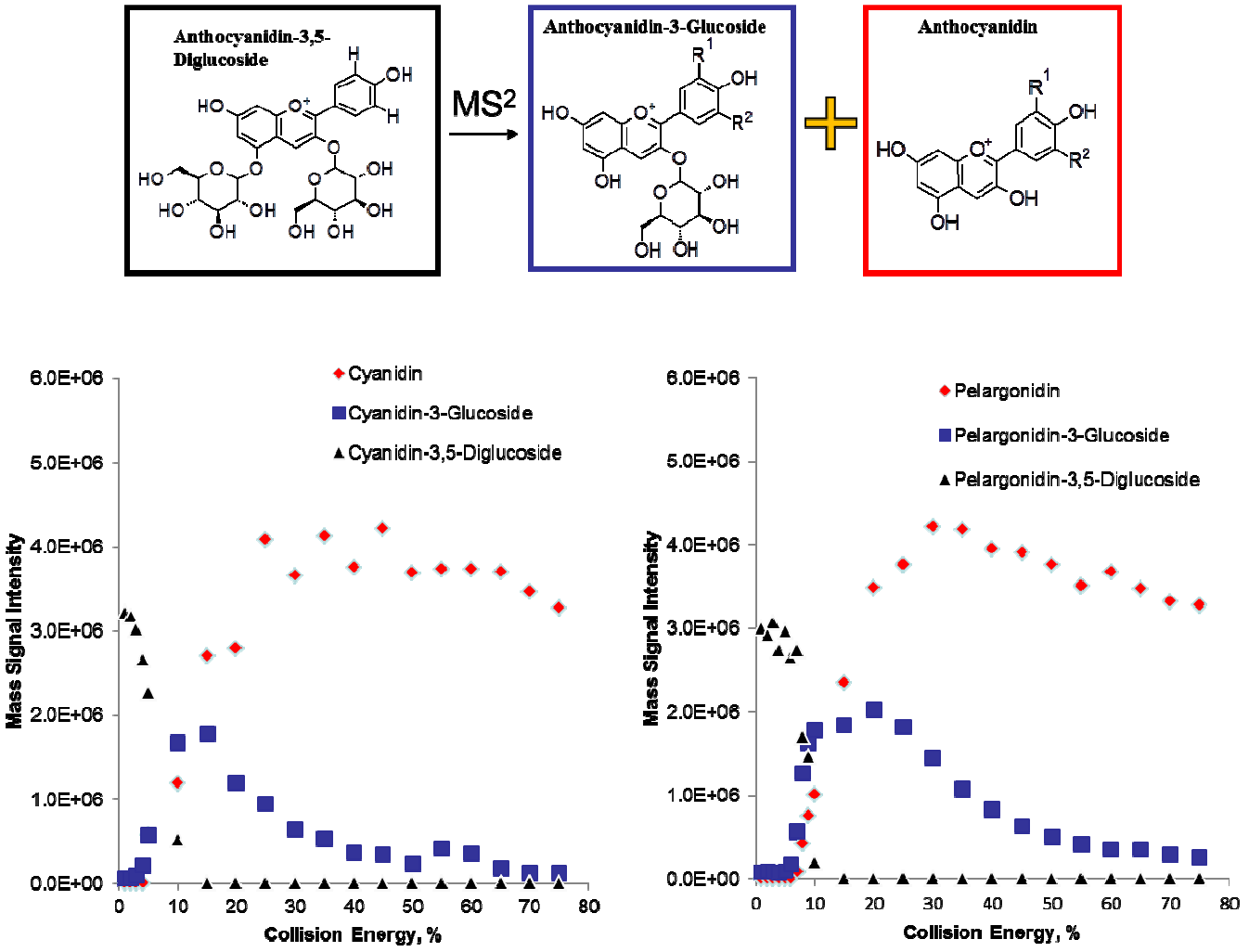

Figure 4.4: The effects of varying the collision energy applied to the ion trap on the major fragment ions of cyanidin-3,5-diglucoside and pelargonidin-3,5-diglucoside at MS-MS stage in the positive mode. For pelargonidin, R^1=R^2=H,. For cyanidin, R^1=OH and R^2=H.

4.4.2 MS^3: Loss of glucoside

Loss of a single glucoside was further studied in the third mass stage by specifically selecting the mono-glucoside and varying the collision energy applied to the trap (Figure 4.5). For cyanidin-monoglucoside, 5% collision energy was not enough to cleave the glucose moiety. At 6% the aglycone cyanidin ion appears in the mass spectrum and grows sharply until it reaches a maximum at 20%. The mono-glucoside signal is absent at this energy, demonstrating that all of the mono-glucoside is being fragmented. For pelargonidin-monoglucoside a different pattern is observed. At 1% collision energy the aglycone signal is near its maximum and the mono-glucoside signal is absent, unlike the cyanidin counterpart.

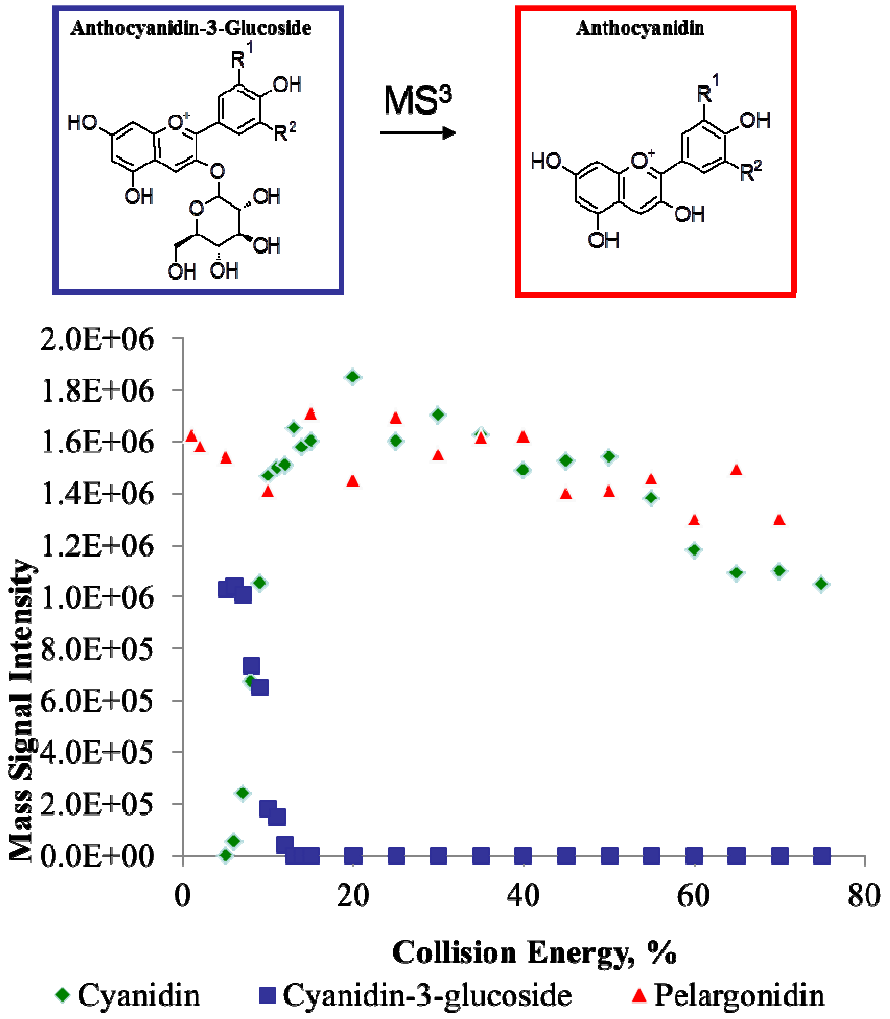

Figure 4.5: The effects of varying the collision energy applied to the ion trap on the major fragment ions of cyanidin-3-glucoside and pelargonidin-3-glucoside at MS^3 stage in the positive mode. For pelargonidin, R^1=R^2=H,. For cyanidin, R^1=OH and R^2=H.

4.4.3 MS^4, MS^5 and MS^6: Fragmentation pathways of Cyanidin and Pelargonidin

It was determined that the maximum amount of signal information from fragmentation of an anthocyanidin can be obtained from within a small window of collision energy values, in our experience from 10 to 20% (Figure 4.6). A default collision energy setting at 50% would not provide any fragmentation signals. The loss of the fragment ion signals at high collision energies may be due to the destabilization of the parent and product ions along the stability diagram as higher excitation amplitudes are reached. The product ions observed for cyanidin fragmentation (Table 4.1) are similar to those reported by Montoro et al.[83] and by Downey and Rochfort[72]. They also matched some high energy

fragments reported by Oliveira et al [82], but contrast significantly in the profile of individual ion intensities. In their study, the CRC fragments are more intense than small molecule loss fragments, while in our spectra, the small molecule loss fragments are more abundant than the CRC fragments (Figure 4.7). The pelargonidin signals (Figure 4.7 and Table 4.2) did show some similarities with those reported by Kammerer et al. in a study of black carrots[83]. The profile of the intensities of the product ions showed similar levels of both CRC fragments and small molecule loss.

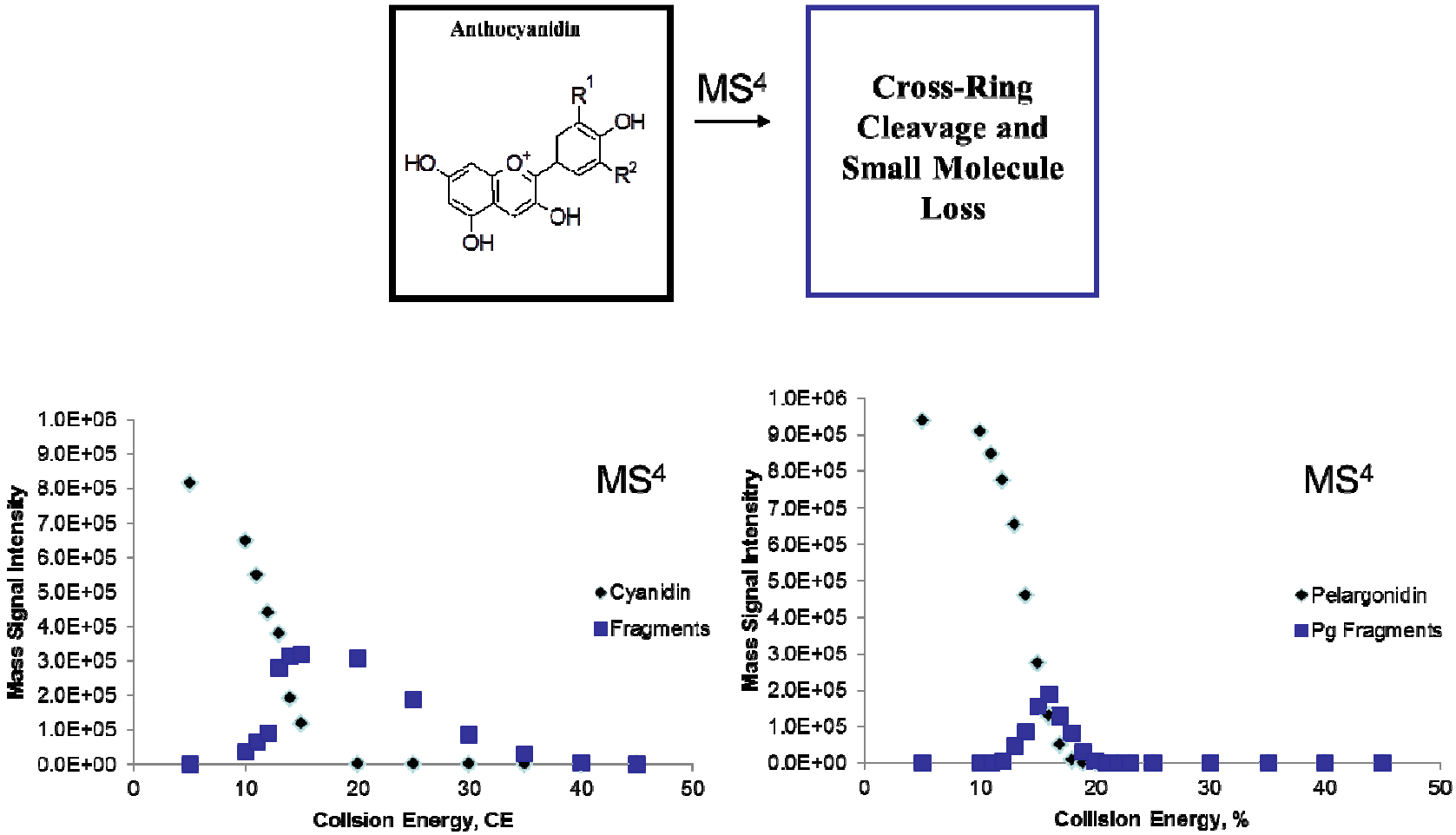

Figure 4.6: The effects of varying the collision energy applied to the ion trap on the major fragment ions of cyanidin and pelargonidin at MS^3 stage in the positive mode. For pelargonidin, R^1=R^2=H,. For cyanidin, R^1=OH and R^2=H.

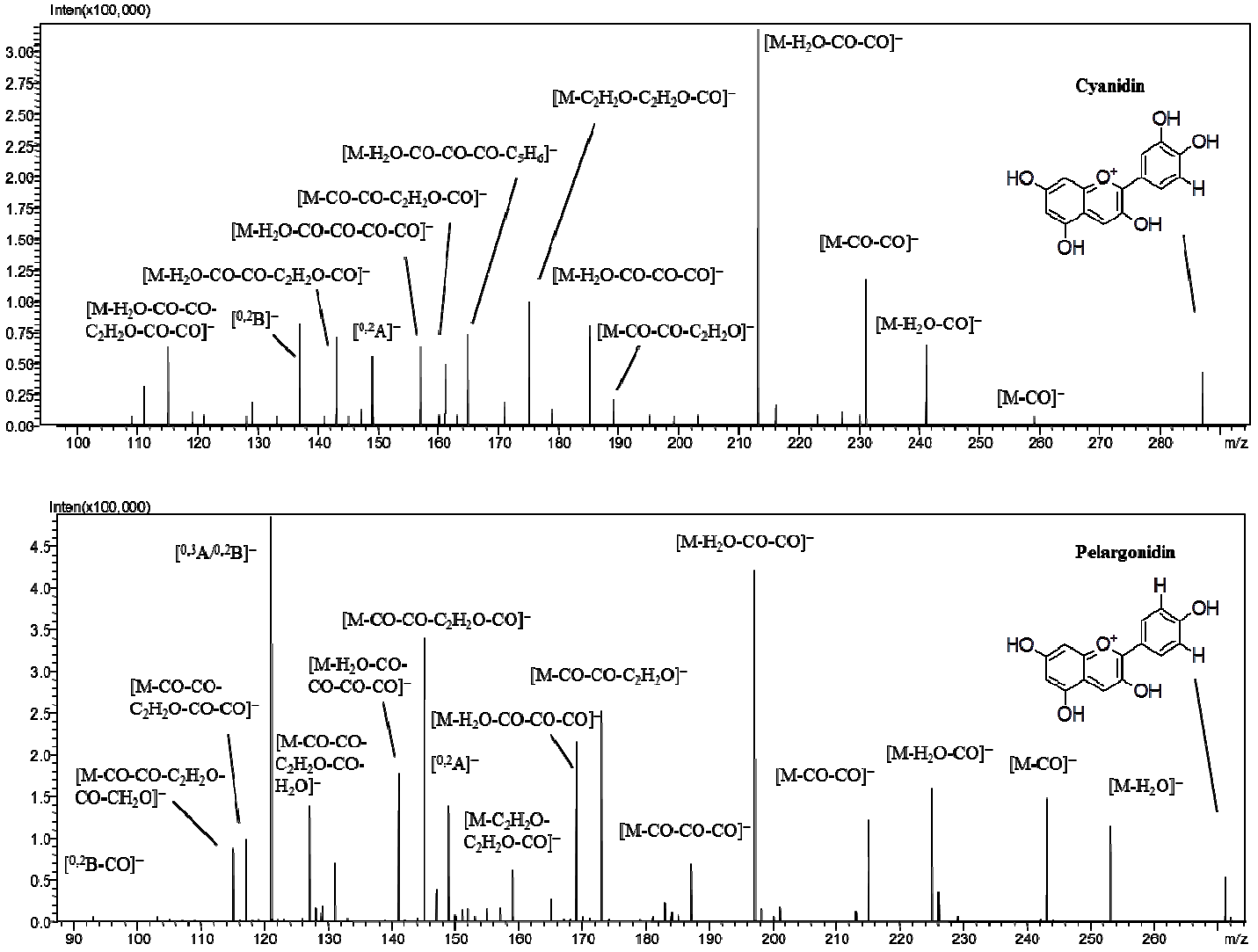

Figure 4.7: The product ion spectra of cyanidin and pelargonidin at MS^4 stage in the positive mode.

Table 4.1: The mass signals observed of cyanidin fragmentation at the MS^4 stage in the positive mode, and their proposed neutral losses based on mass accuracy.

Fragment Type	Theoretical mass, m/z	Measured Signal, *m/z*	error, ppm
Cyanidin-3,5-Diglucoside	611.1607	611.1610	0.6
Cyanidin-3-Diglucoside	449.1078	449.1088	2.1
Cyanidin	287.0550	287.0548	-0.7
$^{0,2}A^+$	149.0233	149.0219	-9.4
$^{0,2}A^{+\bullet}$	150.0311	150.0309	-1.6
$^{0,3}A^+$	121.0284	121.0273	-9.1
$^{0,2}B^+$	137.0233	137.0226	-5.3
$^{O,2}B^+$-CO	109.0251	109.0242	-8.4
O^2B^+-CO-CO	81.0335	81.0337	2.6
M-H_2O	269.0444	269.0424	-7.6
M-CO	259.0601	259.0624	8.9
M-H_2O-CO	241.0495	241.0494	-0.6
M-CO-CO	231.0652	231.0641	-4.7
M-H_2O-C_2H_2O	227.0339	227.0356	7.6
M-H_2O-CO-CO	213.0546	213.0560	6.5
M-CO-CO-CO	203.0703	203.0704	0.6
M-H_2O-CO-C_2H_2O	201.0546	201.0505	-20.5
M-H_2O-CO-C_2H_2O-H_2	199.0390	199.0405	7.7
M-H_2O-CO-CO-H_2O	195.0441	195.0450	4.8
M-CO-CO-C_2H_2O	189.0546	189.0546	-0.1
M-H_2O-CO-CO-CO	185.0597	185.0596	-0.6
M-C_2H_2O-C_2H_2O-CO	175.0390	175.0393	1.9
M-H_2O-CO-CO-C_2H_2O	171.0441	171.0435	-3.2
M-H_2O-CO-CO-CO-H_2O	167.0491	167.0510	11.1
M-CO-CO-C_5H_6	165.0182	165.0160	-13.5
M-CO-CO-C_4H_2O	163.0390	163.0398	5.1
M-CO-CO-C_2H_2O-CO	161.0597	161.0585	-7.5
M-C_2H_2O-C_2H_2O-CO-O+H	160.0519	160.0537	11.4
M-H_2O-CO-CO-CO-CO	157.0648	157.0657	5.8
M-C_2H_2O-C2H_2O-CO-CO	147.0441	147.0428	-8.5
M-H_2O-CO-CO-C_2H_2O-CO	143.0491	143.0511	13.7
M-H_2O-CO-CO-H_2O-CO-CO+H_2	141.0699	141.0702	2.3
M-H_2O-CO-CO-H_2O-CO-CO	139.0542	139.0534	-6.0
M-H_2O-CO-CO-CO-CO-CO	129.0699	129.0714	11.8
M-H_2O-CO-CO-CO-CO-CO-H	128.0621	128.0613	-5.9
M-H_2O-CO-CO-CO-CO-CO-H_2	127.0542	127.0552	7.7
M-C_2H_2O-C_2H_2O-CO-CO-CO	119.0491	119.0469	-18.8

Table 4.1 -- Continued

M-H_2O-CO-CO-C_2H_2O-CO-CO	115.0542	115.0546	3.2

Table 4.2: The mass signals observed of pelargonidin fragmentation at the MS^4 stage in the positive mode, and their proposed neutral losses based on mass accuracy.

Fragment Type	Theoretical mass, m/z	Measured Signal, *m/z*	error, ppm
Pelargonidin-3,5-Diglucoside	595.1657	595.1648	-1.6
Pelargonidin-3-Diglucoside	433.1129	433.1114	-3.5
Pelargonidin	271.0601	271.0594	-2.6
$^{0,2}A^+$	149.0233	149.0225	-5.4
$^{0,2}A^{+\bullet}$	150.0311	150.0287	-16.3
$^{0,3}A^+$	121.0284	121.0279	-4.2
$^{0,2}B^+$	121.0284	121.0279	-4.2
$^{0,2}B^+$-CO	93.0302	93.0313	11.8
M-H_2O	253.0495	253.0501	2.2
M-CO	243.0652	243.0640	-4.9
M-H_2O-CO	225.0546	225.0538	-3.7
M-CO-CO	215.0703	215.0719	7.6
M-H_2O-CO-CO	197.0597	197.0599	1.0
M-CO-CO-CO	187.0754	187.0739	-7.8
M-H_2O-CO-C_2H_2O	183.0441	183.0451	5.7
M-CO-CO-C_2H_2O	173.0597	173.0579	-10.4
M-H_2O-CO-CO-CO	169.0648	169.0650	1.2
M-CO-CO-CO-CO	159.0804	159.0789	-9.7
M-C_2H_2O-C_2H_2O-CO	159.0441	159.0454	8.4
M-H_2O-CO-CO-C_2H_2O	155.0491	155.0490	-0.9
M-H_2O-CO-CO-H2O-CO	151.0542	151.0512	-20.1
M-CO-CO-C_2H_2O-CO	145.0648	145.0653	3.5
M-H_2O-CO-CO-CO-CO	141.0699	141.0693	-4.1
M-CO-CO-C_2H_2O-CO-H_2O	127.0542	127.0528	-11.3
M-CO-CO-C_2H_2O-CO-CO	117.0759	117.0781	18.6
M-CO-CO-C_2H_2O-CO-CH_2O	115.0542	115.0541	-1.1

Table 4.3: The pathways of fragmentation signals observed for cyanidin-3,5-diglucoside in the positive mode.

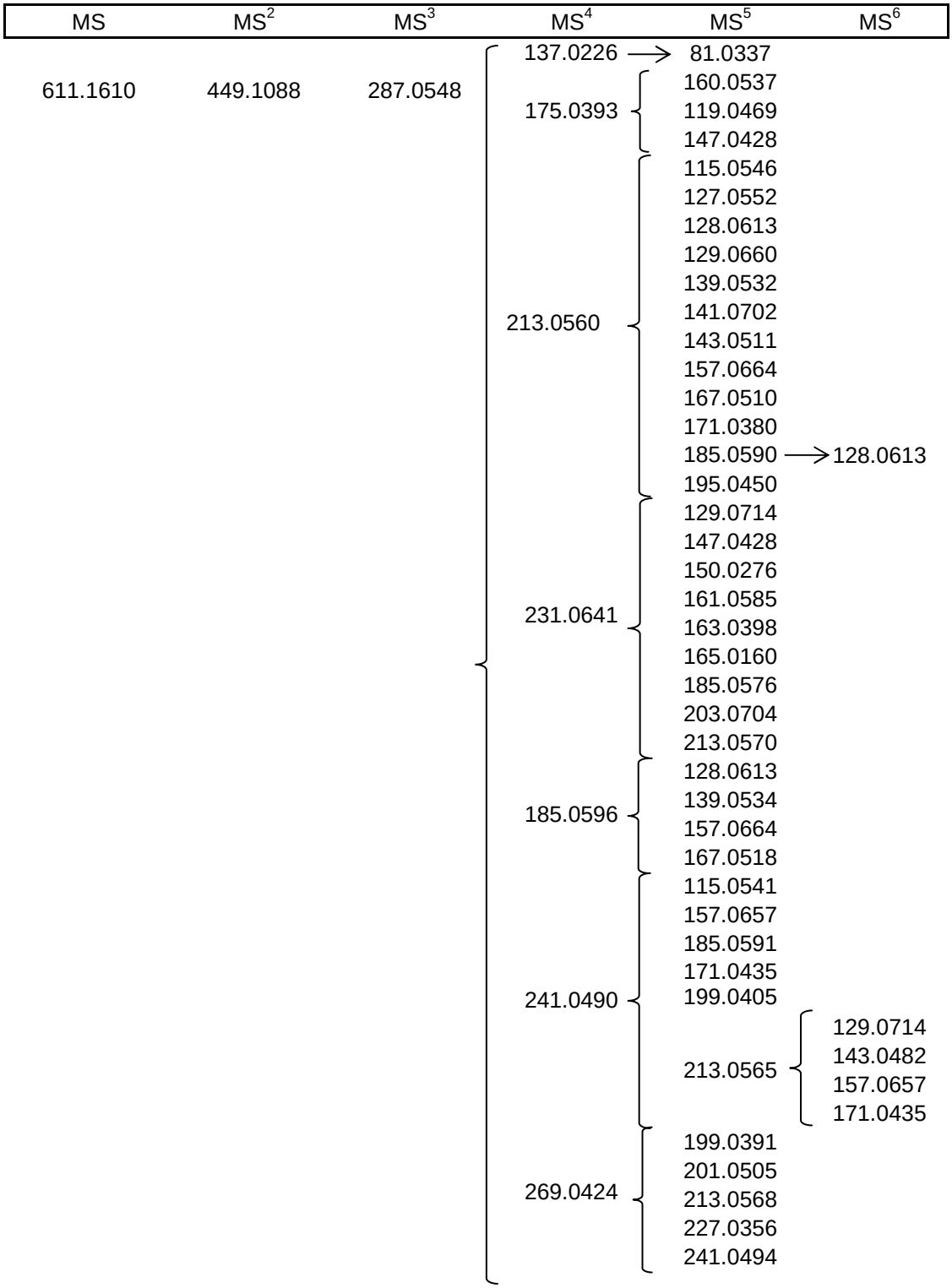

Table 4.4: The pathways of fragmentation signals observed for pelargonidin-3,5-diglucoside in the positive mode.

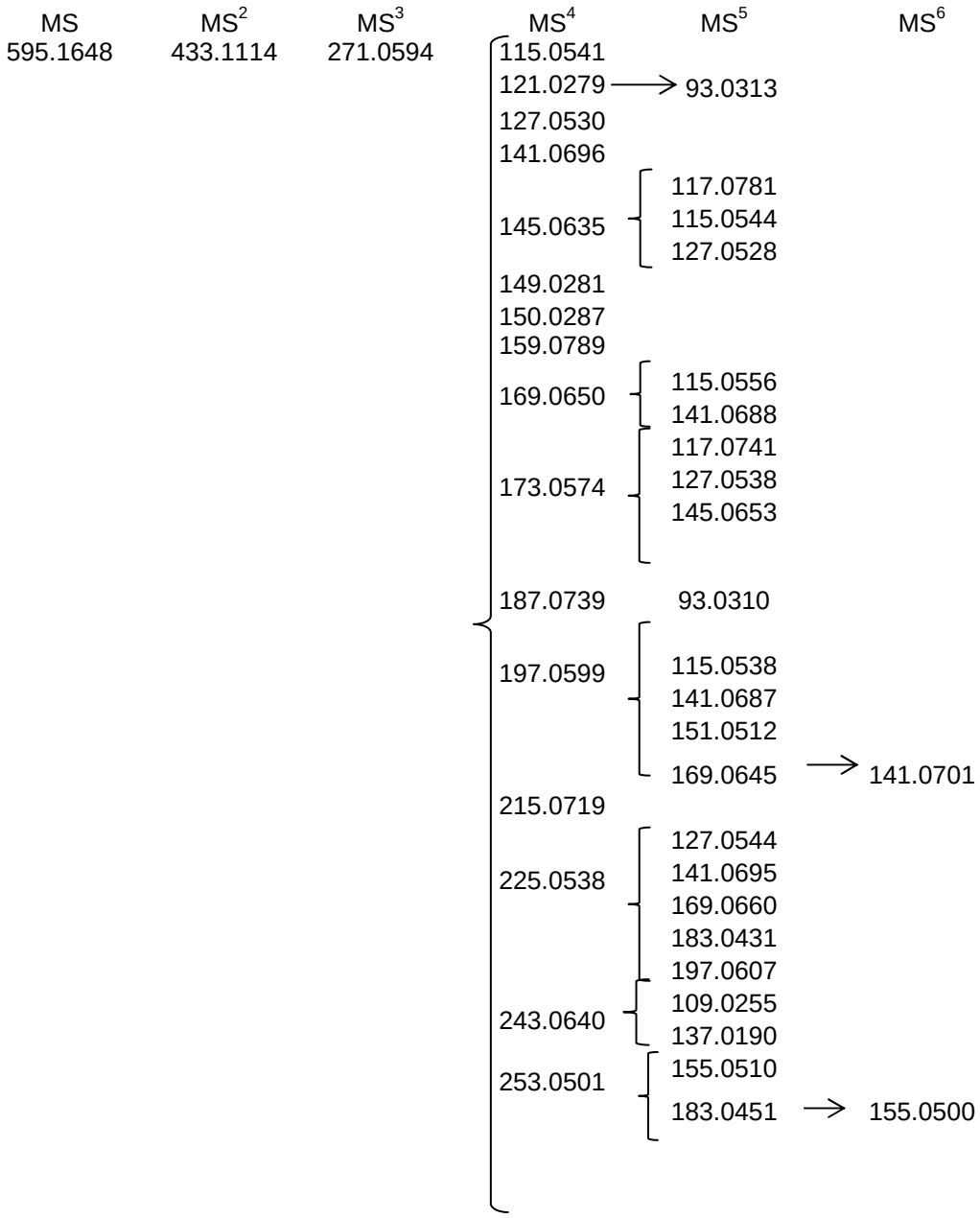

4.4.4 Cross Ring Cleavage (CRC)

The cyanidin CRC fragments observed at MS^4 were $^{0,2}A^{+\bullet}$ (150.031 m/z), $^{0,2}A^{+}$ (149.023 m/z), $^{0,2}B^{+}$ (137.023 m/z), $^{0,2}B^{+}$-CO (109.028 m/z), and $^{0,3}A^{+}$ (121.028 m/z). Further fragmentation (MS^5) of the $^{0,2}B^{+}$ signal revealed a neutral loss of two carbonyls, giving the signal $^{0,2}B^{+}$-CO-CO (81.033 m/z), which to our knowledge has not been reported before. The $^{0,2}A^{+}$ fragment was also observed in fragments of cyanidin, delphinidin, peonidin and malvidin by Montoro et al[79] who used a ESI-IT-MS. Based on computational calculations (refer to section 4.4.4.1-2), a structure and mechanism for the generation of the $^{0,2}A^{+}$ is proposed herein (Figure 4.8). This mechanism is similar to the $^{0,2}A^{+\bullet}$ (150.031 m/z) fragmentation proposed by Oliveira et al [26], but it involves heterolytic cleavage of bond 2 and a hydrogen transfer from the C-3 hydroxyl group to C-2. Plotting the signal strength of the cyanidin CRC fragments against the collision energy applied to the ion trap shows that the $^{0,2}B^{+}$ fragment is by far the strongest signal, followed by the $^{0,2}A^{+}$, the $^{0,3}A^{+}$ signal and then the less intense $^{0,2}A^{+\bullet}$ and $^{0,2}B^{+}$-CO signal (Figure 4.9).

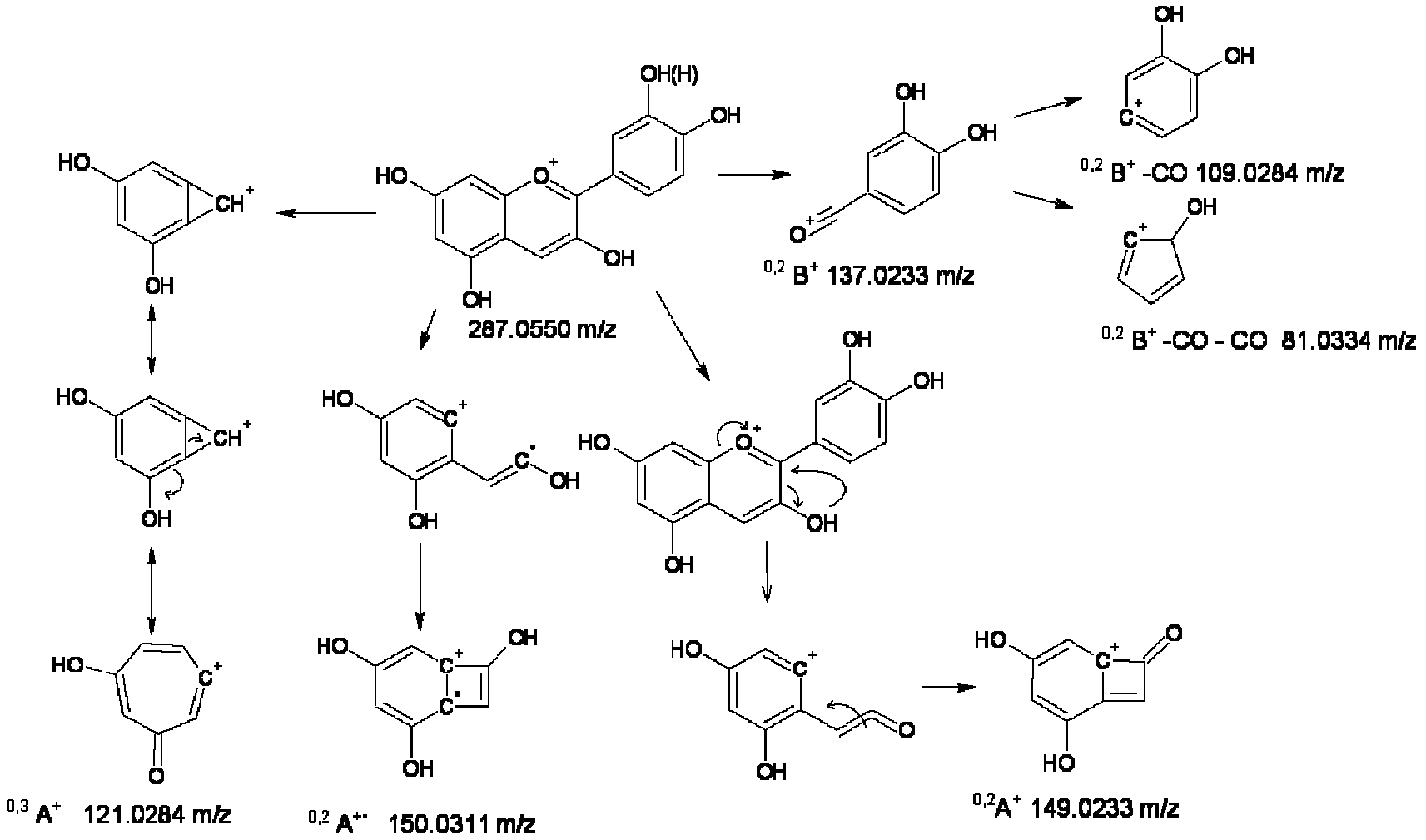

Figure 4.8: Proposed structures and mechanisms for CRC fragmentation of cyanidin.

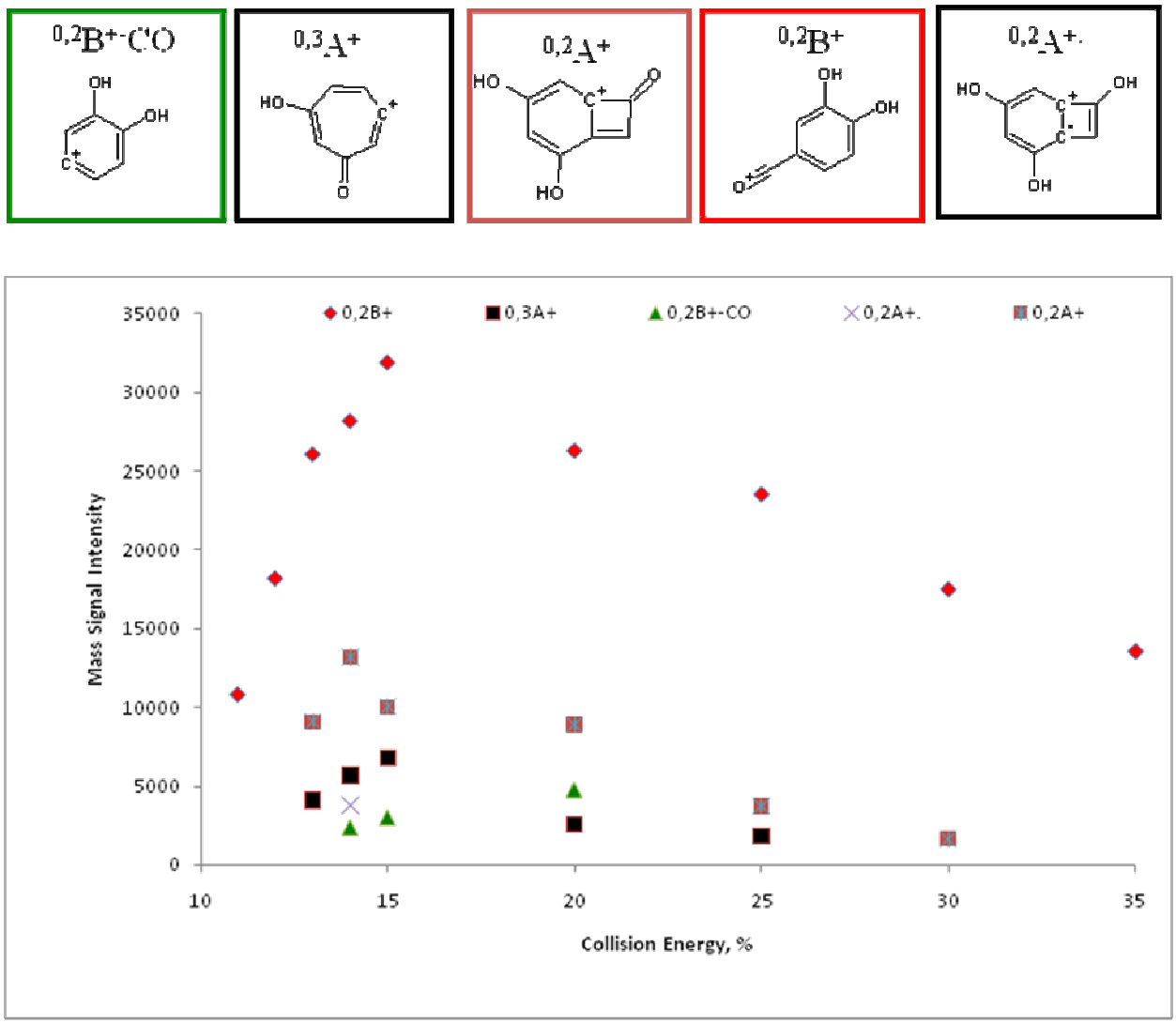

Figure 4.9: The effects of varying the collision energy applied to the ion trap of the CRC fragment ions of cyanidin at MS^4 stage.

For pelargonidin, a fairly intense signal at 121.028 m/z is observed in MS^4 spectra, which corresponds to two isobaric CRC fragments, $^{0,3}A^+$ and $^{0,2}B^+$. Additionally, the $^{0,2}A^+$ •(150.031 m/z), $^{0,2}A^+$ (149.023 m/z), and $^{0,2}B^+$-CO (93.030 m/z) signals are observed. MS^5 fragmentation of the 121.028 m/z resulted in a neutral loss of a carbonyl, giving $^{0,2}B^+$-CO (93.030 m/z). It is assumed that it is not $^{0,3}A^+$-CO because this signal is not observed in the fragmentation of cyanidin and has not been reported previously in the anthocyanidin fragmentation literature.

4.4.4.1 A Computational Study of Natural Conformation of Cross Ring Cleavage Products

A planar cyanidin structure was optimized in Gaussian and portions of the structure were removed to match the CRC fragment types. The lowest energy conformation of the fragment was then computed. The optimized structures were compared to the structures proposed by Oliveira et al.[82] and Montoro et al [83]. The $^{0,2}A^{+}$ structure proposed herein differs from the one proposed by Montoro et al [83]. Their structure suggests that a hydrogen is transferred from the C-4 to C-9, leaving a formal charge on the C-4, and a straight C-C-O chain. All of the calculated structures oriented to the proper configuration further justifying the existence of these structures in the gas phase, including the structure for $^{0,2}A^{+}$ proposed herein (Figure 4.10).

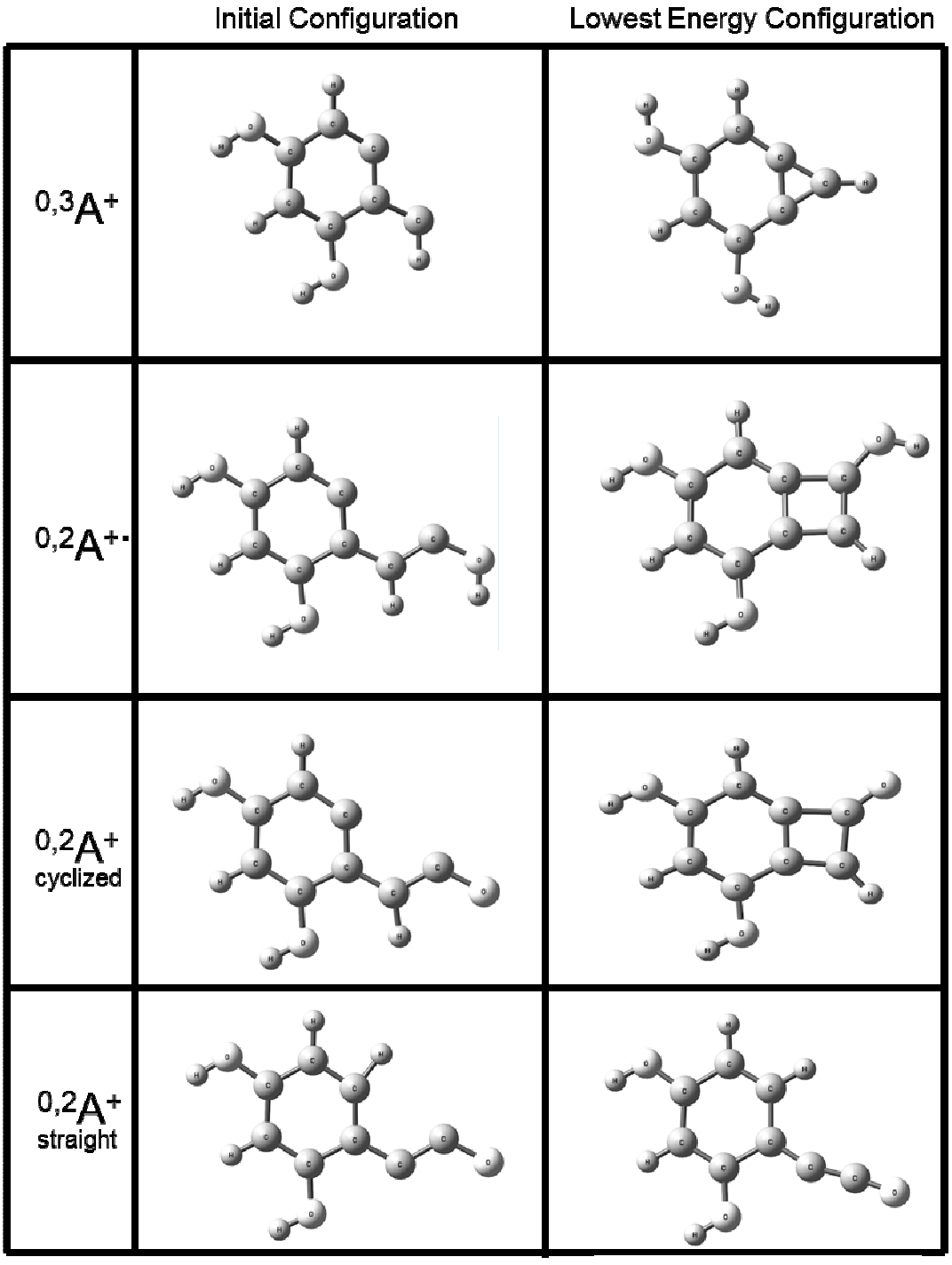

Figure 4.10: Natural conformation of cross-ring cleavage structures by computational analysis.

4.4.4.2 Correlation of Energy Values vs. Observed Fragmentation of Cross-Ring Cleavage

In the CRC fragmentation scheme, the precursor ion fragments to form both charged and neutral species. Software-calculated energy values for each charged and neutral fragments of cyanidin were obtained, compared against each other, and correlated to observed fragmentation intensities (Tables 4.5 and 4.6). The combined energy values are in good agreement with the energy of the non-fragmented species. From estimating the change in energy relative to the charged cyanidin parent ion, it can be determined that the $^{0,2}A^+$ and $^{0,2}B^+$ fragments are the most energetically favorable. Additionally, it can be implied that the $^{0,2}A/B^+$ fragment scheme is more energetically favorable than the $^{0,3}A/B^+$ fragment scheme.

Table 4.5: The calculated energy of CRC fragment species of cyanidin.

Fragment Type	**Calculated Energy, kJ/mol**
$[A+B]^+$ (Cyanidin)	-2701.681
$^{0,2}A^+$ (cyclized)	-1399.441
$^{0,2}A^+$ (straight)	-1399.430
$^{0,2}A^{+\bullet}$	-1401.011
$^{0,2}B^+$-CO	-1001.849
$^{0,2}B^+$-CO-CO	-704.532
$^{0,3}A^+$	-1101.905
$^{0,3}A^+$ (tropylium)	-1101.781
$^{0,3}B^{+\bullet}$	-1598.305
$^{0,2}A$	-1401.632
$^{0,2}B$	-1301.900
$^{0,2}B^{\bullet}$	-1300.137
$^{0,3}A$	-1102.306
$^{0,3}B$	-1599.028

Table 4.6: Combined calculated energy of neutral and charged CRC fragment species of cyanidin.

Fragment Scheme	Combined Energy, kJ/mol	ΔE relative to Cyanidin, kJ/mol
$^{0,2}A^{+}$ (cyclized) + $^{0,2}B$ =	-2701.341	0.341
$^{0,2}A^{+}$ (straight) + $^{0,2}B$=	-2701.331	0.351
$^{0,2}A$ + $^{0,2}B^{+}$ =	-2701.209	0.473
$^{0,2}A^{+\bullet}$ + $^{0,2}B^{\bullet}$ =	-2701.148	0.533
$^{0,3}A^{+}$ + $^{0,3}B$ =	-2700.933	0.748

The computational values for the $^{0,2}A/B^{+}$ scheme are in agreement with the intensities of the CRC fragments observed. Based on the change in energy relative to cyanidin, the $^{0,2}A^{+}$ fragment is energetically the most favorable to be formed compared to the other CRC fragments, but the observed intensities for this fragment are lower than the $^{0,2}B^{+}$ ions (Figure 4.9). The transfer of hydrogen needed to generate the $^{0,2}A^{+}$ fragment may create a higher activation barrier leading to lower fragment intensities. The $^{0,2}A^{+\bullet}$ fragment ions are very low in intensity, which is in contrast to what is suggested by the computational values. The reason for this may be due to the highly reactive nature of the radical in the ion trap, which causes the fragment to be short-lived in the ion trap.

A possible rearrangement of the $^{0,3}A^{+}$ ion into a tropylium configuration was also evaluated based on the energy determined by computational calculations. The calculated energy for tropylium-style ion was higher in energy than the one initial proposed by Oliveira et al [82]. Additionally, when allowed to reconfigure after removing the appropriate atoms from the anthocyanidin in simulation of a cross-ring cleavage (as in the natural conformation simulation above), the structure formed into the one proposed by Oliveira et al [82]. Still, a possibility exists that there may be a more energetically favorable intermediate which would encourage the tropylium structure to form.

4.4.5 Ring Opening and Small Molecule Loss

Due to the high stability of the anthocyanidin, there can be some speculation as to which ring is opening to facilitate fragmentation by small molecule loss. Based on the CRC fragmentation pattern it can be assumed that a cleavage site can be found at bonds 2 or 3 of the C-ring. Loss of CO from the C3

position may then be justifiable. This fragmentation could lead to a number of other possible fragmentations scenarios.

The number of possible fragmentation scenarios is many and due to isobaric uncertainties, the structures related to each of these fragmentation events may not be easily distinguished based on mass signals alone, or readily proven since some of these species may only exist for a short amount of time within the confines of the instrument. Some diagnostic information can be assessed, though, by comparing the type of fragmentation observed for each anthocyanidin species.

In addition to multi-stage fragmentation, high mass accuracy was used in assigning the neutral losses of fragment ions. For example, the loss of CO (27.996 Da) can be differentiated from the loss of C_2H_4 (28.0313 Da) by determining the accuracy of the observed signal and the theoretical monoisotopic mass. The difference between the theoretical masses of $[M\text{-}CO]^+$ (259.060 m/z) and $[M\text{-}C_2H_4]^+$ (259.024 m/z) is ~140 ppm. Another example can be illustrated by two observed signals in the pelargonidin fragmentation: 159.079 m/z and 159.045 m/z. These fragment signals were assigned as $[M\text{-}CO\text{-}CO\text{-}CO\text{-}CO]^+$ (theor. 159.080 m/z, -9.7 ppm error) and $[M\text{-}C_2H_2O\text{-}C_2H_2O\text{-}CO]^+$ (theor. 155.044 m/z, 8.4 ppm error), respectively. In general, assignments were only made when the error was within 25 ppm mass accuracy.

4.4.5.1 Cyanidin Fragmentation

In the case of the cyanidin species the neutral small molecules lost were all either water (H_2O), carbonyl (CO), C_5H_6 and/or a ketene (C_2H_2O). Based on which small molecule is lost, a specific fragmentation pathway was observed. In our experience, fragmentation may continue to occur until there is no more oxygen left in the fragment species, granted the precursor signal is of suitable strength and the appropriate collision energy is applied. For example, the cyanidin fragment ion at 128.0621 m/z observed at the MS^6 stage (Table 4.3) is described as $[M\text{-}H_2O\text{-}CO\text{-}CO\text{-}CO\text{-}CO\text{-}CO\text{-}H]^{+\cdot}$ which is a loss of 6 oxygens, the number of oxygens cyanidin contains. Similarly, the pelargonidin fragment ion at 141.069 m/z observed at the MS^6 stage (Table 4.4) is described as $[M\text{-}H_2O\text{-}CO\text{-}CO\text{-}CO\text{-}CO]^+$, which is the loss of 5 oxygens, the number of oxygens pelargonidin contains. For this reason, the fragment types that include a loss of 6 oxygens (by way of $CO/H_2O/C_2H_2O$ loss) are only observed in cyanidin fragmentation, and not in fragmentation of pelargonidin.

Signals for loss of water, $[M-H_2O]^+$ (269.044 m/z) and loss of a carbonyl $[M-CO]^+$ (259.062 m/z) were observed in the MS^4 spectrum. Iterative fragmentation of $[M-H_2O]^+$ at MS^5 resulted in further losses of CO and C_2H_2O. Further fragmentation of the signals $[M-CO]^+$ could not be collected either due to an insufficient signal level or improper collision energy applied, although, fragmentation of $[M-CO-CO]^+$ was easily obtained.

The fragment at 175.039 m/z is believed to be $[M-C_2H_2O-C_2H_2O-CO]^+$. This fragment was believed to be a primary fragment since it is not observed in the H_2O or CO pathways and since $[M-C_2H_2O]^+$ or $[M-C_2H_2O-C_2H_2O]^+$ is not observed.

There are two routes by which the fragment ion at 213.056 m/z is made, based on the fact that it is observed from two separate parent fragments, $[M-H_2O-CO]^+$ (241.049 m/z) and $[M-CO-CO]^+$ (231.064 m/z)(Table 4.3). This makes proposing structures for the fragments from 213.056 m/z difficult, realizing that each fragmentation event may be coming from two separate species which have the same mass. A combined response of two isobaric fragment ions would help explain why this signal is the most intense in the MS^4 spectrum (Figure 4.7).

4.4.5.2 Pelargonidin Fragmentation

Fragmentation of pelargonidin at MS^4 also demonstrated loss of small neutral molecules CO, H_2O, and C_2H_2O like cyanidin. Pelargonidin differed from cyanidin in losses of CH_2O, and C_5H_2O groups. Also, it is worth noting that further fragmentation of the signals $[M-CO]^+$ was successful (Table 4.4), unlike for cyanidin. However, this may only be due to sufficient signal level or adequate collision energy applied.

Unexpectedly, all of the pelargonidin fragments signals were different from the cyanidin signals by at least one mass unit, except the masses 141.069 m/z and 115.054 m/z, even though the two compounds share many of the same type of fragmented signals (Tables 4.1, 4.2 & 4.5). If a substantial amount of the B-ring was cleaved off, signals with the same mass would be expected to be observed in both fragmentation spectra. This suggests that ring opening and small molecule loss may be primarily originating in the A-C bicycle since the B-ring substituents would provide the 16 unit mass difference observed between the majority of the common fragment signal types shared between the two anthocyanidins.

Table 4.7: Comparison of the fragmentation types observed between pelargonidin and cyanidin in the positive mode.

Fragment Type	Cyanidin	Pelargonidin
$^{0,2}A^{+}$	✓	✓
$^{0,2}A^{+\bullet}$	✓	✓
$^{0,3}A^{+}$	✓	✓
$^{0,2}B^{+}$	✓	✓
$^{0,2}B^{+}$-CO	✓	✓
$^{0,2}B^{+}$-CO-CO	✓	x
M-H_2O	✓	✓
M-H_2O-CO	✓	✓
M-H_2O-CO-CO	✓	✓
M-H_2O-C_2H_2O	✓	x
M-H_2O-CO-C_2H_2O	✓	✓
M-H_2O-CO-CO-CO	✓	✓
M-H_2O-CO-CO-H_2O	✓	x
M-H_2O-CO-CO-CO-CO	✓	✓
M-H_2O-CO-CO-H2O-CO	✓	✓
M-H_2O-CO-CO-C_2H_2O	✓	✓
M-H_2O-CO-C_2H_2O-H_2	✓	x
M-H_2O-CO-CO-H_2O-CO-CO+H_2	✓	x
M-H_2O-CO-CO-H_2O-CO-CO	✓	x
M-H_2O-CO-CO-CO-CO-CO	✓	x
M-H_2O-CO-CO-CO-CO-CO-H	✓	x
M-H_2O-CO-CO-CO-CO-CO-H_2	✓	x
M-H_2O-CO-CO-C_2H_2O-CO-CO	✓	x
M-CO	✓	✓
M-CO-CO	✓	✓
M-CO-CO-CO	✓	✓
M-CO-CO-CO-CO	✓	✓
M-CO-CO-C_2H_2O	✓	✓
M-CO-CO-C_2H_2O-CO-H_2O	✓	✓
M-CO-CO-C_2H_2O-CO	✓	✓
M-CO-CO-C_5H_6	✓	x
M-CO-CO-C_4H_2O	✓	x
M-CO-CO-C_2H_2O-CO-CO	x	✓
M-CO-CO-C_2H_2O-CO-CH_2O	x	✓
M-C_2H_2O-C_2H_2O-CO	✓	✓
M-C_2H_2O-C_2H_2O-CO-O+H	✓	x
M-C_2H_2O-C2H_2O-CO-CO	✓	x
M-C_2H_2O-C_2H_2O-CO-CO-CO	✓	x

Finally, the substituents of the B-ring may be directing certain fragmentation pathways. This would lead to unique fragment ions that are only observed in fragment spectra of certain anthocyanidin species. For example, $[M-H_2O-C_2H_2O]^+$ is observed in the cyanidin spectra, but not in the pelargonidin spectra. This fragment pathway may be directed by the fact that cyanidin has two hydroxyl groups in the B-ring which are both being lost in consecutive fragmentation events (Figure 4.11). Pelargonidin would not be able to follow this pathway, since it has only one hydroxyl group.

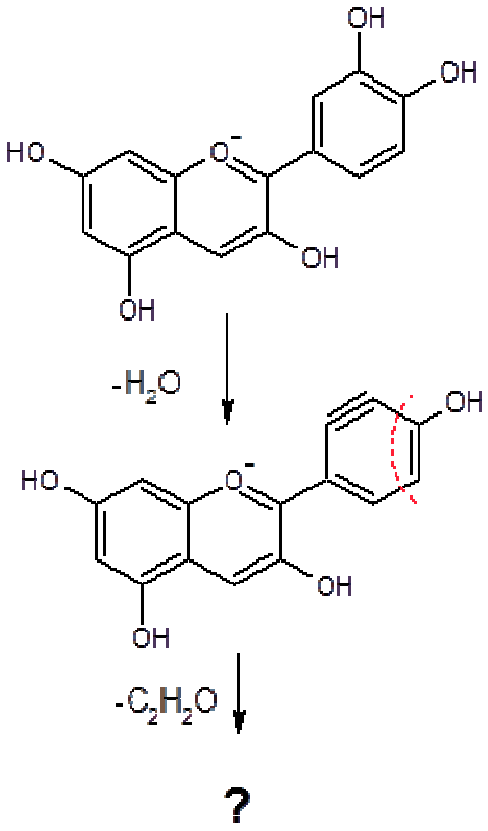

Figure 4.11: Proposed mechanisms for ring opening fragmentation and neutral loss of H_2O and C_2H_2O from cyanidin.

4.5 Conclusion

Fragmentation of cyanidin-3,5-diglucoside and pelargonidin-3,5-diglucoside was shown to be greatly affected by the amount of energy applied to the ion trap. Optimization of this energy was shown to increase the signal strength of the desired product ion, which improves the ability to achieve higher

order fragmentation. Fragmentation of cyanidin and pelargonidin was found to occur within a narrow range of collision energy to give cross-ring cleavage and small neutral molecule loss products.

The cross ring cleavage fragments of cyanidin generated by breaking the C_9-O_1 and C_2-C_3 bonds (0,2 pathway) were found to be in greater intensity than the fragments generated from cleaving the C_9-O_1 and C_3-C_4 bonds (0,3 pathway) and this trend was further justified by computational calculations.

Ring opening fragments of cyanidin and pelargonidin were found to lose CO, H_2O and C_2H_2O, while pelargonidin also showed losses of CH_2O and C_5H_2O. Additionally, all of the CRC product ions from the CID of each anthocyanidin, except for two, were shown to be diagnostic in differentiating between cyanidin and pelargonidin.

CHAPTER 5

CONCLUSIONS/FURTHER WORK

Some of the earliest methods of chromatography can be traced back to Mikhail Tswett and the separation of plant pigments. Recent advances in analytical instrumentation have greatly improved on the ability to analyze complex matrices of plant extracts. Anthocyanins, in particular, have been found to be particularly well-suited for analysis by LC-MS and as new hyphenated techniques emerge, less effort is needed for their definitive identification.

Although there has been an abundant amount of research performed on anthocyanins, the literature is lacking in studies of solvent extractions from natural products, specifically blueberries. Thus, a systematic approach was taken for optimizing the extraction process of anthocyanins using blueberries as a model system. It was determined that a mixture of methanol:water:trifluoroacetic acid (70:30:1, v:v:v) was the most efficient extraction system from those investigated. Additionally, a general method of identification without the need for authentic standards was reviewed and applied using the complementary techniques provided by RP-HPLC-ESI-IT-TOF-MS.

Based on these experiences, it was observed that more definitive identification could be obtained by investigating the fragmentation pathways of the anthocyanidin. Through this, individual anthocyanins could be differentiated from themselves and from other interfering flavonoids without the need of sample cleanup or standards. Cyanidin-3,5-diglucoside and pelargonidin-3,5-diglucoside were extracted from red hybrid-tea rose petals and their common fragmentation pathways were investigated by using multi-dimensional tandem mass spectrometry (MS^n) with high mass accuracy. Variations in product ion intensities were observed as the collision energy of the ion trap was adjusted. Computational calculations were then applied to further investigate the observed fragment signals.

The fragment ions of anthocyanidins were determined to contain many isobaric uncertainties. These uncertainties limit the ability to understand the mechanisms by which the fragmentation events are occurring and hinder the characterization of the fragment structures. To improve on this situation, a

number of studies may be performed. The use of metal complexation may be helpful in determining which ring may be opening in fragmentation, causing small neutral molecule loss. Harborne used one such technique when he added aluminum chloride to his solutions to differentiate between anthocyanidins with adjacent hydroxyl groups by shifting UV spectra[74]. This could also be used in observation of fragment signals. Metal complexation may alter the observed fragment spectra leading to new insight of the fragmentation pathways. In a similar manner, isotope labeling could be used to help determine the mechanisms by which fragmentation is occurring.

Finally, computational models can be used to justify the proposed fragment structures determined by additional knowledge of fragmentation patterns. In addition to calculating the optimized energy levels of structures, HOMO/LUMO and mulliken charge calculations may be used to assess the location of formal charges and possibilities of resonance structures. These methods may provide some further support in understanding the complexities of these colorful compounds.

REFERENCES

[1] J. B. Harborne, The Flavonoids: Advances in Research Since 1986. Chapman and Hall, University Press, Cambridge, Great Britain, 1994.

[2] O. M. Anderson, K. R. Markham, Flavonoids: Chemistry, Biochemistry and Application. CRC Press,Taylor and Francis, Boca Raton, Florida, 2006.

[3] R. J. Robbins et al. J Cardiovasc. Pharamcol. 2006, 47:S110-S118

[4] Q. Tian et al. J Chromatogr. A. 2005, 1091:72-82

[5] V. Vukicks and A. Guttman, Mass Spec Reviews, 2010, 29:1-16

[6] K. R. Markham, Techniques of Flavonoid Identification. Academic Press New York, 1982.

[7] C. A. Williams, R. J. Grayer. Nat. Prod. Rep. 2004, 21:539-573

[8] C. R. Welch et al. Anal Chem. 2008, 4: 75–101.

[9] X. Wu et al. J. Agric. Food Chem. 2006, 54:4069-4075

[10] J. B. Harborne, The Flavonoids: Advances in Research Since 1986. Chapman and Hall, University Press, Cambridge, Great Britain, 1994.

[11] H. Stafford. Flavanoid Metabolism, CRC Press, Fl, USA 1990

[12] K. Simpson, in T. Richardson, J. Finley (eds), Chemical Changes in Food During Processing. AVI Publishing Co., Westport, CT, 1985, p. 409-441.

[13] G.J. Wagner. Recent Advances in Phytochemistry, 16, Plenum Press, New York, pp. 1-45

[14] C.J. Small and R.C. Pecket. Planta, 1982, 154:97-99.

[15] S. Conn, C. Franco, W. Zhang. Planta, 2010, 231:1343-1360

[16] D. Lee, K. Gould, Adv. In Bot. Research, 2002, 37:1-16.

[17] R. Klaper et al. Phytochem. 1996, 63: 811-813.

[18] C. Costa-Arbuhi et al. Journal of Chem. Ecology 2001, 27: 273-283.

[19] P.A. Hedin et al. In Plant Resistance to Insects pp. 347-367, Amer. Chem. Soc., Washington. . 1983.

[20] L. Chalker-Scott. Photochemistry and Photobiology 1999, 70:1-9.

[21] R. L. Nicholson et al. Proceedings of the National Academy Sciences, USA 1987, 84: 5520-5524.

[22] A. Faria et al. J. Agric. Food Chem. 2005, 53, 6896-6902.

[23] A. Mente et al. Arch Intern Med 2009, 169: 659–669.

[24] J. Vinson et al. J. Am. Coll. Nutr. 2005, 24:1 44-50.

[25] R. Moyer et al. J. Agric. Food Chem. 2002, 50: 519-525.

[26] C. Rice-Evans et al. Trends in Plant Science, 1997, 2:152-159.

[27] D. Huang et al. J. Agric. Food Chem. 2005, 53:1841-1856.

[28] A. Faria et al. J. Agric. Food Chem. 2005, 53 6896-6902.

[29] I. Fernandes et al. J Agric Food Chem. 2010, 58:3785-3792

[30] H. B. Park et al. J Orthop. Res. 2010, 28:1162-1169.

[31] K. Gould et al. Roles of Anthocyanins in Plant Defence. Springer, New York, 2009, pp 10-12

[32] D. Hou. Curr. Mol. Med. 2003, 3:149-159

[33] S. Meiers et al. J. Agric. Food Chem. 49:958-962.

[34] W. Yi, et al. J. Agric. Food Chem., 2005, 53:7320-7329

[35] W. Yi, et al. J. Agric. Food Chem., 2006, 54:5651-5658

[36] T. K. McGhie et al. J. Agric. Food Chem. 2003:51:4539-4548.

[37] G. Cao et al. Amer J. Clin. Nutri. 2001:73:920-926

[38] B. Davis et al. J Mass Spectrom. 2006, 41:911-920

[39] X. Wu et al. J. Nutrition 2002, 132:1865-1871

[40] J. Beattie et al. Curr. Nutri. Food Science, 2005, 1:71-86

[41] N. Katsube et al. 2003, 51:68-75.

[42] A. Sarma et al. Phytochemistry 1997, 45:671-674

[43] P. Pawlowicz. Ginekol Pol. 2000, 71:848-853.

[44] L. Estevez, R. A. Mosquero. J. Phys. Chem. A 2008, 112:10614-10623

[45] L. Estevez, N. Otero, R. A. Mosquero. J. Phys. Chem. B 2010, 114: 9706-9712

[46] R. Guzman et al. J. Mol. Structure 2009, 935:110-114

[47] R. Willstatter, T. J. Nolan, Ann. Chem. 1914, 408:1-14.

[48] M. S Onslow. The Anthocyanin Pigments of Plants. Cambridge Press, Cambridge, 1926

[49] A. Castañeda-Ovando, et al. Food Chem. 2009, 113: 859-871.

[50] E. Revilla et al. J. Agric. Food Chem. 1998, 46:4592-4597.

[51] R. Brouillard, Anthocyanins as Food Colors. Academic Press, New York, 1982.

[52] T. Goto, T. Kondo, Angew. Chem. Int. Ed. Engl. 1991, 30:17-33.

[53] J. F. Gonnet, Food Chem. 1998, 63:409-415.

[54] A. Liazid et al. J. Chromatogr. A , 2007,1140: 29-34.

[55] M. O. Downey et al. Am. J. Enol.Vitic. 2007, 58:358-364.

[56] G. Fan et al. LWT- Food Science and Tech. 2008, 41:155-160.

[57] R. Jackman et al. J. Food Biochem. 1998, 11: 279-308.

[58] J. E. Cacace, G. Mazza. J. Food Engineering. 2003, 59:379-389.

[59] M. A. Rostagno et al. J. Chromatogr. A 2003, 1012:119-128.

[60] J. Prasain et al. Free Radical Bio. Med. 2004, 37:1324-1350.

[61] X. Wu, R. L. Prior. J. Agric. Food Chem. 2005, 53: 2589-2599.

[62] R.P. Metivier et al. J. Food Science. 1980, 45:1099-1100.

[63] C. Sandoval et al. J. Soln Chem. 2003, 32:781-790.

[64] E. Nicoue et al. J. Agric. Food Chem. 2007, 55:5626-5635.

[65] C. Peri, V. Bonini. J. Food Technol. 1976, 11:283-296.

[66] J. Pissara et al. J Food Sci. 2003, 68:476-481.

[67] B. Sun et al. J. Chromatogr. A. 2006, 1128:27-38.

[68] F. Kader et al. Food Chem. 1996:55:35-40.

[69] V. Hong and R. E. Wrolstad J. Agric. Food Chem. 1990, 38, 708-715

[70] V. L. Singleton, J. A. Rossi. Am. J. Enol. Vitic. 1965, 16, 144-158.

[71] M. M Giusti,.; R. E. Wrolstad, In Current Protocols in Food Analytical Chemistry. John Wiley & Sons: New York, 2001.

[72] M. O. Downey, S. Rochfort. J. Chromatogr. A. 2008, 1201:43-47.

[73] J. Harnly et al. J. Agric. Food Chem. 2006, 54:9966-9977.

[74] J. B. Harborne, Biochem. J. 1958, 70:22-28.

[75] I. Idaka, et al. Agric. Biol. Chem., 1987, 51:2215-2220.

[76] H. M. Merken, G. R. Beecher. J. Agric. Food Chem. 2000, 48:577-599.

[77] M. Stobieck, Phytochemistry 2000, 54: 237-256.

[78] M. Giusti et al. J. Agric. Food Chem. 1999, 47:4657-4664.

[79] P. Montoro et al. J Chrom. A, 2006, 1112, 232-240

[80] I. Revilla et al. J. Chromatogr. A. 1999. 847:83-90.

[81] R. Kostiainen, T. J. Kauppila. J.Chromatogr. A, 2009,1216:685–699

[82] M.C. Oliveira et al. Rapid Comm in Mass Spectrom. 2001, 15:1525-1532

[83] D. Kammerer et al. Rapid Commun Mass Spectrom. 2003, 17:2407-2412.

[84] Y. L. Ma et al. Rapid Comm in Mass Spectrom. 1997, 11:1357-1364

[85] N. Fabre et al. Amer. Soc. Mass Spec. 2001, 12:707-715

[86] D. Callemien, S. Collin. Amer. Soc. Brewing Chemists. 2008, pg 1-7

[87] H. Li, M. Deinzer. Anal. Chem. 2007, 79, 1739-1748

[88] V. Vukics and A. Guttman, Mass Spec Reviews, 2010, 29, 1-16.

[89] E. Petersson et al. Electrophoresis. 2008, 29:2723-2730.

[90] H. Li et al. Rapid Commun. Mass Spectrom. 2007, 21:2497-2504

[91] R. E. March, X. Miao. Inter J of Mass Spec. 2004, 231:157-167

[92] G. Robinson, R. Robinson, Biochem J. 1932, 26 :1647–1664.

[93] W. E. Ballinger et al. J. Am. Soc. Hortic. Sci. 1970, 95:283-285.

[94] W. E. Ballinger et al. J. Am. Soc. Hortic. Sci. 1972, 97:381-384.

[95] V. V. Vershkovski et al. Prir. Soedin. 1985, 4:570.

[96] G. M. Sapers et al. J. Am. Soc. Hortic. Sci. 1984, 109:105-111.

[97] Z. Zhang et al. J. Agric. Food Chem. 2004, 52:688-691.

[98] V. Lohachoompol et al. Food Chem. 2008, 111:249-254.

[99] K. R. Price et al. Food Chem. 1999, 66:489-494.

[100]L. Lin, J. Harnly. J. Agric. Food Chem. 2007, 55:1084-1096.

[101]D. Amic, D. Davidovic-Amic, J. Chromatogr. A. 1993, 653:115-121.

[102]I. Konczak, W. Zhang, J. Biomed. Biotech. 2004, 2004:239-240.

[103]S. Hakkinen, S. Auriol, J. Chromatogr. A. 1998, 829:91-100.

[104]Y. Mikanagi et al. Biochem. System. Ecol. 2000; 28:887-902

[105]C. H. Eugster, E. Märki-Fischer, Angew. Chem. Int. Ed. Engl. 1991, 30:654-672.

[106] J. S. Barnes et al. J Chromatogr. A. 2009, 1216: 4728-4735

[107] J. Kang et al. Rapid Commun. Mass Spectrom. 2007, 21:857-868.

[108] B. Davis et al. J. Mass Spectrom. 2006, 41:911-920.

[109]K. V.Wood, et al. Rapid Commun Mass Spectrom., 1993, 7:400–403

[110] J. Woodford. Chemical Physics Letters 2005, 410:182–187

[111] M. Wolniak, I. Wawer. Solid State Nuclear Magnetic Resonance 2008, 34:44–51.

[112] K. Sakata et al. Tetrahedron 2006, 62:3721–3731

[113] G. K. Pereira et al. J Mol. Structure. 1997, 392:169-179.

[114] L. Estevez, R. A. Mosquero. J. Phys. Chem. A 2007, 111:11100-11109

[115] Gaussian 03, Revision C.02, M. J. Frisch, G. W. Trucks, H. B. Schlegel, G. E. Scuseria, M. A. Robb, J. R. Cheeseman, J. A. Montgomery, Jr., T. Vreven, K. N. Kudin, J. C. Burant, J. M. Millam, S. S. Iyengar, J. Tomasi, V. Barone, B. Mennucci, M. Cossi, G. Scalmani, N. Rega, G. A. Petersson, H. Nakatsuji, M. Hada, M. Ehara, K. Toyota, R. Fukuda, J. Hasegawa, M. Ishida, T. Nakajima, Y. Honda, O. Kitao, H. Nakai, M. Klene, X. Li, J. E. Knox, H. P. Hratchian, J. B. Cross, V. Bakken, C. Adamo, J. Jaramillo, R. Gomperts, R. E. Stratmann, O. Yazyev, A. J. Austin, R. Cammi, C. Pomelli, J. W. Ochterski, P. Y. Ayala, K. Morokuma, G. A. Voth, P. Salvador, J. J. Dannenberg, V. G. Zakrzewski, S. Dapprich, A. D. Daniels, M. C. Strain, O. Farkas, D. K. Malick, A. D. Rabuck, K. Raghavachari, J. B. Foresman, J. V. Ortiz, Q. Cui, A. G. Baboul, S. Clifford, J. Cioslowski, B. B. Stefanov, G. Liu, A. Liashenko, P. Piskorz, I. Komaromi, R. L. Martin, D. J. Fox, T. Keith, M. A. Al-Laham, C. Y. Peng, A. Nanayakkara, M. Challacombe, P. M. W. Gill, B. Johnson, W. Chen, M. W. Wong, C. Gonzalez, and J. A. Pople, Gaussian, Inc., Wallingford CT, 2004.

BIOGRAPHICAL INFORMATION

Jeremy Barnes was born on May 14th, 1979. He was raised in Mansfield, Texas by his father on a small ranch. He spent his time with his brother, who is two years older, playing video games and exploring nature. He graduated from Mansfield High School in 1997. He earned an Associates' Degree in Liberal Arts from Tarrant County College in 1999, then a Bachelor's in Science (Biology) from the University of Texas-Arlington in 2002. He is happily married, enjoys American Football, and dreams about having the time to play more golf and video games in the future.